Functionally Adaptive Myosite Selection using conformable HD sEMG electrodes for movement-pattern classification

by

Sapna Kumar

A thesis submitted to Johns Hopkins University in conformity with the requirements for the degree of Master of Science

Baltimore, Maryland

May, 2018

ABSTRACT

Myoelectric prosthesis systems currently use advanced control schemes such as pattern recognition to classify muscle activation signals as intended movement classes. For this classification, generally, untargeted, equally spaced electrodes placed circumferentially around the muscle belly of the forearm, are used for acquisition of surface electromyogram (sEMG) for tran-radial amputee subjects. We propose a novel system, consisting of a hardware and software component. We built the hardware component in the form of a flexible and conformable high-density sEMG array. We tested the signal quality and electrode-skin contact characteristics to demonstrate the quality and conformability of the electrode array. We built the software component of the system based on separability criteria. This proposed system is called functionally adaptive myoelectrode site (myosite) selection (FAMS) and is to identify optimal myosites for pattern recognition. Our study investigates the effects of optimal myosite selection with increase in the number of movement classes and inclusion of fine motor movements. We also used myosite selection from current clinical and research procedures and compared the performances of FAMS to existing systems. Results of our study indicate that using optimal myosites selected using FAMS for movement pattern classification improves performance and this becomes more evident with increase in the number of selected myosites. The significance of using optimal myosites increases when more movement classes are included. This work also shows that the optimal myosites change spatially with the type and number of movement classes included for classification.

We then explored other future applications of 1) FAMS in temporal adaptations to help prosthetic users begin early use of pattern recognition based prosthesis system and 2)

extending FAMS to site selection for direct control so as to make FAMS a universal electrode interface for myoelectric prosthesis. Preliminary study results in these areas are presented in this work. The electrode design was further improved to fit inside of a prosthesis. This system has the capabilities to become an off-the-shelf universal system that can be prescribed for any myoelectric prosthesis user irrespective of their level of amputation and experience with using a myoelectric prosthesis. This system can reduce pre-prosthetic training time and facilitate early fitting. This system also removes the need for refitting every time the user changes the movement classes controlled by the prosthesis.

Thesis Committee Chair: Dr. Eileen Haase

Thesis Project Adviser and Thesis Committee Member: Dr. Nitish. V. Thakor

Thesis Committee Member: Dr. David Kraemer

PREFACE

This thesis has been a great learning experience and it would have not been possible without the help and guidance of my mentors and peers. First and foremost, would like to thank my adviser, Dr. Nitish. V. Thakor, for his mentorship and support throughout the period of this research. I would also like to thank him for his motivation and guidance in becoming a better person. In addition, I would like to thank Dr. Rahul Kaliki for his guidance and insights in this research and also for being a great mentor and bringing out the best in me.

I would also like to thank Dr. Eileen Haase and Dr. David Kraemer for taking the time out to review my thesis. I would like to extend my gratitude to my colleagues at Infinite Biomedical Technologies, particularly Damini Agarwal, George Levay, Megan Hodgson, Tina Lee and Dan Schlattman for their help and encouragement during the period of this research. I would like to extend a special thank you to Joseph Betthauser for building the algorithm section of FAMS work and being a guide and collaboratively working with me to make this work successful. I would also like to thank Matthew Fifer, Robert. S. Armiger and Applied Physics Laboratory for their collaboration and MiniVIE software. I am also grateful to my colleagues in the lab, Luke Osborn and Christopher Hunt for their willingness to offer advice whenever needed and other graduate and undergraduate students in the lab for making this a fun experience. I am honored to have had a such great people to support and guide me during my research.

DEDICATION

I would like to dedicate this thesis to my family and friends. Thank you for having confidence in me and encouraging me to pursue my passion. I also dedicate this to all my teachers and professors who have been the reason for my passion and love for science.

Table of Contents

List of figures

Chapter 1:

Chapter 2:

Chapter 3:

List of tables

Chapter 1: Introduction

1.2.1. History of prosthetics:

The history and evolution of prosthetic technology takes us back to times where they used peg legs and hand hooks as replacements for the lost limb. Initially prostheses were worn to get a sense of "wholeness" than for functional purposes [1]. Later when more such limb losses occurred during times of battles, there emerged a need for artificial limbs that could substitute a specific function like to hold a shield. This led to the evolution of body-powered prostheses, mechanically more functional prostheses, initially made by watchmakers by adding small mechanical components like springs and gears that could improve functionality of the limb. The materials used in making these earlier versions were iron, steel, wood, copper etc. The need to make the prostheses lightweight and more functional were the main goals that were set in this era of body-powered prostheses. Then, during the US civil war, the number of amputations increased tremendously bringing in the need for better material, technology for the veterans to improve their quality of life. This marked the birth of the industry in the US. Around this time, James Edward Hanger launched the era of modern prosthetics [2]. He founded the company Hanger Inc. which is still a key player in the field.

1.2.2. Upper limb amputation and prosthetics in Clinical practice:

Though the percentage of upper limb amputations is not as high as the lower limb amputations, upper extremity amputation can be more devastating in some ways than lower limb amputations [3]. In 2005, 541,000 American suffered from different levels of upper limb amputation. This number is expected to double at least by 2050 [4]. About 3500 and

5200 upper limb amputations have been reported each year in Italy and in UK respectively [5].

Upper limb amputations can be of two main types: Congenital and Acquired. The most common cause of acquired amputations is trauma due to accidents/war injuries. Tumor and vascular insufficiencies are some other causes contributing to acquired upper limb amputations [3]. Prostheses have been playing a major role in rehabilitation of persons with amputation. There are 2 major types of prostheses: Passive and active prostheses. Passive prostheses include cosmetic and functional prostheses. Active prostheses include body-powered and externally powered prostheses.

1.2.2.1. Postsurgical care:

Upper limb amputation surgeries are performed at various levels. Fig. 1.1 shows the various levels of upper extremity amputations. The most occurring levels of amputations are 61% trans-carpal, 16% trans-humeral, 12% trans-radial in Italy and UK [5]. The motivation of upper limb amputation surgeries is to preserve as much length as possible, stabilize the severed muscles, resect nerves to prevent neuromas, improve wound healing and help in maximizing the chances of having a functional residual limb [3].

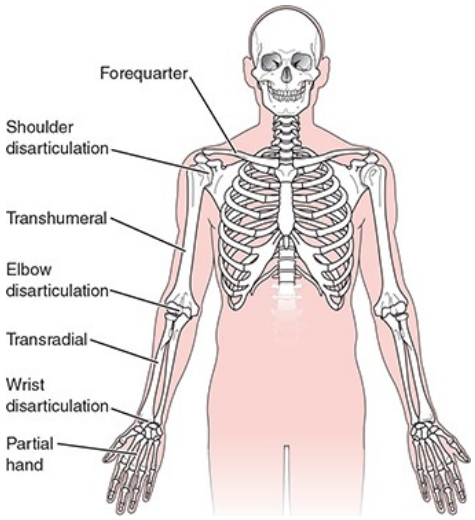

Fig. 1.1. Upper extremity amputation levels [3].

The postsurgical care of amputees is an important part of rehabilitation for upper limb amputees. This involves enhancing residual limb healing, preventing muscle weakness in

areas adjacent to the site of amputation, regaining independence in performing functional activities, preparing the residual limb for a definitive prosthetic fitting process, preventing postural deformities and assisting in gaining emotional adjustments [3]. In cases where the patient is opting for a myoelectric prosthesis, the step involving preparation for prosthetic fitting include shrinking or stabilizing the shape of the residual limb and determining possible sites for myoelectric control [3].

1.2.3. Prosthesis Rejection/Abandonment:

The ultimate aim of any research/ product design is that the solution/ product satisfies the user needs. Any solution that fails to do so is eventually rejected by the target population it is built for. The second important factor that contributes to the success of a solution is how well it satisfies the need and how favorable the outcomes are. The field of prosthetics is no different. Various studies have examined the reasons for prosthesis rejection [6,7]. One such study by K. Østlie et al. [6] surveyed users of cosmetic prostheses, body-powered prostheses, myoelectric prostheses, aesthetic prostheses and hybrid prostheses. This study also quantified 2 types of rejection: Primary and secondary rejections. Primary rejection is where the person with amputation never used the prosthesis and secondary rejection means that they have discontinued the use of prosthesis after a certain period of use.

The results in this work showed that primary and secondary prosthesis rejection was found to be 4.5% and 13.4% in amputees respectively. The reasons reported for the primary rejection were that the users did not perceive a need to use a prosthesis and if they did, there was a huge gap between perceived need and the capabilities of the prosthesis available on market. The reasons for secondary rejection included dissatisfaction with prosthetic

comfort, function and control. Among the secondary prosthetic rejection, the average time from prosthetic fitting to rejection was shown to be 6.5 years.

There is also a group of people comprising passive wearers of body-powered or electric prostheses, who do not use the active capabilities of their device, rather, they wear the prosthesis for cosmetic purposes [8]. The percentage of this type of users seem to range between 16% [9] and 47% [10] with a weighted average of 27%.

1.2.4. Introduction to myoelectric prostheses:

With increased occurrences of amputations, there came the need for improved technology that could substitute for functions and enhance the quality of lives of the users. This gave rise to the first ever prosthetic controlled by electrical activity of the muscle - Myoelectric prosthetic. The first myoelectric prosthesis we know of was created in the period 1944-1948 by Reinhold Reiter, then a physics student at Munich University. This was before the invention of transistors and hence, Reiter was forced to use vacuum tubes in the electronic systems. Due to its bulky nature, it was not portable to be of any practical use to the persons with amputations [1]. His system controlled opening and closing of the artificial limb using signals from a single muscle. His work was neither accepted, nor published. His work was however, reinvented by the time it was discovered by other researchers. Around 1957, research groups from various countries started working on the myoelectric control. This was more obvious and practical after the availability of transistors [1]. Various groups started contributing to the field of myoelectric prosthesis. Groups led by Bottomley in England; Herberts in Sweden; Kato in Japan; Kobrinski in Moscow; Reswick, Lyman and Childress in the USA, Scott at UNB were among the pioneers [1]. From the beginning since now, it can be argued that though the technology has advanced in a relatively noteworthy

pace with parallel advancements in electronics, data analysis tools and techniques, there is still a gap in understanding adequately the needs of the persons with amputations and exploiting the technological advancements to bring about meaningful outcomes.

Myoelectric prosthetics are superior over body-powered prosthesis since it has hands-free control ability based on user's intension [11], more like a human hand, eliminates the need for harness, grips stronger than a body-powered prosthesis [3] etc. However, it is more difficult to learn control, has a very slow response time, the components are not as durable. In specific cases like trans-humeral amputees it is even more difficult to control the myoelectric prosthetic hand since it is not as intuitive as for a trans-radial prosthetic [3]. The next section would dwell on attempting to understand the drawbacks and shortcomings in the performance of the myoelectric prostheses from a user's perspective.

1.2.5. Common drawbacks and shortcomings of myoelectric prosthetic from a User perspective:

There have been a lot of studies and surveys which have been conducted to analyze the issues faced by upper limb amputees in myoelectric prostheses, to study their needs and infer how the technology can be applied to improve the functionality of the prosthesis to satisfy user needs. This section reviews some of these works and summarizes the needs of myoelectric prosthetic users.

Firstly, there are the most frequently used Activities of Daily Living(ADL) that the prosthesis needs to be able to perform in order to be considered effective and in order for the user to feel the need to even use one. This is because, as stated earlier the lack of need to use a prosthesis is one of the major causes of abandonment. This means that the prosthesis should be able to perform better than what the users can achieve through mere

adaptation with their residual limb and/or other healthy limb. Better performance could hence mean that the user is able to exhibit more consistency, reliability and less effort while performing ADL or is able to perform specialized functions that they cannot perform by mere adaptation.

Some of the activities that the users want a myoelectric prosthetic to perform are stated in Pylatiuk et al., [12] internet survey, they include handicrafts, personal hygiene, using cutlery, dressing. In Biddiss et al. [13], the activities highlighted are related to household maintenance, heavy lifting, sports, activities of daily living (i.e., cooking, eating, dressing, personal hygiene, typing) and hobbies (i.e., playing a musical instrument). The most desired activity however is using cutlery, followed by handicrafts, personal hygiene, opening and closing a door, dressing and undressing; the least desired activity is writing with the prosthesis.

The other set of user feedback and recommendations from users falls into the category of "improving performance". These recommendations mainly include feedback and improved control [12]. The users wished to have a reduced demand of visual attention, ability to feel the grip force, temperature of objects being grasped, ability to avoid object slippage etc. On the other hand, the recommendations to improve the capabilities or performance of the prosthesis included ability to adapt to object shape, index point, individual finger movements, performing wrist flexion/ extension, improved dexterity and fine motor control to operate a computer keyboard etc. Apart from these needs, issues with using their existing prostheses were also reported in Pylatiuk et al.'s [12] work. These included, issues with glove material, weight of the prostheses resulting in back pain, noise produced by the

prosthesis, prosthesis grasping speed too low, electrodes being too sensitive to interference [12], [14] etc.

1.2.6. Introduction to control strategies:

Myoelectric control schemes for upper limb prosthesis control have evolved from two site direct control [1] to more advanced schemes such as pattern recognition [15] over the years. In direct control, the user can perform only very limited number of motions which are activated by threshold based control signals [1]. In pattern recognition, the user can perform as many control movements as possible based on the capabilities and extent of muscles retained post amputation. Pattern recognition system is one of the advanced classification algorithm-based control system that has helped improve the number of motions that a myoelectric prosthetic user can perform based on the ability of the subject to produce consistent and distinguishable patterns. The state-of-the-art control scheme widely used in research as well as state-of-the-art commercial system [16] use the pattern recognition based control strategy. Studies have shown that this control scheme outperforms conventional direct control strategy by providing more functionality in TMR patients [17], [18]. The concept of simultaneous control has also been investigated with the use of this control strategy [19]. However, there are many factors that affect the classification performance of this control strategy which include location of electrodes, level of amputation and type of surgical procedure [18], [20].

1.2.7. Preparation for myoelectric prosthetic fitting:

One of the essential and critical part of preparation for myoelectric prosthetic fitting as stated in section 1.2.2.1 is myoelectrode site (myosite) testing/control site selection. The

electrode site identification usually happens in the occupational therapy center post amputation. The ideal period of prosthetic fitting is said to be 30 days from the amputation. This period is termed as the "golden window". Research has demonstrated that persons with amputations fit with a prosthesis during this golden window exhibited a 93% rehabilitation success rate with a 100% return to work rate within 4 months of injury. Those fit beyond this period showed a 42% rehabilitation success rate with a 15% return to work rate within 6 to 24 months [21]. Within 2 to 3 weeks of injury/amputation, the electrode site identification and training is initiated. The important goals of this early training phase is to "identify, instruct, and train the patient to independently, correctly, and efficiently use specific residual limb musculature to activate and perform basic myoelectric prosthesis functions resulting in the ability to immediately operate the myoelectric prosthesis at first fitting" [22].

As stated in the previous section, the location of electrodes has a major role to play in how the myoelectric prosthesis performs. The positioning of electrodes depends on factors including level of amputation, type of surgical procedure performed and type of control system used by the myoelectric prosthesis. For a two site direct control system for trans-radial amputations, site selection process is fairly simple. The myosite testing or myosite selection occurs at the OT using palpation/socket electrodes (shown in Fig. 1.2) [23], where the electrodes are used to visualize the quality of the signal using biofeedback system such as the MyoBoy (Otto Bock, Minneapolis, Minn), or the MyoLabII (Motion Control, Inc., Salt Lake City, Utah) [23], [24]. Myotester is a device that is used to test the muscle activity signals from various muscles of the residual limb in order to arrive at the locations to be used for the placement of electrodes for a myoelectric prosthetic device [3]. However, to

use this equipment advanced training is essential and usually therapists and prosthetists work together to identify the best sites for electrode placements. The most commonly used sites are flexors and extensors for a two site direct control system. The clinician starts control site identification with palpation, while asking the person with amputation to perform the intended motions (for instance, wrist flexion and extension). Once the region of interest is located, bipolar socket electrodes are used to visualize the best possible signal sites. One such example of socket electrode used for this purpose (Otto Bock electrodes) is shown in Fig. 1.2(a).

One more critical step in successful use of the selected sites is learning how to use the muscle pairs associated with these sites i.e. learning to contract one muscle group isometrically while maintaining relaxation (least muscle activity) in the antagonist group. Usually real time graphs (using MyoBoy, MyoLabII as stated above, or BioSim from Touch Bionics [23]) are used to visualize the signals from the selected myosites. These act as biofeedback during the training and fitting sessions. An example of a good signal or optimal graph and a poor signal as depicted in the "*Training Protocol for Therapists"* [23] is shown below in Fig. 1.2(b) and 1.2(c).

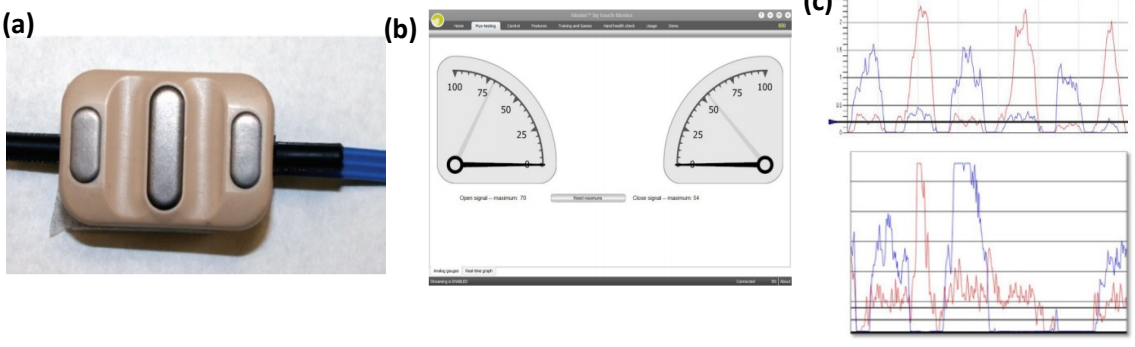

Fig. 1.2: a) Socket electrode for myoelectric testing. [Photograph courtesy of Otto Bock.] b) BioSim GUI [24] c) (top) optimal signal graph for 2 site control (bottom) poor signals for 2 site control [23].

Some of the cases where the person does not have two available antagonistic sites, due to higher level of amputation or loss of the relevant muscle activity, the skills and creativity of the team of clinicians is what decides how well the site selection occurs and in turn how efficient the myoelectric prosthesis will perform.

Some other issues as reported by Smurr et. al., [22] are "(a) scar and graft site locations because the signal is not as easily transmitted through dense tissue, (b) identification of an appropriate superficial muscle site for a stronger signal, and (c) continuous contact between the skin and electrode at the selected myosite throughout the maximum Range of Motion (ROM) of the residual limb. The latter requires special attention during this process".

In case of electrode locations for pattern recognition systems there are different conventional methods followed: 1) 8 equally spaced electrodes placed on the muscle belly of the forearm (for trans-radial amputations) 2) Site selection using palpation and EMG tester method for higher level of amputations like trans-humeral amputees and special cases such as TMR patients. Fig. 1.3. summarizes the various methods of electrode placements for a pattern recognition based prosthetic control system.

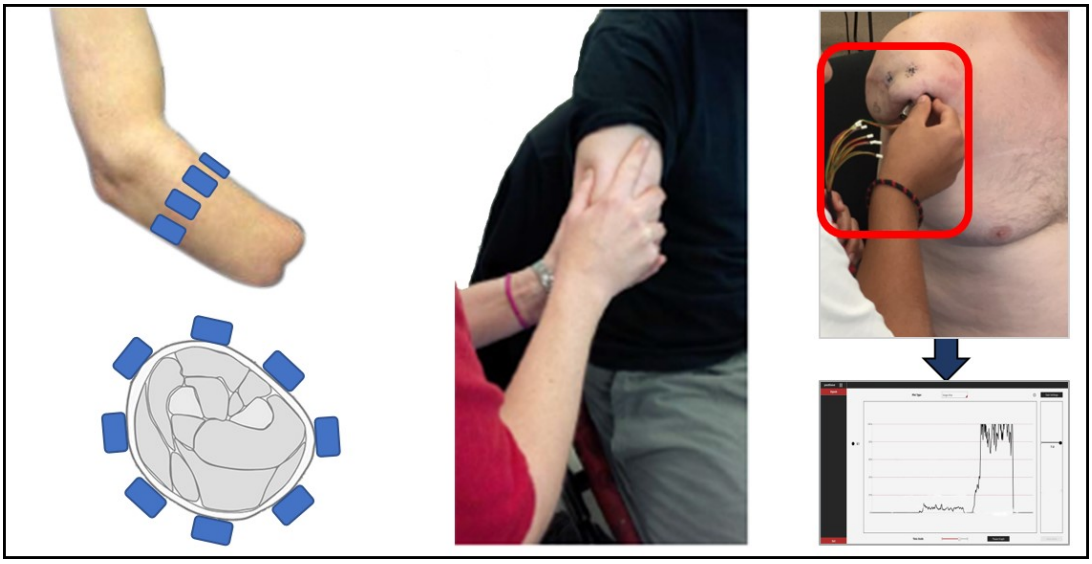

Fig. 1.3. a) Conventional electrode placement for trans-radial amputation: Electrodes are equally spaced along the circumference of the forearm. b) Myosite selection for targeted electrode placement: 1) Palpating residual limb for myosite selection 2) EMG tester method -Testing signals with differential electrode placed on the myosite and Visualizing EMG signals to select sites with maximum amplitude.

Fig. 1.4 depicts a flowchart of the conventional process of site selection performed on a trans-humeral amputee at Infinite Biomedical Technologies (IBT, Baltimore). First, the residual limb is palpated to find regions of high muscle activity during contraction. Then a socket electrode (in this case, IBT element electrode) is placed in this region. The electrode is then moved in all directions from the starting location to find the optimum site where the signal amplitude is maximum. This spot is then marked for future use. The biofeedback used here is Infinite Biomedical Technology (IBT)'s Element^{TM} graphical user interface. This is used to visualize the real time amplitude of the EMG signal during contraction.

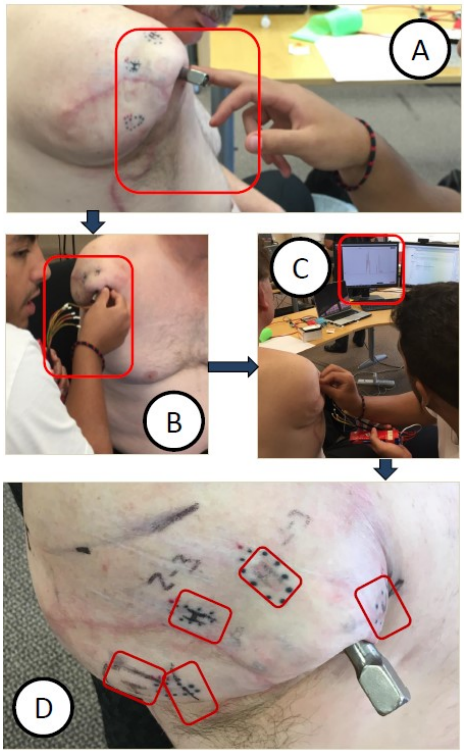

Fig. 1.4. Conventional process of myosite selection for trans-humeral amputee: (a) Palpating residual limb with finger to locate myosite (b) Testing signals with differential electrode placed on the myosite selected by manual palpation (c) Visualizing EMG signals (c) Selected location with high muscle activities marked on residual limb.

Recently, researchers have used high-density surface EMG (HD sEMG) electrodes to visualize muscle activity of a residual limb [25], [26]. These are densely arranged EMG electrodes that can be used to study the muscle activity of different regions of the residual limb simultaneously. There have also been works that have used HD sEMG electrodes for identifying best control sites [25]-[33] and these have been discussed in detail in chapter 2.

1.2.8. Thesis Overview:

It is evident from the above sections that the quality of EMG signal plays an important role in deciding the performance of a myoelectric prosthesis. Myosite selection is hence a crucial step in the prosthetic fitting process. However, this step as of today is highly dependent on the skills and experience of the clinicians involved in the prosthetic fitting process. Hence, there is a need to automate the process of site selection and to introduce a more quantitative signal analysis approach. This would in turn improve the quality of signals used to drive the myoelectric prosthesis improving the performance of the same. There is also a need to account for consistency in electrode contact within the prosthesis, reducing motion artifacts and electrode lift offs that can affect the quality of the signal. The aim of this thesis is to

use the state-of-the-art technologies to help satisfy the user need of (a)making the myoelectric prosthesis perform more consistently and reliably to help improve their quality of life, (b)making the pattern recognition system adaptable to include more functionality without compromising performance. This thesis is projected to have a clinical impact that would not only standardize the process of myosite selection for prosthetic fitting, but also make it less time consuming and more efficient. At the end of this work we intend to have an off-the-shelf system that can be used with any control strategy and with people with any level of amputation.

There have been various works that uses different algorithms with different type of electrode placements to perform myosite selection and to examine best myosite configuration. These are reviewed in chapter 2. The custom designed high-density surface electromyography (HD sEMG) array along with the study design to quantify motion artifacts is presented in Chapter 3. Chapter 4 illustrates how high density (HD) sEMG is used in myosite selection and its effect on improving prosthetic functionality. The possible future directions are discussed in chapter 5, concluding the thesis.

Chapter 2: Limitations with pattern recognition based myoelectric prosthesis and current electrode placement methods

Surface EMG signals have long been a major means of controlling electrically driven prosthesis, especially upper limb. A myoelectric upper limb prosthesis, with a pattern recognition based control system, is the closest to the maximum function that an amputee can perform with a prosthesis. This is especially true, if the amputee is bilateral or has a lot of ADL involving basic grips that a commercial myoelectric prosthesis has to offer. However, there have been a lot of functional limitations and practical issues that are still hindering some of the state-of-the-art research related to pattern recognition based myoelectric prosthesis control from becoming a reality. There has also been a lot of research that compares and evaluate different kind of electrode placements and machine learning algorithms and combinations of those to arrive at optimal performance for a myoelectric pattern recognition based prosthesis system [25]- [33].

For a pattern recognition system to perform well the patterns under consideration should be consistent and distinguishable [34]. It is, thus, necessary not only to identify the high intensity signal sources but also to identify the sites that produce co-contractions during a movement class which are unique to that movement class. The ability to simultaneously visualize the muscle activity from various regions of the residual limb will be highly useful in achieving best results for selecting such unique sites for pattern recognition based control. HD sEMG technology has also been used in the recent times to study muscle activity patterns visually using image [25], [26]. Some of the previous works that investigated optimal electrode placement that uses both low-density and high-density

sEMG electrodes and different machine learning algorithms are reviewed here in this chapter.

2.1. Review of different electrode locations used for pattern recognition based myoelectric prosthesis control.

2.2.1. Conventional electrode placements and no site selection:

Farrell and Weir performed experiments [35] to study the effects of targeted vs untargeted surface vs implanted EMG electrodes. The movement classes under consideration for this study included mostly gross movements (except finger point): (A) Wrist flexion. (B) Wrist extension. (C) Pronation. (D) Supination. (E) Hand open. (F) Palmar prehension. (G) Radial deviation. (H) Ulnar deviation. (I) Lateral prehension. (J) Power prehension. (K) "Point." (L) "Hand flat". They used 8 bipolar surface electrodes to study surface electrode location effects. The placement of these electrodes in targeted and untargeted configurations is shown in Fig. 2.1(a) and 2.1(b) respectively. They showed that there is not much difference in the performance of pattern recognition with targeted surface EMG electrodes vs equally spaced surface EMG electrodes. They used the EMG tester method to identify the sites that produced high intensity EMG signals during each movement class. The method of site selection employed, for placement of targeted surface electrodes, here was subject to the skills of the clinician involved in selecting sites. Also, this study involved

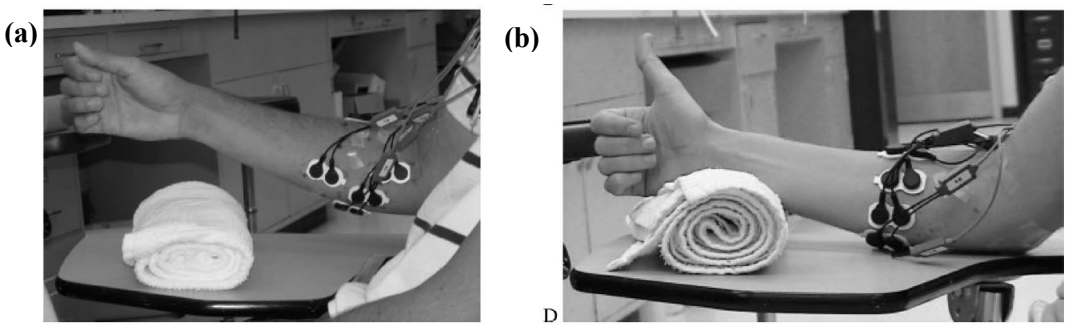

Fig. 2.1. Electrode configuration used in Farrell and Weir's work: (a) Targeted surface electrode placement, (b) untargeted surface electrode placement [35].

only able-bodied subjects and hence arriving at any generalization that can be applied to people with amputations is difficult.

The first work presented in decoding individual finger movements in amputee subject was presented in 2009 by Tenore et al. [36]. Five able bodied and 1 amputee subject were recruited in this study. They demonstrated the ability to decode 10 finger movements (individual fingers flexion and extension) with greater than 90% accuracy in a trans radial amputee subject using surface EMG technique. They used different number of electrodes with different levels of amputation as shown in the figure below (Fig. 2.2 (a)). They used up to 32 bipolar electrodes placed on the subject's limb based on SENIAM recommendations [37]. The subjects performed 12 finger movements namely, flexion of each individual finger, extension of each individual finger, flexion of middle, ring and little group (MRP-middle ring pinky) and extension of MRP group. The performance accuracy of decoding varied with the level of amputation as well. This is shown in the tabular column in Fig. 2.2 (b). In the tabular column shown below, subject B refers to the trans radial amputee. With the use of 19 channels, they were successful in demonstrating an accuracy of 82%-87% with four time-domain features. One of the important points to note here is that most of the movement classes involved in this study physically recruit very different muscles and thus the chances of misclassification is very less. Wrist and precision grip classes were not involved in this study.

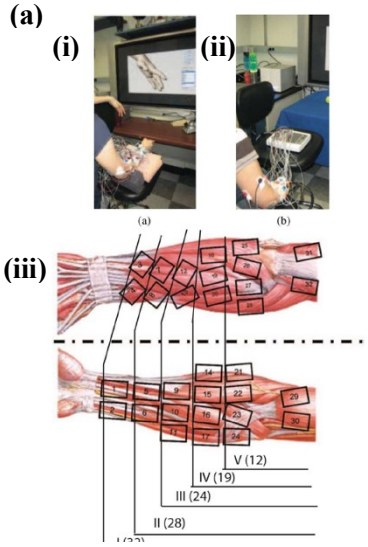

(b)

TABLE I
SUMMARY OF DECODING ACCURACY FOR ALL SUBJECTS (IN PERCENTAGE)

Subject	No. elec. (Level)	Feat.	Acc.	Subject	No. elec. (Level)	Feat.	Acc.
A	32 (I)	MAV	98.8±1.1	D	32 (I)	MAV	92.5±6.4
		Var	98.8±0.9			Var	90.9±8.4
		WA	98.6±2.5			WA	84.9±4.6
		WL	99.7±0.3			WL	95.0±6.1
	19 (IV)	MAV	98.3±2.1		19 (IV)	MAV	88.8±9.4
		Var	98.1±2.3			Var	87.8±10.0
		WA	98.0±2.7			WA	80.0±13.0
		WL	99.1±1.3			WL	94.3±5.7
B	19 (IV)	MAV	82.3±15.7	E	32 (I)	MAV	92.1±5.8
		Var	83.8±13.1			Var	86.9±8.2
		WA	83.3±14.8			WA	91.4±6.0
		WL	87.8±12.3			WL	93.5±3.6
					19 (IV)	MAV	88.9±7.4
						Var	81.6±16.7
						WA	87.5±8.9
						WL	91.5±6.4
C	32 (I)	MAV	88.8±8.0	F	32 (I)	MAV	89.2±7.5
		Var	87.7±8.0			Var	86.4±7.1
		WA	86.9±9.8			WA	89.4±6.9
		WL	93.6±6.2			WL	89.6±5.1
	19 (IV)	MAV	84.4±10.9		19 (IV)	MAV	89.2±5.9
		Var	84.8±11.2			Var	85.6±6.5
		WA	86.9±11.8			WA	89.2±6.2
		WL	92.7±7.6			WL	89.1±5.7

Fig. 2.2. Electrode configuration and results from Tenore et al.'s work (a) Experimental setup for (i) able bodied subject (ii) amputee subject (iii) approximate location of electrodes as a function of level of amputation [36], (b) Summary of decoding accuracy for all subjects [30].

In 2013, Al-Timemy et al. [38] used 12 channels of bipolar electrodes to decode up to 15 finger movements, namely, little finger flexion and extension (f1, e1), ring flexion and extension (f2, e2), middle flexion and extension (f3, e3), index flexion and extension (f4, e4), rest position, thumb flexion and extension (f5, e5), thumb abduction (a5). The other movements included finger combinations and these were included only in the data gathering for able-bodied subjects: little and ring fingers flexion (f12), flexion of the ring, middle, and index fingers (f234); flexion of the little, ring, middle, and index fingers (f1234). The amputee persons performed 12 movement classes, whereas the able-bodied subjects performed 15 movement classes. Electrodes were placed in two rows around the circumference of the forearm as shown in Fig. 2.3. (a). Two types of feature reduction and 2 types of classification algorithms were used and hence 4 combinations of algorithms were used on the data for classification and were compared. Error rates for able-bodied and amputee subjects with 5,9,12(common to able bodied and amputees) and 15(only for able

bodied) movement classes were presented which is shown below in Fig 2.3.(b). Also, 11 EMG features were used for this study.

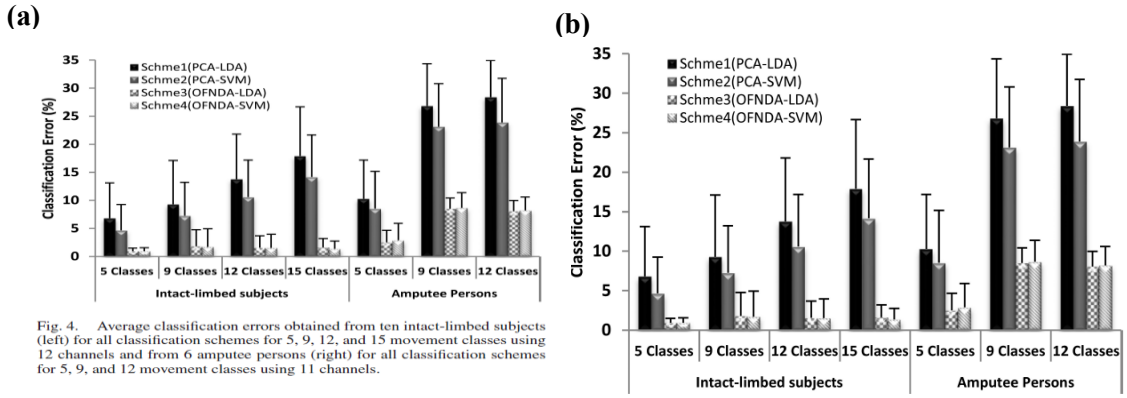

Fig. 4. Average classification errors obtained from ten intact-limbed subjects (left) for all classification schemes for 5, 9, 12, and 15 movement classes using 12 channels and from 6 amputee persons (right) for all classification schemes for 5, 9, and 12 movement classes using 11 channels.

Fig. 2.3. Results from Al-Timemy et al's work: (a) Electrode placements (i) anterior view of forearm (ii) posterior view of forearm [38], (b) average classification errors [38].

2 feature reduction techniques, namely, principal component analysis(PCA) [39] and orthogonal fuzzy neighborhood discriminant analysis (OFNDA) [40] were used for feature reduction with linear discriminant analysis (LDA) and support vector machine(SVM) as classifiers. All 4 possible combinations were tested to arrive at best possible algorithm. This experiment showed that with increase in number of classes for classification, the error rate increased. Also, the error rates are higher in amputee subjects when compared to able-bodied subjects. The performance accuracy obtained for the 12 individual finger motions in the 6 amputee subjects was 90.57%. Gross movements like hand motions and precision grips were not included in the study. Including this along with the finger motions could drastically reduce the performance numbers. The number of EMG features used were also high.

Fang et al. [41] proposed a new generic electrode configuration to reduce the interferences due to electrode shift. This configuration was called zig configuration and was compared to conventional placement of 2 rows of 8 electrodes around the circumference of the forearm. The representation of the 2 configurations tested are shown in Fig. 2.4.(a) and 2.4.(b).

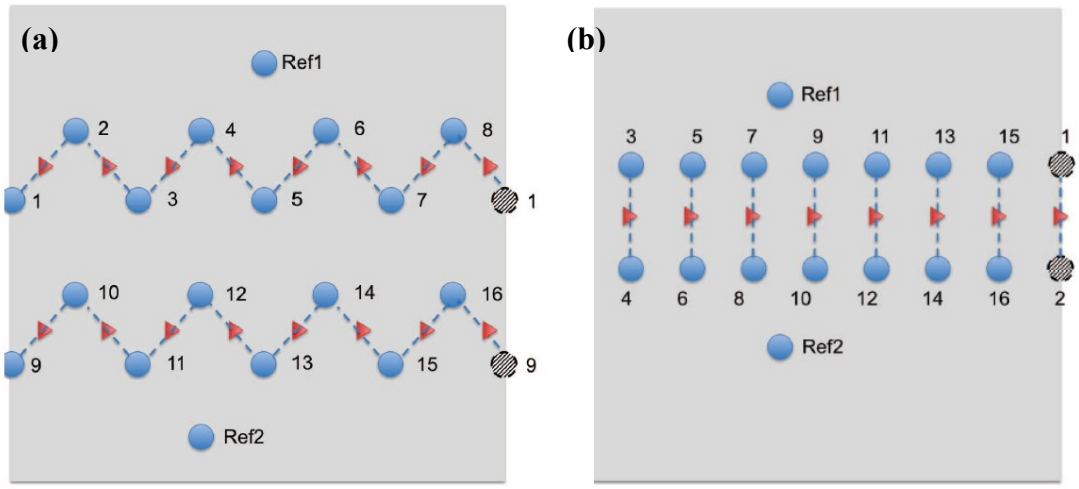

Fig. 2.4. Electrode configuration used in Fang et al.'s work: (a) Zig-zag configuration [41], (b) traditional sEMG configuration [41].

Only two able-bodied subjects were considered for this study. Ten hand motions included in the study were: Hand-Close, Hand-Open, Wrist-Flexion, Wrist-Extension, Supination, Pronation, and using thumb to touch index finger, middle finger, ring finger and little finger. Classification was performed using kNN and LDA classifiers. Results showed that hand motion recognition accuracies were improved by 4% when using kNN and 8% when using LDA classifiers. However, the number of subjects included in the study was small and no amputee subjects were included.

Similarly, Castro et al. [42] decoded 5 finger movements and 5 grasp patterns with 5 pair of electrodes with an average accuracy of 80%. The electrode placements that they used were based on standards for low density electrode placements [43]. Signals were recorded from forearm muscles: flexor digitorum superficialis, palmaris longus, abductor pollicis longus, extensor digiti minimi and extensor communis digitorum. Fig. 2.5. shows the placement of these electrodes.

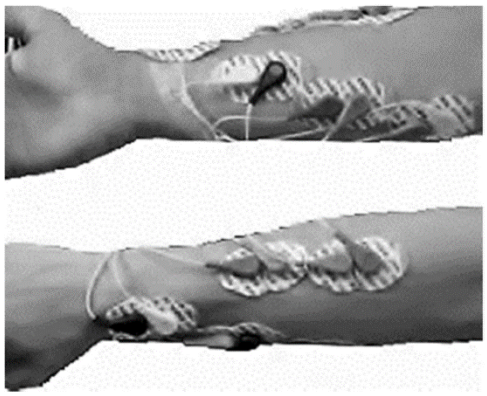

Fig. 2.5. Electrode configuration used in Castro et al.'s work: (Top) Targeted electrode placements [42] (Bottom) traditional sEMG configuration [42].

Their study was aimed at sub-selecting highly performing classes to improve the average accuracy, sensitivity and specificity of the system that they proposed, which was based on a metric called positive- negative performance measurement index(PNM). They showed that accuracy, sensitivity and specificity increased from 80%, 80% and 97.8% to 96.5%, 96.5% and 99.3% respectively. However, this was validated only in able-bodies subjects. Also, the true goal of pattern recognition system is in including more functionality and hence there is a need for a system to adapt to increased functionality.

In another work, Mayor et al. [44] showed successful recognition of dexterous gestures using only 4 electrode pairs on amputees with different classifiers and features selected from the data. The locations of the electrodes used in this study are shown in Fig. 2.6. These electrodes were placed in accordance with the movement classes considered for the study, namely, individual finger movements, which included thumb flexion (F1), index flexion (F2), middle flexion (F3), ring flexion (F4), little flexion (F5), hand close (HC) and hand

open (HO); hand grasps, which included large diameter(LD) and medium diameter(MD) hand grasps, lateral grasp (LT), tripod grasp (TR) and tip pinch (TP).

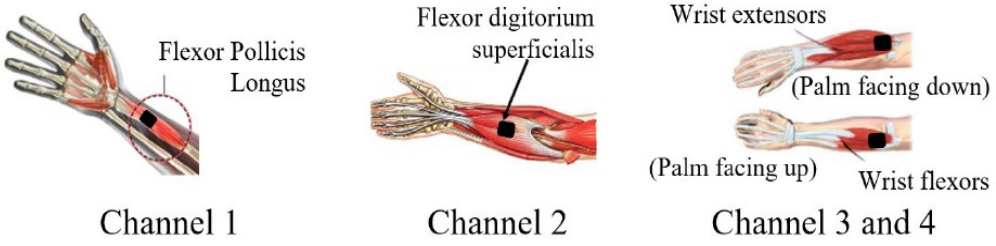

Fig. 2.6. Electrode configuration used in Mayor et al.'s work: Targeted electrode placement of 4 bipolar electrodes [44].

This experiment was conducted on 10 able bodied volunteer and 10 trans-radial subjects. However, the emphasis of their work on how using different features and different classification algorithm improved average accuracies from using baseline of using LDA algorithm. The results showed that for all task categories, SVM showed the best performance, followed by KNN and LDA, respectively.

2.2.2. Conventional placements with site selection algorithm:

Fukuda et al. [45] conducted a study to prove discrimination capabilities of a novel statistical neural network called log-linearized Gaussian mixture network (LLGMN). For this study, only gross motion classes were included namely (E) extension, (F) flexion, (UF) ulnar flexion, (RF) radial flexion, (S) supination, (P) pronation, (HO) hand open, and (HG) hand grasp. The number of EMG electrodes used were 6. The electrode placements were based on precise anatomical positions. For able bodied subjects, the anatomical locations were ch. 1 Flexor Carpi Radialis; ch. 2 Flexor Carpi Ulnaris; ch. 3 Pronator Teres; ch. 4 Supinator; ch. 5 Biceps Brachii; ch. 6 Brachialis muscles. For amputee subjects, the muscle locations included four electrodes (ch.1–4) on the muscles near the amputated part, and two electrodes on the upper arm muscles (ch. 5 Biceps Brachii, ch. 6 Triceps Brachii).

Since the anatomical locations were precise in this study, the drawbacks of such electrode placements include, 1) electrode positions are fixed and cannot be changed over time with practice, 2) electrode positions need alterations with different level of amputations, 3) the electrode locations does not take into account the extent of damage or level of activity retained in the residual muscles.

Li et al. [46], in 2010, performed studies on intact and amputated arms of trans-radial amputee subjects to evaluate real-time control of virtual arm by the subjects. 12 self-adhesive bipolar snap electrodes were positioned on the arm. For the amputated arm, 8 of the 12 electrodes were uniformly placed around the proximal portion of the forearm over the apex of the muscle bulge (2–3 cm distal to the elbow crease), and the other 4 electrodes were positioned on the distal end, as illustrated in Fig. 2.7.(a). For intact arm, the electrode locations were: 6 bipolar electrodes around the apex of the muscle bulge, (2–3 cm distal to the elbow crease), the wrist (3 around, 2–3 cm proximal to the wrist crease), and the hand (the thenar, first dorsal interosseous, and hypothenar muscles), as illustrated in Fig. 2.7.(b). They collected sEMG signals for 10 movement classes which included wrist flexion and extension, wrist pronation and supination, hand open, and 5 hand-grasp patterns including chuck grip, key grip, power grip, fine pinch grip, and tool grip.

For classification, they used LDA algorithm and 4 sEMG TD features namely, mean absolute value, number of zero crossings, waveform length, and number of slope sign changes. They also studied the performance of optimal sets of electrodes from the 12 bipolar pairs. They used a straightforward exhaustive search algorithm to arrive at optimal set of channels. They showed that 6-8 electrodes were able to produce comparable classification accuracies for all 10 classes. They concluded that the muscles in the residual

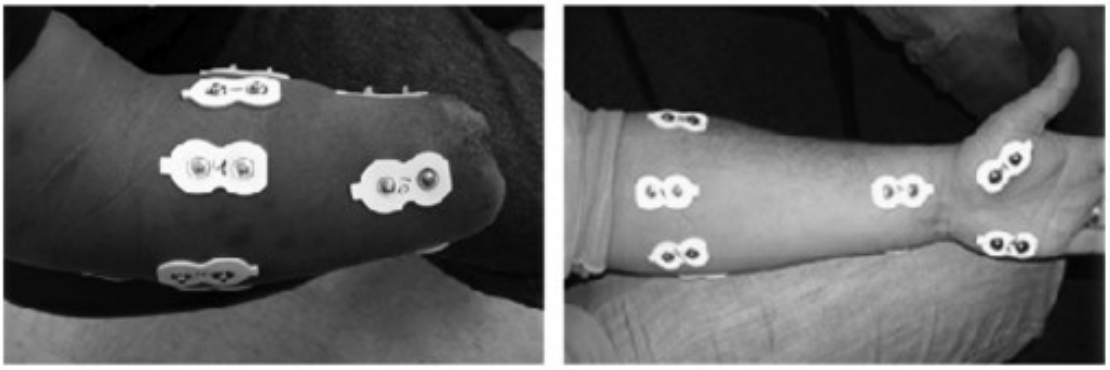

Fig. 2.7. Electrode configuration used in Li et al.'s work: Untargeted electrode placement (a) on the residual limb of an amputee (b) on an able-bodied subject's arm [46].

limb of the amputated arm could produce quality sEMG signals to control wrist(gross) movements but the signals for grasp motions were not of comparable quality. Hence, there is a need to include grasp movement classes for prosthesis control without compromising the performance of the system.

2.2.3. HD sEMG with site selection algorithm:

Huang et al. [27] performed experiments with 4 TMR subjects (3 trans-humeral subjects and 1 shoulder disarticulation subject). The aim of their study was to investigate the optimal number and placement configuration to obtain sufficient amount of information to control 16 movement classes: namely, elbow flexion/extension, wrist flexion/extension, pronation/supination, and hand open/close, thumb adduction/abduction, thumb flexion/extension, index finger flexion/extension, and third/fifth finger flexion/extension. They compared 3 different electrode placement configurations for a 16 movement class and 8 movement class classification. Amongst this, the electrode configuration that was setup by selecting a subset of optimal channels from many available electrode channels

was called as suboptimally selected channels. 1) Configuration 1: Suboptimal selection: For this they used a HDEMG system along with a Sequential Forward Selection (SFS) algorithm. 2) Configuration 2: Geometrical configuration: Approximately equally distributed electrodes on the residual limb. 3) Configuration 3: Clinical configuration: Electrodes placed on re-innervated sites, based on the clinical knowledge of the TMR surgery performed on the subject. The images of the system they used along with the practical configurations and suboptimally selected electrode configurations are shown in Fig. 2.8 (a) and 2.8 (b) respectively. Their results showed that for 12 sub-optimally selected channels, performance accuracy for 16 movement classification was 93±3.3%. For clinical placements, it was 88.7±4.5% and for geometrical placement it was only 72.9%. The result graphs from the study is shown in Fig. 2.8. (c). This study was performed on TMR subjects, who are in a sense best scenario cases since the residual muscles are re-innervated in a favorable fashion. There is a lack of such studies on amputees without TMR, where

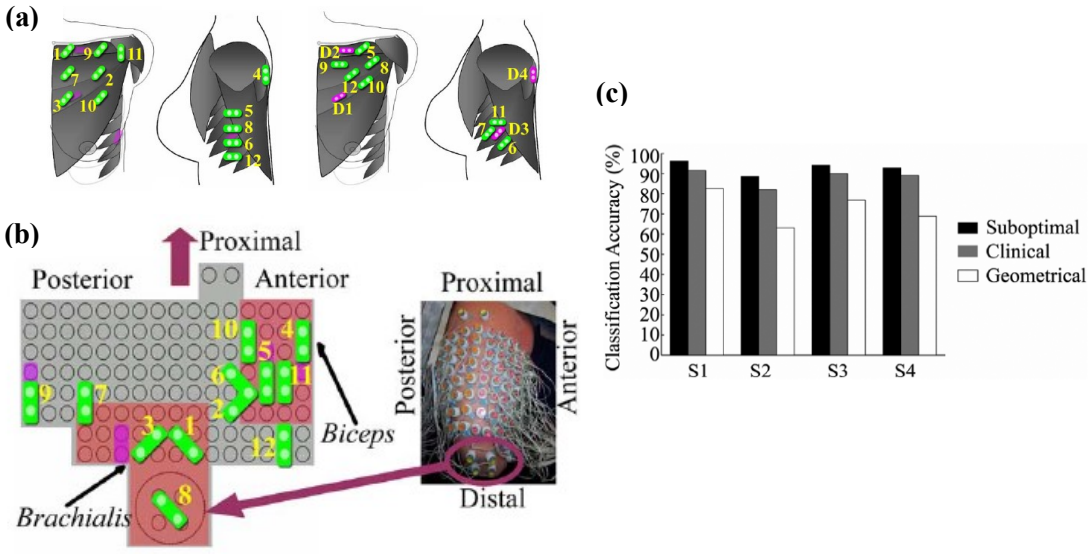

Fig. 2.8. Electrode placements and results from Huang et al.'s work [27]: (a) geometrical and clinical configuration of electrode placements, (b) sub-optimally selected electrode configurations shown by green markings and direct control sites shown by purple markings for reference, (c) classification accuracies of the 3 different electrode configurations for four subjects [27].

identification of optimal sites is more difficult since there is minimal knowledge on the capabilities of the residual muscles.

In 2011, Li et al. [28] studied how different signal processing methods (different filtering cut off frequencies) could affect the performance accuracy of pattern recognition system. In an attempt to demonstrate this, they used a 12 electrode bipolar sEMG system on 5 able-bodied subjects and 8 amputee subjects, of which 5 were trans-radial (TR) amputees and 3 were shoulder disarticulation(SD) subjects. One of the shoulder disarticulation subject had a TMR surgery done as well. The electrode placements they used were different for able-bodied, trans-radial and SD subjects. The electrode placements for SD subjects were loosely based on Huang et al.'s work [27] which is also reviewed in this chapter.

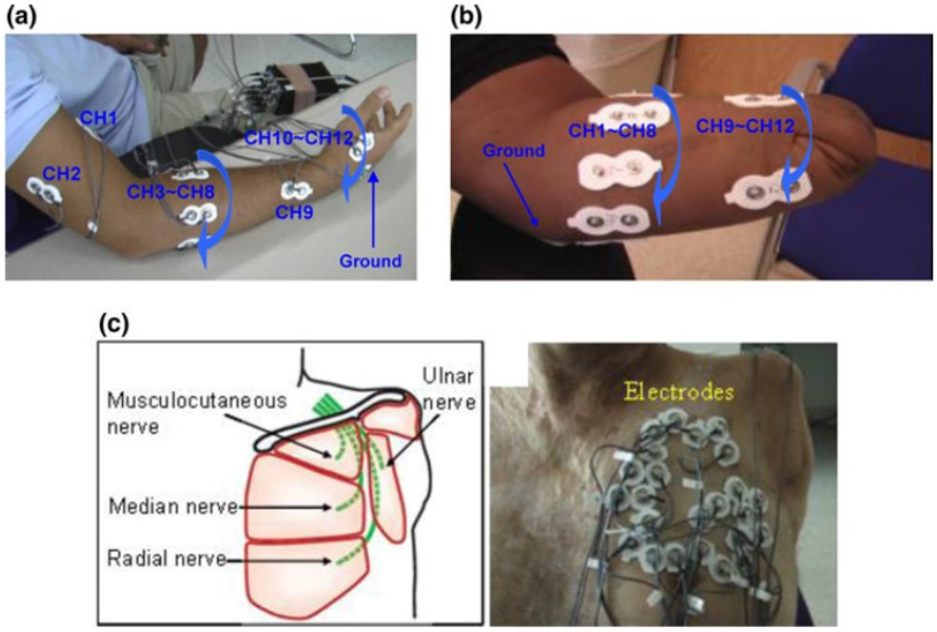

Fig. 2.9. Electrode configuration used in Li et al.'s work: Twelve bipolar electrode placements for (a) able-bodied subject (b) trans-radial amputee subject (c) shoulder disarticulation subject [28].

Fig. 2.9 shows the different electrode placements used in this study, for different levels of amputations. They used 4 TD features for classification with LDA algorithm was used. The best results obtained was an average performance accuracy of 97.5% for able-bodied subjects, 71.3% for TR subjects and 88.2% for SD subjects. The drawback in this work is that the electrode placement system was not uniform across all subjects which might have contributed to the classification accuracy values. According to their results, SD average classification accuracy was higher than TR, which might be because of the different electrode placement systems followed or inclusion of a TMR subject. TMR subjects tend to have a higher classification accuracy due to the better knowledge of correlation of muscle activity with the residual muscles. This was evident from Huang et al's work [27]. Hence, there is a need to have a standardized, quantitative method of electrode placement system, in order to compare performances of people with difference levels of amputation.

Tkach et al. [29] performed studies with 2 TMR patients with trans-humeral amputation. They demonstrated that untargeted placements of electrodes perform better than targeted placements for TMR patients. They tested 2 conditions:1) Targeted placements: Electrodes placed on 4 DC sites and 4 additional sites based on recommendations by Huang et al. 2) 15 electrodes placed in 3 rows around the circumference of the residual limb. These configurations are shown in Fig. 2.10.(a) and 2.10.(b). 15 Bipolar combinations were derived from these electrodes. 9 movement classes were included in this study: wrist pronation, wrist supination, wrist flexion, wrist extension, hand open, hand close, elbow flexion, elbow extension and rest. They used 4 TD features along with AR features for classification using LDA classifier.

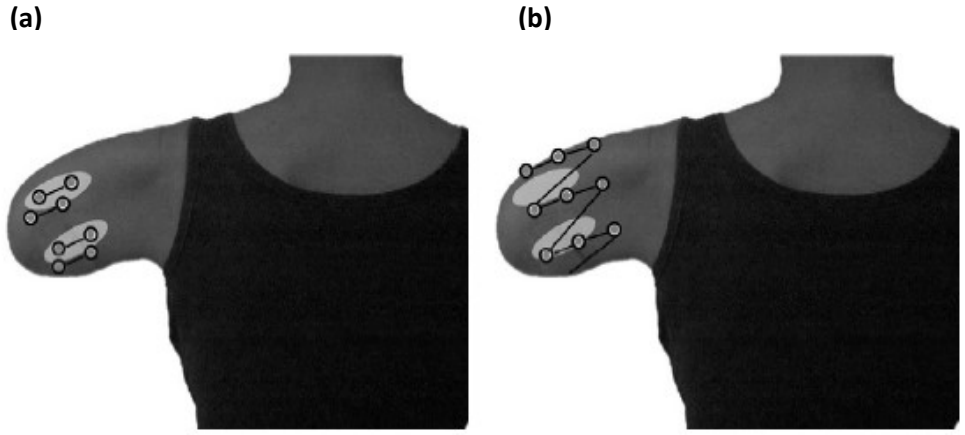

Fig. 2.10. Electrode configuration used in Tkach et al.'s work : Electrode placements in (a) clinical configuration targeting reinnervated sites, (b) grid configuration [29].

Their results show that least error was obtained in grid configuration and highest error was seen in the 4 DC site configuration. This is represented from the Fig. 2.11 (a). They also performed channels reduction to reduce computational cost and their results showed that a subset of 7 channels from the grid were needed to reach error plateau as shown in Fig. 2.11(b).

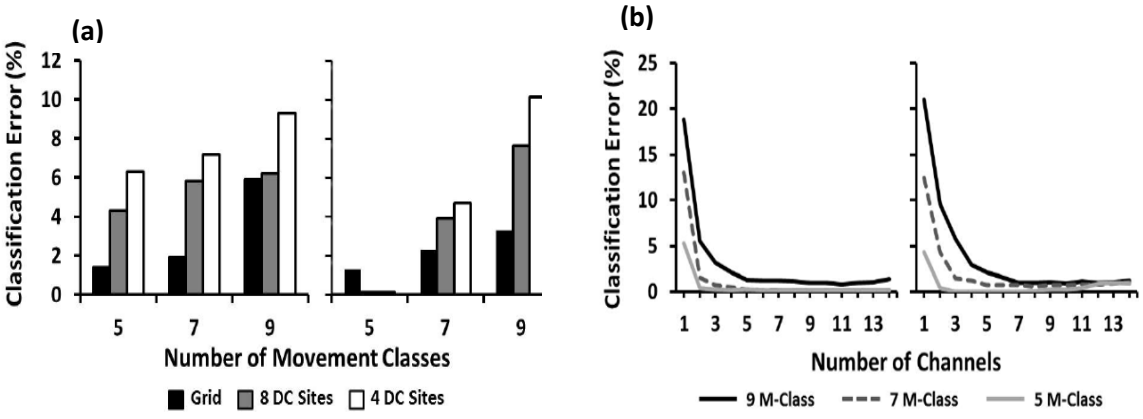

Fig. 2.11. Results from Tkach et al.'s work: (a) Classification error percentages for the 3 electrode configurations with increase in number of movement classes, (b) Classification error percentages for the 3 electrode configurations with increase in number of selected channels [29].

This study, in a way, conveys that the best electrode sites for PR are not conventional targeted placements (which pick up high intensity signals). This also introduces the idea that electrode sub-selection provides a more quantitative way of arriving at optimal electrode locations for PR.

Daley et al. [30] conducted a study using HD surface EMG electrodes to show that individuals can perform distinguishable muscle patterns and to show that HD sEMG can be used to determine optimal electrode locations. They used sequential forward selection method based on classification performance of the channels to select 8 optimal channels. Their work showed that optimally selected channels performed significantly better than equally spaced electrode channels for able-bodied subjects. They also concluded that there was no significant difference in classification performance when the electrodes were reduced to 8 in amputee subjects, irrespective of whether they were placed optimally or distributed equally. To obtain best results, they optimized the number of classes that a subject can perform best and showed that the amputee subjects were able to perform only 4-6 classes with a classification accuracy better than 80%. However, the ultimate goal of pattern recognition based control system is to increase the number of movements that an amputee can perform.

Another related work that presented a novel method of channel and feature reduction for gesture recognition was the work of Mesa et al [31] in 2014. They used 32 sEMG electrodes, placed in 4 rows of 8 electrodes each around the forearm as shown in Fig. 2.12 86 EMG features were considered for this work. They used a feature selection method called mRMR-FCO with an SVM classifier. The gestures included for classification were 14 hand gestures pertaining to sign language for alphabets A, B, C, D, E, I, K, L, N, O, P, Q, R, U. Seventeen able-bodied subjects participated in the study. The channels and features from the data collected were ranked based using their algorithm and best channels and features were selected based on maximum number of occurrences of a channel or feature in the top 50 channel-feature combination rank list. Seven best electrode locations selected by the system were {A6, A5, A4, D6, C6, B6, B1}. The selected locations consisted of a combination of site around and along the forearm. This result also is in agreement with Daley et al.'s [30] work.

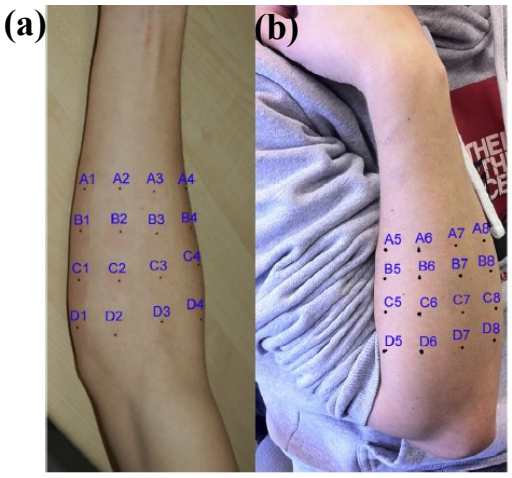

Fig. 2.12. Electrode configuration used in Mesa et al.'s work: Placement of 32 electrodes distribute as 4 rows of 8 electrodes each. Figure shows (a) anterior forearm, (b) posterior forearm [31].

Their results showed that, for a given set of gestures, best information can be obtained from the reduced electrode locations and feature. This puts forward an important point for consideration that the best signal source is specific to the nature of selected movements. Another important point of discussion from their work is that the muscles proximal to the wrist are more superficial, whereas those distal to the wrist have more cross-talk. The sites

selected in the work included sites in the middle region indicating that cross-talk is a desirable feature for classification. Their study showed a performance accuracy of 86.4%, however, it was performed only on able-bodied subjects.

In 2014, Geng et al. [32] performed a comparative study of two types of electrode number and location optimization algorithms namely, SFS and FMS. They also introduced a novel algorithm called multi class common spatial pattern. Twelve mildly-impaired traumatic brain injury patients participated in the study. A set of 21 forearm and hand movements were considered in the study. HD sEMG electrode system from Refa-128 (TMS International BV, Netherlands) that consisted of 56 monopolar contacts were used in the study, placement of which is shown in Fig. 2.13(a).

All 3 algorithms were applied on both monopolar and bipolar electrode configurations of the system. 18 optimal electrodes were set as the number of electrodes for performance comparison purposes. The results indicated that the best combination of feature-classifier was TD-KNN when MCCSP based electrode selection algorithm was applied. The classification accuracy values with the selected number of channels from 1-18 using the optimal algorithm combination is shown in Fig. 2.13(b). Also, MCCSP selected same

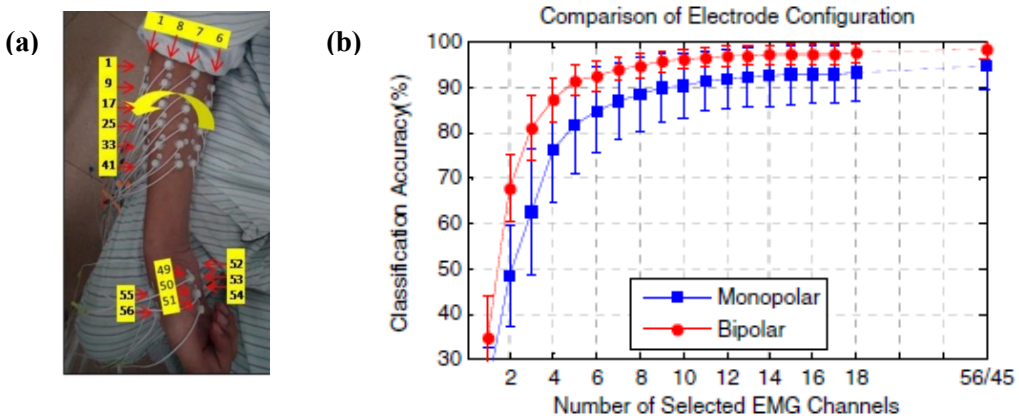

Fig. 2.13. Electrode configuration used in Geng et al.'s work (a) Refa-128 HD sEMG electrodes, (b) graph showing classification accuracy with increase in number of selected channels [32].

channels irrespective of which classification algorithm was selected, unlike the SFS and FMS methods.

Paleari et al. [33] performed studies using flexible HD sEMG channels to arrive at best possible generic electrode placements which does not need the involvement of specialist for electrode localizations. They used OtBioelecttronica^{TM} (OT Bioelettronica s.r.l., Toronto) electrodes with 192 electrode contacts for sEMG data acquisition. 8 able-bodied subjects were asked to perform 11 movements for the study, namely, wrist flexion, extension, abduction and adduction, all fingers- flexion, extension, wrist and finger combination- flexion, extension, abduction and adduction with an object in hand.

Levenberg-Marquardt feed-forward back-propagation artificial neural network (ANN) was used for classification.

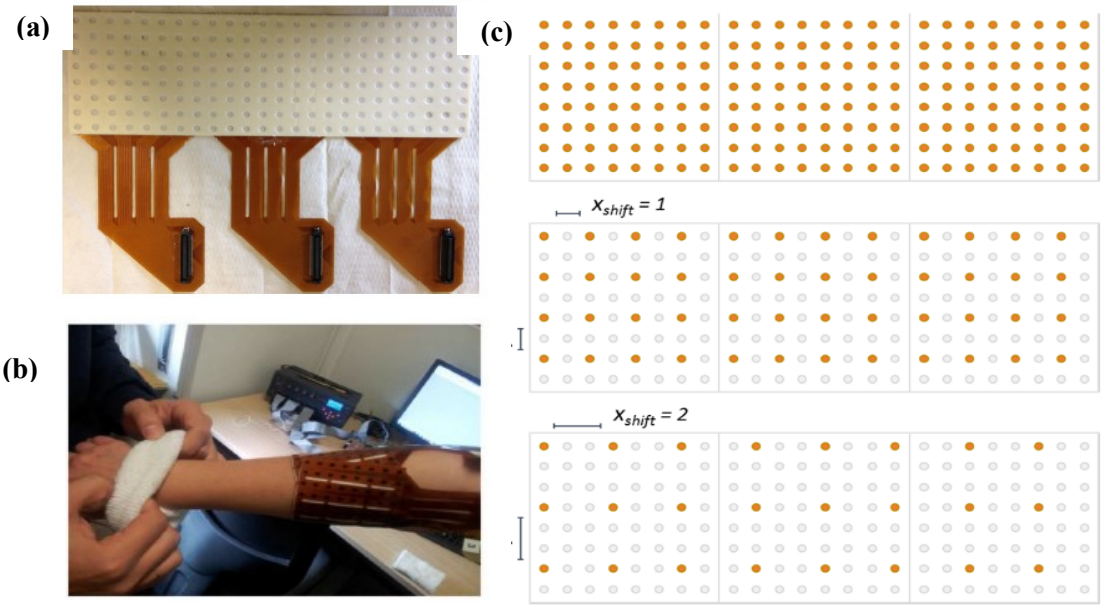

Fig. 2.14. Electrode configuration used in Paleari et al.'s work: (a) OtBioelecttronica^{TM} electrodes with 192 electrode contacts, (b) Electrode setup on forearm of the subject, (c) examples of resampled electrode matrices considered for testing [33].

They tested different electrode configurations, all of which were regular symmetrical matrices. All possible symmetrical configurations by skipping sites on x direction and y direction were tested. It was observed that reduction in number of electrodes in medio-lateral direction affected the performance more than in proximo-distal direction.

They also concluded that 16 electrodes placed in 2 rows as far away from each other as possible on the first third of the forearm provided the closest result to using all 192 electrodes. However, the drawbacks of the study were that only symmetrical combinations were tested, amputee subjects were not included in the study, and grips/individual finger movements were not included.

Celadon et al. [25] investigated the methods for selective estimation of individual finger movements with the least possible amount of interference from the other fingers using HD sEMG signals. Nine healthy subjects participated in the study and 4 individual finger flexion and extension, and no movement classes were included in the study. They

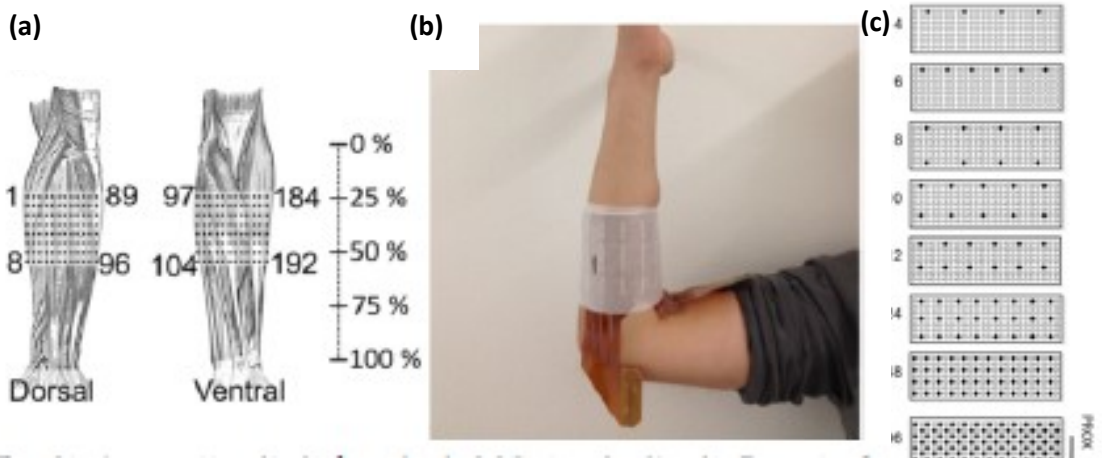

Fig. 2.15. Electrode configuration used in Celedon et al.'s work: (a) Distribution of 192 electrode contacts on the forearm, (b) Electrode setup on forearm of the subject, (c) examples of resampled electrode matrices considered for testing [25].

compared the performance of 3 types of classification algorithm: 2 Machine learning algorithms: LDA and Common spatial patterns proportional estimator(CSP-PE) and a thresholding algorithm(THR) for direct control classification. HD sEMG electrodes from Ot Bioelectronica^{TM} with 192 channels was used in this study, distribution and positioning of which is shown in the Fig. 2.15 (a) and 2.15 (b). Different symmetric combinations of electrode numbers were tested, namely, 192, 96, 48, 24, 12, 10, 8, 6 and 4 and these are shown in Fig. 2.15 (c).

Results showed that the performance of all 192 electrodes vs 10 reduced electrodes did not show much difference in performance pertaining to the individual finger movement classes. Though this study shows compelling results, it considered only symmetric combinations of electrode locations and finger movement for classification. As stated earlier, inclusion of both gross and finger movement classes introduces more error rates in classification, which is a significant hindrance to improving functionality of a pattern recognition based control system.

Recently, Geng et al. [26] presented the concept of using HD sEMG spatial images at a specific instant of time for gesture recognition with classification using deep convolution

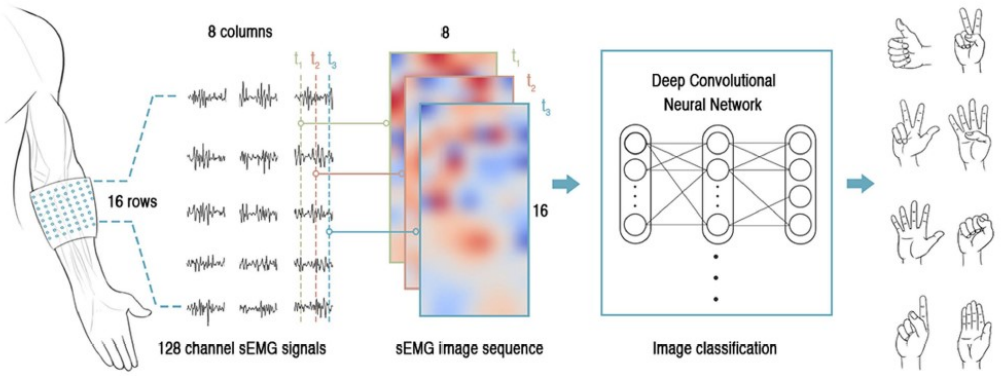

Fig. 2.16. Schematic representation of gesture recognition by instantaneous sEMG images [26].

network. Here data from all 128 channels were used to produce image sequences for image based classification. There was no channel selection or channel reduction performed prior to classification. Their system demonstrated 89.3% accuracy on 8 gestures with a single frame recognition system and 99% accuracy with 40 frames at a 1000Hz sampling rate. This is the state of the art with respect to gesture recognition based on surface EMG. A schematic illustration of this system is shown in Fig. 2.16.

This system was validated by NinaPro and CSL-HDEMG databases as well. These kind of image recognition based system might be much faster than the current data-based recognition systems. However, this study was performed only on able-bodied subjects and further investigation would be needed in justifying the extent of validity of the system with amputee subjects.

2.2. Summary

The above literature review clarifies that the number and position of electrodes along with the classification algorithms used play a major role in deciding the effectiveness of the pattern recognition system as a whole. Most of the above mentioned works follow the SENIAM standards for electrode placement [37] to decide which muscles are chosen for the placement of the electrodes. Unlike in direct control systems, pattern recognition system needs careful selection of myosites, since, unique activation sites associated with each type of motion is of high importance. Unlike in a direct control problem where co-contraction is considered cross-talk or undesired signal, co-contractions are the source of generation of desirable “patterns” that are required to train a classifier in a pattern recognition system.

One of the major functional limitation seen from the review is that when both gross and fine motor classes are included in a pattern recognition system, especially in patients with no special surgeries such as the TMR, the performance gets poor and most researchers found an optimal subset of movement classes to improve performance.

The next 2 chapters will aim at custom designing a high-density array and building a system for sub-selecting the best electrode locations to be used based on the problem presented. This high-density system can be used for selecting multiple sites for pattern recognition based system to have a more intuitive control with very little knowledge about the residual muscle architecture, selecting multiple sites based on the motions of interest which may include gross control motions or finer grip type motions. The main objective here is to improve the number of movement classes that a user can perform without compromising performance.

Chapter 3: Conformable HD-EMG array design and characterization

3.1. Introduction:

3.1.1. State-of-the-art electrode technology: Flexible high-density sEMG for upper limb prosthesis control:

Advancements in flexible materials for electronics and readily available interface systems for signal acquisition and processing has allowed the design of different types of high-density sEMG sensors for use with sEMG based research. A review of such flexible electrode technology was presented in Agarwal's work [47]. Previous chapter outlined how HD sEMG can play a major role in myosite selection for improving pattern recognition based prosthesis control. This chapter describes how a more conformable electrode design was built to ensure more reliable signals with reduced electrode lift offs and motion artifacts.

*3.1.2. **F**lexible high-density sEMG design and contact material:*

Various studies have used flexible arrays for high-density sEMG data acquisition [25], [26], [33]. Some of the important factors to consider while designing flexible electronics for sEMG data acquisition are:

1) Contact material characteristics:
    - Settling time of contact material (lower the better).
    - Complex impedance characterization of electrode-skin interface (lower the better).
    - Signal to Noise ratio (higher the better).

2) Skin-electrode contact quality to have minimal electrode lift offs when attached to the skin surface as well as low motion artifact during the limb a prosthesis use for bio-signal acquisition.

The first design consideration mentioned above was covered in Agarwal's work [47], where, various contact materials were tested and a standard method of characterization of different types of contact materials were established. Her work also used a custom-made polyimide high-density sEMG electrode array design and signal quality was tested and presented.

The aim of the proposed design is to improve on the previous design and prototype a more conformable alternative, so that, it can be fit into a prosthesis socket to have maximum spatial coverage and obtain maximum information from the residual limb, while maintaining contact with the residual limb irrespective of the shape and size of the same. This will then be used for the myosite selection application discussed in Chapter 4 and 5.

3.1.3. Electrode Design: Issues with previous design of flexible HD sEMG electrode array:

In myoelectric prostheses, changes in electrode conductivity, electrode shifts and loss of electrode contact have been shown to add noise to the recorded sEMG signals [48], [49]. The chances of such occurrences become higher with HD sEMG arrays which have smaller regions of contacts, especially when they are not adherent to the skin surface. Some HD sEMG electrodes used in research use adhesives to be attached to the region of interest to reduce motion artifacts [33], [50]. This is however, not a practical solution, especially for use as an interface in upper limb prosthesis, where, the user should be able to don and doff the system whenever desired. Also, in a pattern recognition based system, with

disturbances to sensor interfaces, the stability of classification is highly affected [48], [24] since such disturbances can cause significant changes in the recognized patterns of the corresponding intended motion. Chadwell et al's [24] work also showed that the performance of the prosthesis in term of response times of the user is affected due to change in the electrode interface. The term called contact security, which was defined as the perceived contact of the electrodes on the skin by the prosthesis wearer, was introduced in Head et al.'s work [51]. They showed that using bipolar electrodes, which have the capability to be aligned and adjusted for contact security, provide better prosthetic functionality based on their Southampton Hand Assessment Procedure (SHAP) [52] scores. Hence, there is a need to make the custom designed electrodes more conformable in order minimize deterioration in performances of the pattern recognition system due to electrode lift offs motion artifacts.

The previously developed flexible array shown in Fig. 3.1 (a) [47] consists of a polyimide array with electroless nickel immersion gold (ENIG) finish contacts. It was designed such that it can easily be wrapped around the residual limb for signal acquisition. However, while using this design for data acquisition, there is a higher chance of electrode lift offs or non-contact in cases where the residual limbs are irregularly shaped and the polyimide arrays are not able to conform well to the shape of the residual limb. Also, there is a high chance of relative motion between the contacts of the array and the residual limb at different positions of the limb during contractions that involve high rotational movements such as pronation and supination [22].

This chapter will summarize the evolution of the flexible HD sEMG design used in Agarwal's work [47], to a more conformable design. The reduction in electrode lift offs

and motion artifacts will be justified using complex impedance characterization. The sEMG signals from different iterations of the design will also be visualized as image maps in order to demonstrate the quality of signals with different iterations of the design.

3.1.4. Improved design for prosthetic sockets to reduce electrode lift offs and motion artifact:

Agarwal's work [47] showed a comparison report of different contact materials that could be used for EMG data acquisition. Contact impedance and Signal to Noise Ratio (SNR) were considered for this comparison. Results showed that Silicone contacts with carbon nanotube doping showed the best results with respect to having a low settling time, <75kOhms skin electrode complex impedance (SECI) and >20 signal to noise ratio(SNR) values. Hence, this material was chosen as contact material to incorporate conformability into the HD sEMG design.

3.2. Methods: Design and testing of conformable electrode arrays for HD sEMG data acquisition

The different designs tested in this chapter will be named based on the iteration number 1, 2, 3 etc. Tests were performed to compare the signal quality and conformability of the four design iterations.

1) The initial design or design iteration 0 (DI0) is the polyimide array with ENIG finish contacts from Agarwal's work [47]. This will also be referred to as the conjoined array(CNJ) design.
2) Design iteration 1(DI1) will also be referred to as Strip design. This is DI0 cut into strips to improve conformability.

3) Design iteration 2(DI2) will also be referred to as silicone patch design. These are electrode array patches made from silicone with the CNT doped silicone contact material.

4) Design Iteration 3(DI3) will also be referred to as hybrid design. This design is a combination of the design versions DI1 and DI2. Gold plated spring pins were used to attach the polyimide arrays to the silicone patches. This is shown in Fig. 3.1 (e) The images of each of these designs are shown in Fig. 3.1 (a)-(f) below.

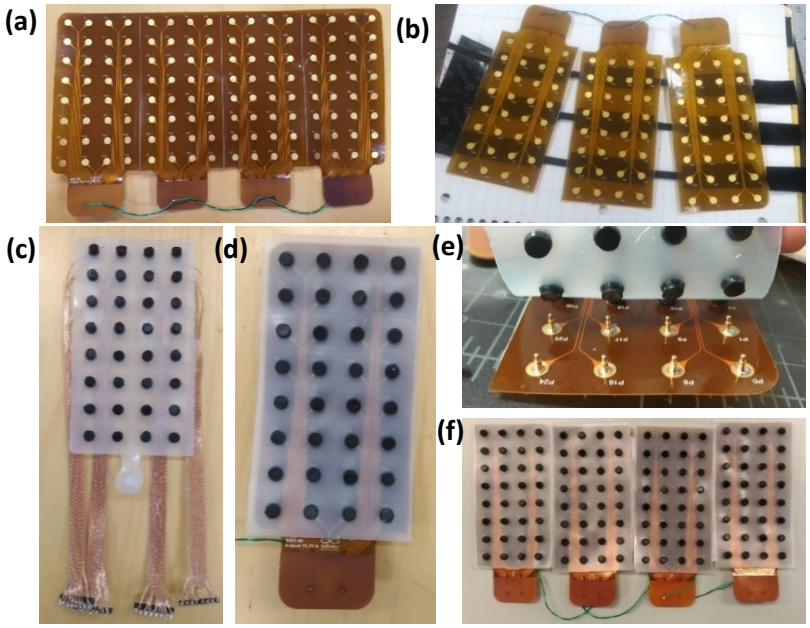

Fig 3.1. Images of different iterations of flexible electrode array design: (a) Conjoined arrays (DI0) [47], (b) strip design (DI1), (c) silicone design with CNT doped silicone contacts (DI2), (d) a strip of hybrid design (DI3), (e) the interconnecting spring pins in hybrid design, (f) hybrid design with 128 electrode contacts.

3.2.1. Experimental setup and data processing:

The electrode array consisting of 32 contacts was placed on the wrist flexor muscle region of the forearm placed about an inch distal from the elbow joint as shown in Fig.3.2 (a). The array was secured using a surgical tape and wrapped around to secure contacts throughout the data gathering process. The reference electrode was placed on the lateral epicondyle (bony region as reference). This system gathers monopolar signals and hence this electrode act as the reference for all the 32 electrodes used. Proper care was taken in the positioning of the reference electrode to get the ideal baseline (for example, the average baseline noise should not be higher ±500 microvolts). The array was connected to the Intan interface board (Intan Technologies, LLC, California) which has 4 SPI ports, out of which only 1 ports were used for 32 channels. To connect the arrays to the Intan amplifier board, standard Omnetics SPI interface connector cables (Omnetics Connector Corp, Minneapolis) were used along with Intan 32 channel (unipolar input) amplifier boards (RHD2132). Intan RHD2000 Interface software (Intan Technologies, LLC, California) was used to view and record the EMG signals. An image of the experimental setup used is shown in Fig. 3.2 (b) The experimental setup followed throughout chapters 3, 4 and 5 for both able-bodied and amputee subjects is similar to this setup (the number of arrays used might be different depending on the experiment and the coverage area needed) unless specified otherwise.

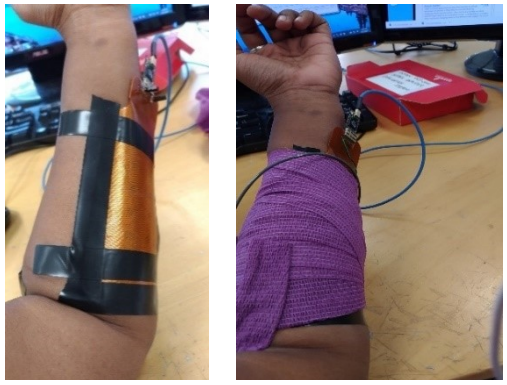

Fig 3.2. Electrode setup (a) Electrode attached to skin on wrist flexor region, (b) electrode setup with contact security.

Data pre-processing: After collecting the EMG data from the subjects, the next step is to pre-process data. The pre-processing steps include filtering data with a i) 3rd order Butterworth bandpass filter between (30 – 300 Hz) and ii) 1st order IIR comb filter to remove 60 Hz noise and the resonant frequencies. The EMG time domain feature used throughout this work is mean average value (MAV). The mathematical representation of MAV is shown below:

$$\boldsymbol{MAV} = \frac{\mathbf{1}}{\boldsymbol{S}}\sum_{\mathbf{1}}^{\boldsymbol{S}} |\boldsymbol{f}(\boldsymbol{s})| \qquad \textit{Eq. 1}$$

where S is the sliding window length and f (s) is the HD sEMG sensor data at index s within the window. The window size used is 200ms with a step size of 50 ms. HD sEMG activity maps are generated by calculating the mean of MAV for each channel and normalizing them across that particular trial. Data interpolation is used to produce smoothened image maps to create better visualizations. They are then plotted in the 2D space based on their location on the residual limb.

The HD sEMG image maps generated for classes wrist flexion(WF) and wrist extension(WE) classes for an able bodied subject is shown in Fig. 3.3.

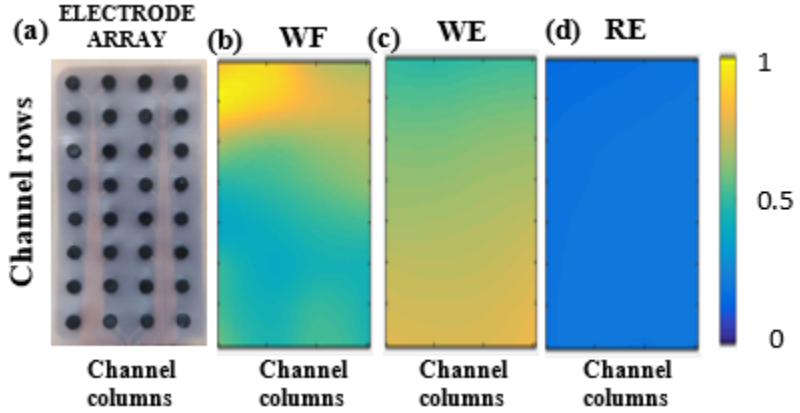

Fig. 3.3. Muscle activity maps: (a) DI3 electrode arrays showing 32 electrode contacts, (b) Muscle activity map for WF, (c) Muscle activity map for WE, (d) Muscle activity map for RE.

3.2.2. Electrode lift/ motion artifact characterization:

Quality of signals and amount of motion artifacts were compared among different design iterations to demonstrate the impact of design changes. Two parameters were used to characterize these, namely mean squared error (MSE) and skin electrode contact impedance (SECI).

3.2.3. Mean squared error:

3.2.3.1. Method:

Mean squared error (MSE) is the parameter used to estimate the closeness of data from different trials to one another. It can be mathematically expressed as follows:

$$\boldsymbol{MSE} = \frac{\mathbf{1}}{\boldsymbol{n}}\sum_{\mathbf{1}}^{\boldsymbol{n}} [\boldsymbol{A(n)} - \boldsymbol{B(n)}]^{\mathbf{2}} \qquad \textit{Eq. 2}$$

where A(n) and B(n) are mean MAV values from different trials and n is the number of electrode contacts under consideration, which in this case is 32 electrode contacts. The experimental setup was made as explained in the previous section on the forearm of an able-bodied subject. The subject was asked to perform the antagonistic movement classes of wrist flexion and extension and the activity of the wrist flexor muscle was visualized as explained in the previous section using image maps. For data recording the subject was asked to get into the contraction phase from rest phase (3sec) and hold the contraction for a period of 5 seconds and get back to rest phase(3sec). A total data of 11 secs was recorded for each contraction. A single trial consisted of WF, WE data recording and 3 such

repetitions were performed. This was repeated with all 4 design iterations used on the same location on the forearm (marked for reference).

This was repeated in an amputee subject with 128 electrodes. The experimental setup for the amputee subject with 128 electrodes is shown in Fig. 3.4. However, only DI0 and DI3 were compared. Hand open(HO) and hand close(HC) classes were recorded for 3 repetitions using both DI0 and DI3 and MSE was calculated. These classes were chosen since they were the movement classes most practiced by the amputee.

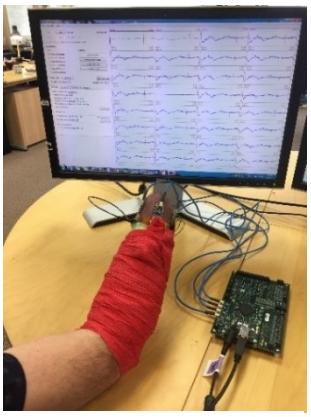

Fig.3.4. Experimental setup used for the subject with trans-radial amputation.

3.2.2.2. Results and discussion:

Data from all the design iterations from able-bodied subject(AB1) were run through the same MATLAB processing and visualization codes and the data acquisition setup was also the same for all the design iterations. Hence, the variations in the MSE values are attributed to the quality of electrode interface. The assumption made here is that the subject is experienced in performing repeated antagonistic contractions. The percentage mean squared error between different trials from each of the design iterations were averaged and is presented below in Fig. 3.5. It can be seen that with each design iteration, the MSE value slightly decreases which is

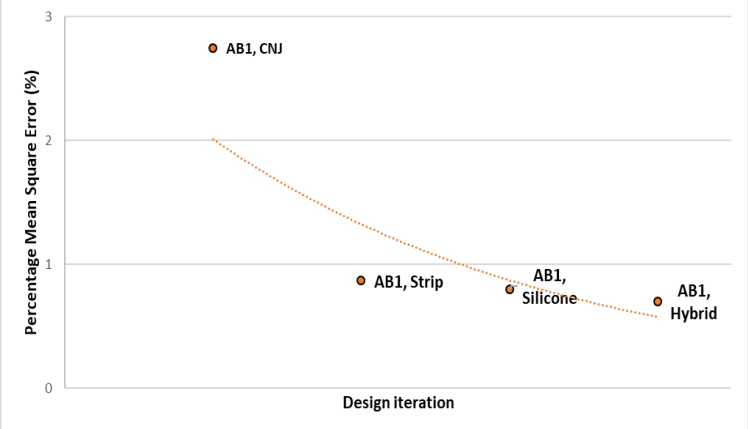

Fig. 3.5. Graph showing percentage mean squared error for each of the electrode design iteration for an able-bodied (AB1) subject.

represented by the exponential trend line in the graph. This shows that the electrode interface has improved with each design iteration. The image maps were also visually

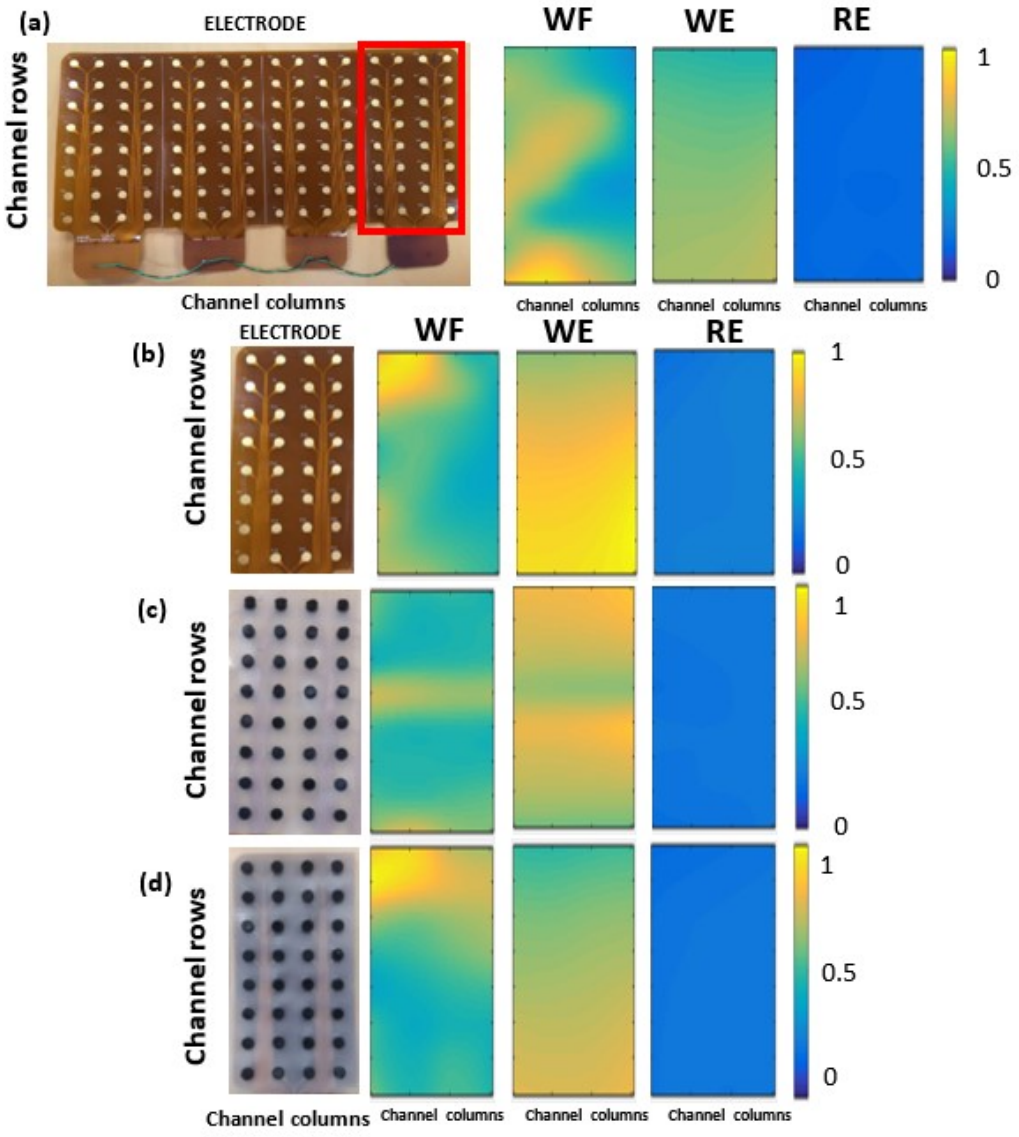

Fig. 3.6. Electrode design iteration with muscle activity maps for WF, WE and RE using (a) DI0 array (b) DI1 array (c) DI2 array (d) DI3 array.

compared from each of the design iterations and are shown below to represent that the image patterns remain fairly similar across design iterations in correspondence to the region of high muscle activity during WF and WE.

The result of data comparison for the amputee subject is shown in Fig. 3.7(a). The trend of reduction in MSE value is seen from DI0 to DI3 design, however, the amplitude values are much lower.

This might be because the level of muscle activity retained by the amputee subject might be lower than that of an able-bodied subject and hence, the regions with maximum activation (~1 in the image maps in Fig.3.7 (b) and (c)) is much smaller than that of able-bodied subject as shown in Fig.3.6.

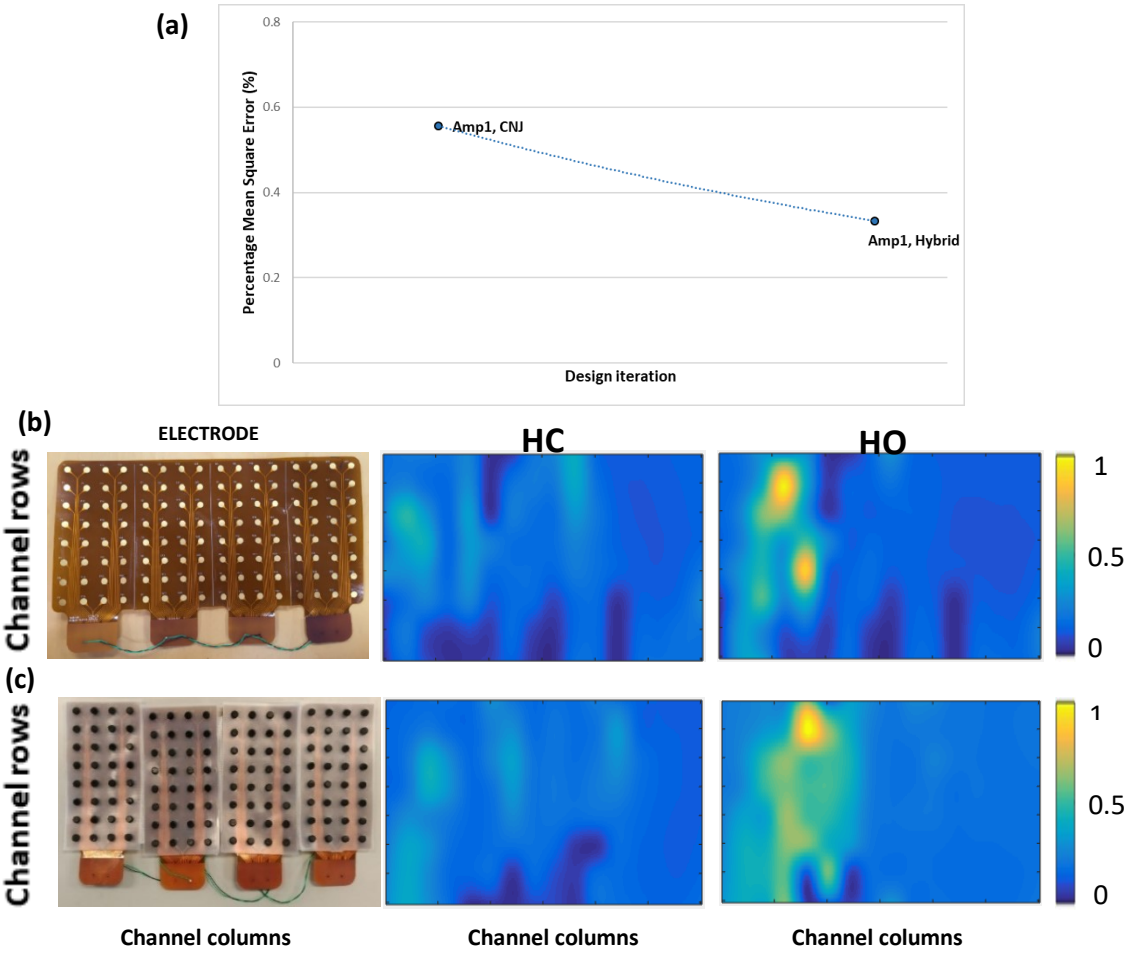

Fig. 3.7. Results for Amputee (Amp1) subject: (a) Graph showing mean squared error for DI0 and DI3, (b) electrode design iteration with muscle activity maps for HO, HC for DI0, (c) electrode design iteration with muscle activity maps for HO, HC for DI3.

3.2.4.1. Method:

Electrode-skin contact is one of the major factor that affects the quality of surface bio-signals [51], in this case EMG signals, especially in case of dry electrodes. There have been different noise reduction algorithms to accommodate for motion artifacts [48], [53] and electrode signal quality tests that have been done when new electrodes are designed for surface bio signal acquisition [54]. Skin-electrode contact impedance has been used as one of the common metrics in various studies [54]- [57] to characterize the extent of electrode-skin contact and motion artifact. The aim of our study is to use the skin-electrode contact impedance to quantify conformability of the flexible HD sEMG electrode designs and to provide design justification of the improved DI3 design to be used within a socket for myoelectric prosthetic control.

The experimental setup for measuring contact impedances across different design iterations was similar to that described earlier in section 3.2.1. The skin electrode complex impedances were measured using the Intan interface software. Two types of impedance measurements were made in order to quantify skin-electrode contact.

a) Firstly, static electrode contact characterization was made. For this, each of the designs was attached to an able-bodied subject's forearm, with and without the contact security. To provide contact security, a wet wrap was used to hold the electrodes in place by wrapping it around the electrode arrays. Images of a setup for one of the design iterations with and without contact security is shown in Fig.3.7. Thus, the impedance measurements were made in a total of 8 setups. To make an impedance measurement, the input signal frequency was set at 5KHz. A higher frequency was chosen because experiments have shown that at higher

frequencies, the components of the measured impedance are greatly influenced by the skin-electrode contact and the variable dynamic impedance components do not affect the readings [47], [56]. First three measurements were made at rest position with an interval of 2 minutes between each reading. After which contractions were performed between each of the remaining 5 measurements. The contractions included wrist flexion(WF), wrist extension(WE), wrist pronation(PR) and wrist supination(WS). These movements were chosen to simulate motion artifacts that could occur while using a prosthesis. The subject performed 1 set of these 4 movements with a contraction period of about 11 secs and an interval of about 5 seconds between each movement. The measured contact impedance values were then averaged across the 32 contacts and 8 measurements for each of the design iteration.

b) The second set of measurements was done to quantify electrode lift offs during a contraction with maximum range of motion. For this, wrist pronation (PR) was selected. The setup was similar to that described in the previous section. SECI was measured at 3 different positions of a wrist pronation - position 1-rest, position 2-mid-pronation, position 3- complete pronation.

3.2.4.2. Result and discussion:

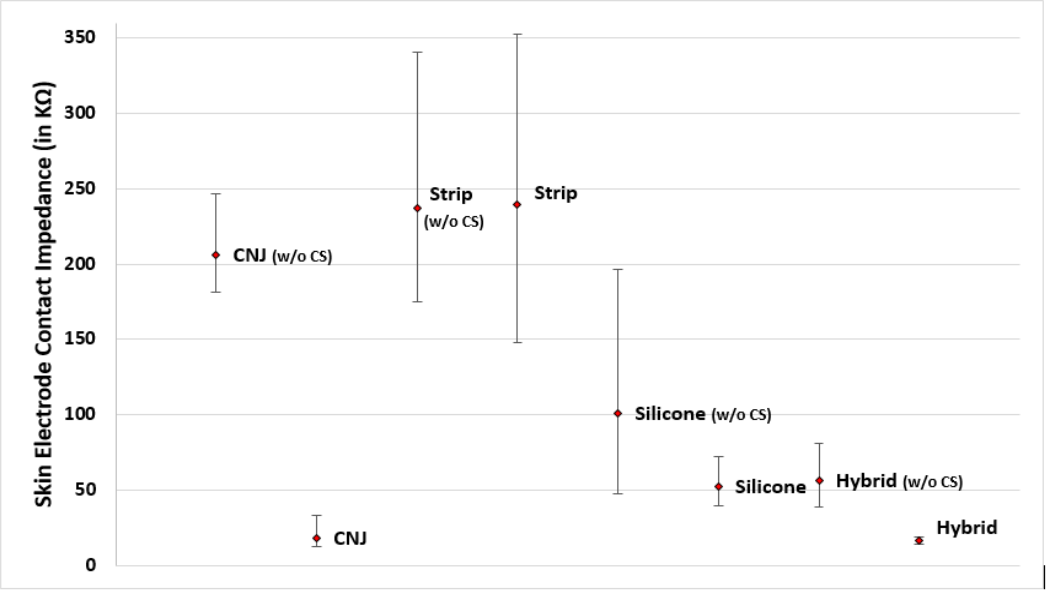

Fig. 3.8. Graphical representation of SECI data of the 4 design iterations tested with and without contact security for static electrode characterization. (The SECI values of setups without contact security are marked as (w/o CS)).

From the given graph in Fig.3.8, it can be seen that CNJ and Hybrid designs with contact security has the best possible average SECI values indicating the best case scenario. It is known that ideal SECI value for sEMG signal acquisition should be <75kΩ [47]. DI0, DI2 and DI3 with contact security satisfies this constraint, however, DI3 is the only design that has good SECI value even in the absence of contact security. This indicates that the hybrid design is the ideal design for use with a prosthesis socket. This is due to the fact that with the same amount of contact security given to all 4 design iterations, DI3 shows minimum variability in SECI value and hence will show maximum stability of the sEMG signal values. Also, it can be seen that, hybrid design with contact security has the least variability (denoted by shorter error bars) in SECI indicating the least electrode lift offs.

Similar calculations were performed i.e. average SECI of 32 contacts were calculated for the 3 positions during contraction and are plotted as average SECI for 3 positions with error

bars showing variances in Fig. 3.9 (a). Results of the best 4 configurations which had a desirable SECI range of <75kΩ are shown separately in Fig.3.9 (b) for better visualization.

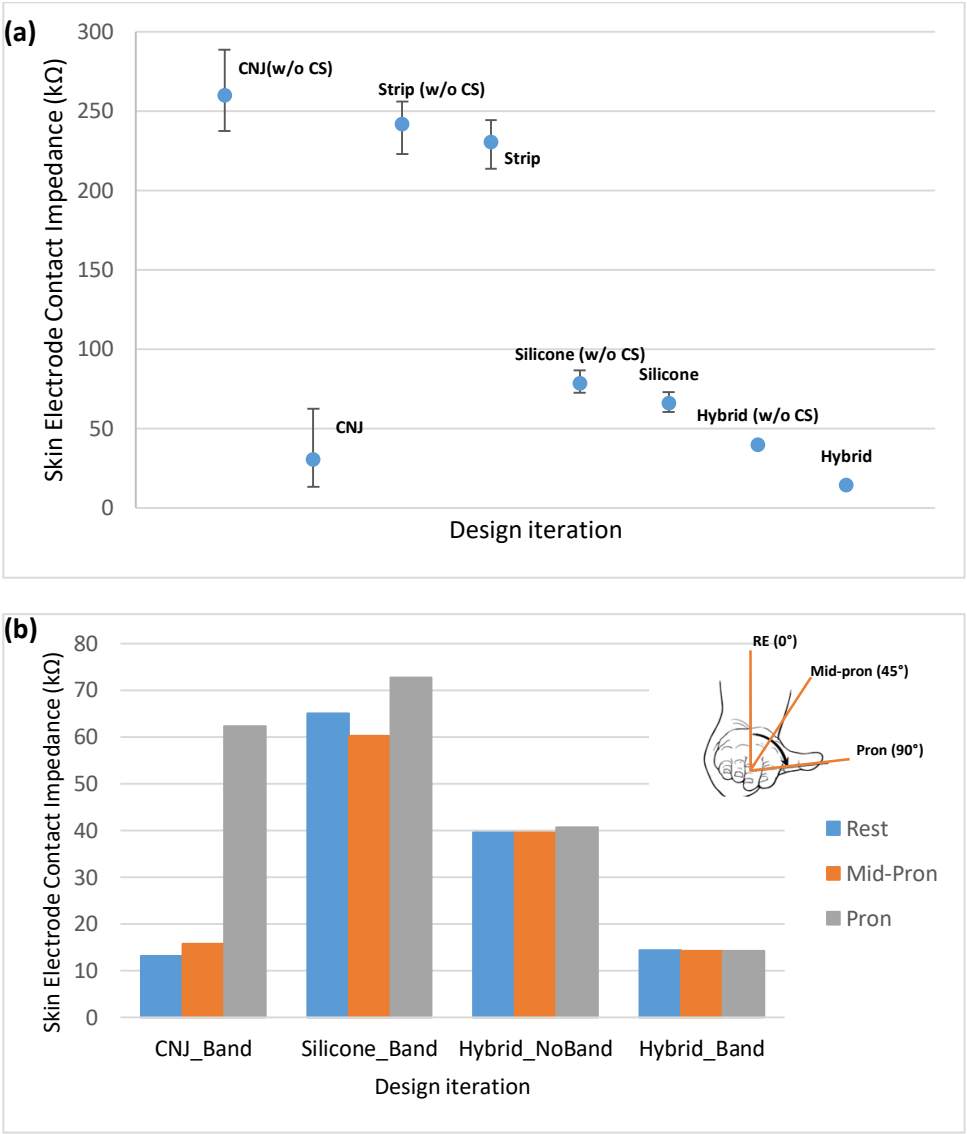

Fig. 3.9. SECI for 3 positions during contraction: (a) Graphical representation of SECI of the 4 design iterations tested with and without contact security during maximum range of motion, here PR (The SECI values of setups without contact security are marked as (w/o CS)), (b) detailed graphical

These results are in agreement with the results of the previous experiment showing the least electrode lift off for the hybrid design, with or without contact security.

3.3. Summary:

Conformability of flexible electrode array on the residual limb of the forearm is a major factor that influences signal quality based on change in electrode skin contact. The proposed design was prototypes via various design iterations and each iteration was tested for analyzing electrode skin contact and signal quality based on mean squared error (MSE) and skin-electrode contact impedance (SECI). The proposed hybrid prototype with conformable contacts had minimal amount of electrode lift offs both in static condition as well as during contraction.

Chapter 4: Myosite selection using high-density sEMG

As stated in chapter 2, prior research has investigated different combinations of movement pattern classifier along with feature selection algorithms to improve the performance of pattern recognition system. In this chapter, the problem of "myosite" (defined as the sites of placement of EMG electrodes on the residual arm of the amputee) will be studied, particularly the context of HD electrode designs. Further, two different types of myosite selection algorithms will be presented and their effect on performance will be investigated- (i) The first algorithm is built for offline analysis in order to select myosites for positioning bipolar electrodes during a clinical fitting process. (ii) The second algorithm is built in order to work with both offline as well as online systems. The goal of the later algorithm presented in this chapter is to accommodate functional changes or improvements in a fitted myoelectric prosthesis by varying the number or type of movements controlled by the system without compromising the performance of the system. Also, this novel method accommodates for these functional adaptations without the need for refitting, thus enabling a pattern recognition based myoelectric prosthesis to perform both gross and fine motor movements with optimal performance.

The work presented in this chapter will investigate how the number and the nature of movement classes included in the pattern recognition system affects the spatial locations of the optimal control sites and, in turn, the overall performance of the system. The effects of training on myosite selection and optimization is also investigated in this chapter.

The hybrid HD sEMG electrode array built in chapter 3 will be used in this work. It consists of 128 monopolar electrode channels, integrated on a polyimide flexible substrate (confirm), to gather data from the residual limb of healthy subjects as well as amputees.

The HD sEMG data from 128 channels needs to be processed to remove redundant and irrelevant data to arrive at the data required for the application of pattern recognition; and the preferred goal is to reduce the selection down to 8 electrode locations, which is the industrial standard for the system [58]. Identifying channels with useful information is important for the efficient performance of subsequent data processing tasks and also for saving computational power required by the processor.

4.1. Introduction to feature subset selection:

A feature is a basic, quantifiable unit that can be used to describe some aspects of any recorded data. Feature subset selection is a method that can enhance the efficiency of machine learning algorithms by identifying the subset of most relevant features from all available features [59]. In our case, electrode channels are analogous to feature and hence, we will be applying the methods of feature subset selection to select the optimal myosites.

There are 2 major methods of feature subset selection namely, wrapper based method [59], and filter based method [60].

1) Wrapper based method: This method uses classifier's accuracy as the performance measure and hence is a classifier dependent method.
2) Filter based method: This uses indirect performance measures like distance measures, information measures etc. and this is a classifier independent method.

4.2. Wrapper algorithm:

4.2.1. Objective:

This algorithm was built in order to provide a more quantitative method of selecting optimal locations for placing the bipolar electrodes during a pattern recognition based

prosthesis fitting process. This algorithm, if proven effective, could be used in selecting myosites during prosthetic fitting process.

4.2.2. Introduction to wrapper based method:

The wrapper based method uses the classifier's predictive accuracy to determine relevant channels. A flowchart depicting the wrapper model is shown in Fig. 4.1. The full data set is analyzed to select the best possible feature, in our case myosites, and data from these myosites are used as input to the learning algorithm. The classifier used for pattern classification is a basic linear discriminant analysis (LDA), since it is the most commonly used multivariate classifier among the upper limb prosthetic pattern recognition systems and it is easy to implement and train [16], [61].

The advantages of using a wrapper method algorithm is that the highest accuracy is obtained by mostly using exhaustive search strategy and hence there are minimal chances of missing optimal subsets. The algorithm that we built analyzes offline data and arrives at the optimum sites. As computation time is not a binding factor in this application (offline and needed only for optimum site selection, not for real time control), it is acceptable even if the algorithm takes a long time to run. This justifies how one of the most common disadvantages of wrapper method, which is that it is highly time consuming and computationally costly [60], is not a major concern for the chosen problem statement.

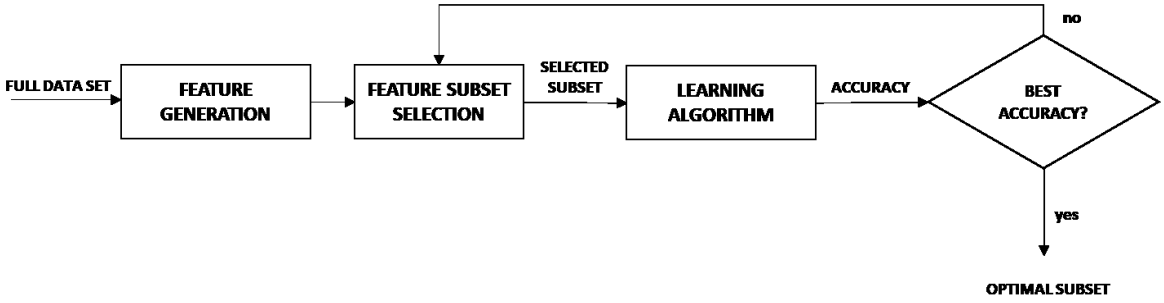

Fig. 4.1. Flowchart for wrapper model of feature selection.

4.2.3. Methods:

4.2.3.1. Algorithm implementation for myosite selection:

The data stored after collection are pre-processed as mentioned in the previous section. The MAV of the 128 channels is then run individually through the pattern recognition LDA algorithm and the classification accuracies are recorded. The channels with highest classification accuracies are sub-selected. One channel is selected among the sub-selected channels at random and is fixed as optimal channel 1. This channel is then combined with one channel (from 1 to 128), giving 128 two-channel combinations to be tested again based on performance accuracies after running through the LDA algorithm. This process is repeated untill the 8 optimal electrode combination is reached and the maximum performance accuracies are noted down for each of the combination stages (1 to 8). Since this algorithm involves a random selection process, the code is run for 100 iterations and the best accuracies attained from the 100 trials is used with the corresponding electrode combinations.

As an intermediate visualization step, the histogram count is plotted. This shows how many occurrences of each electrode is present in the finally selected 8 optimal electrode combinations. The most occurring electrodes are those which occur the maximum number of times in the selected optimal combinations. These are identified from the histogram. The combination with the maximum number of most occurring electrodes is then selected as the optimal combination. This is summarized as a flowchart in Fig. 4.2.

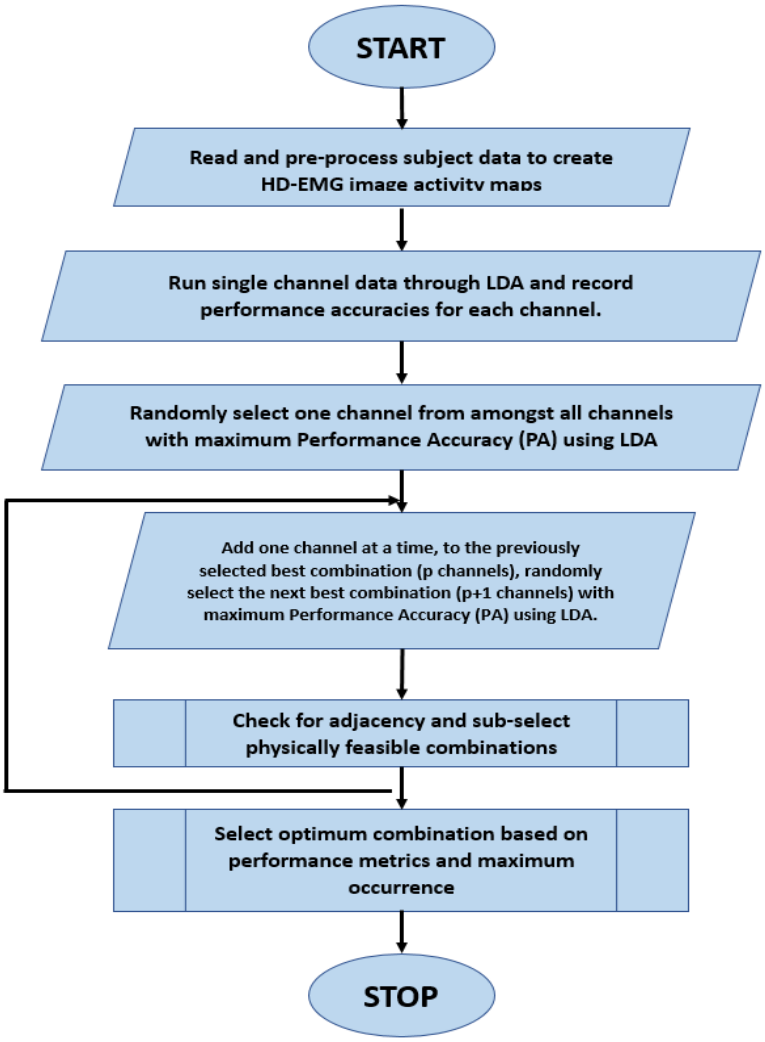

Fig. 4.2. Flowchart for wrapper algorithm implemented for myosite selection.

4.2.3.2. Experimental setup:

The experimental setup used for this data collection is the standard setup described in chapter 3. The electrode setup wrapped around the subject's residual limb for this study is shown in Fig.4.3.

Fig. 4.3. Electrode setup on residual limb of a trans-humeral amputee subject, used for evaluation of wrapper algorithm based myosite selection.

4.2.3.3. Subject Demographics:

Two subjects with trans-humeral non-congenital amputations were considered for this study. Informed consent was obtained from the subjects. The study was approved by Johns Hopkins Medicine Institutional Review Board.

4.2.3.4. Data gathering procedure:

Data were collected from the subjects for 6 movement classes (widely used gross movement classes), 3 repetitions each. The 6 classes used for data collection and evaluation for the 2 subjects are 1) hand open, 2) hand close, 3) pronation, 4) supination, 5) elbow extension, 6) elbow flexion shown in Fig. 4.4. These movement classes were selected based on the most practiced and comfortable classes for the subjects. Also, these are the most widely used movement classes for gross function used by trans-humeral amputees for pattern recognition. Data were collected for all 6 classes for trial 1 and then the process was repeated again for trial 2, and trial 3. The pre-processing steps are also the same as described in chapter 3. As a good practice, the data are visualized at intermediate stages throughout the process to have a more informed and interactive process of building the code.

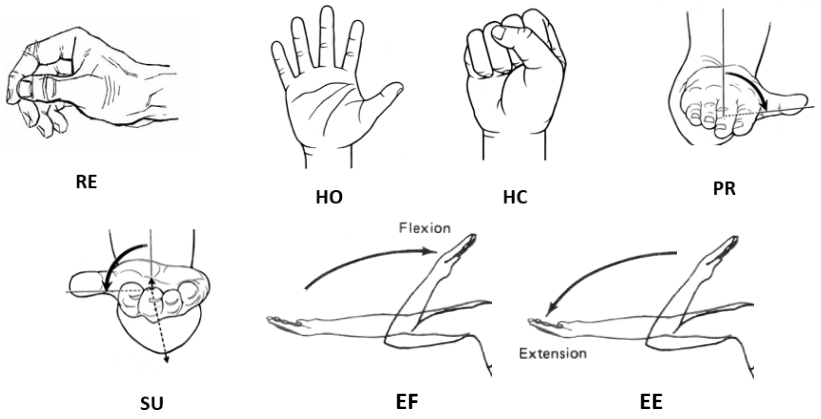

Fig. 4.4. Movement classes used for the study: RE, HO, HC, PR, SU, EF, EE.

4.2.4. Results and Discussion:

a) Manual site selection for comparison:

The muscle activity maps generated from the MAV values were visually analyzed to select 8 sites manually - channels with high intensity for specific classes as well as unique to different classes. This is analogous to the current method of myosite selection using palpation. This is used as a control to compare the algorithmically selected sites with. The muscle activity maps used to select these sites along with the myosites selected manually are shown in Fig. 4.5(a)-(f) and 4.5(g) respectively.

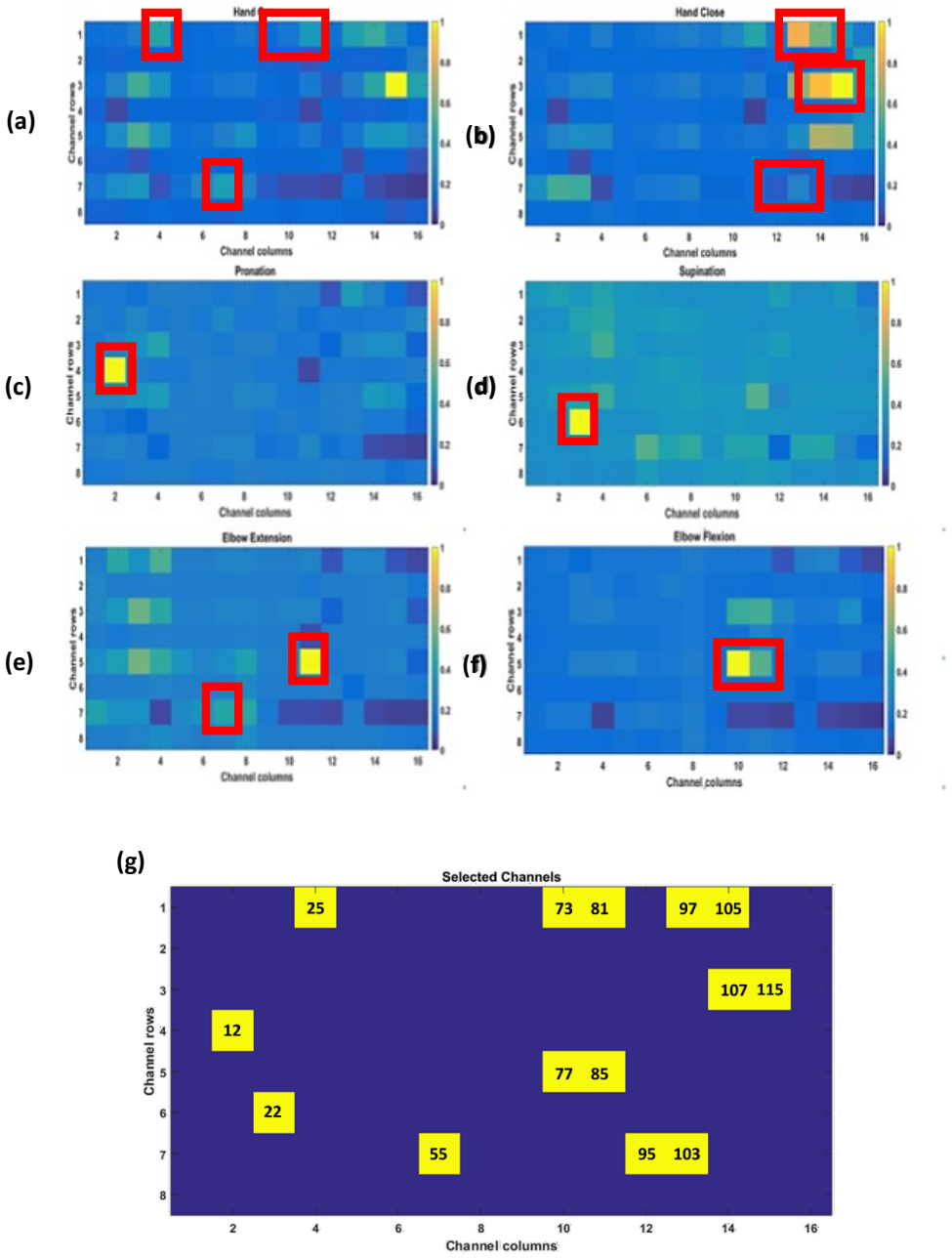

Fig. 4.5. Muscle activity map with marking of manually selected myosites for (a) HO, (b) HC, (c) PR, (d) SU, (e) EE, (f) EF (g) map of HD sEMG array showing the manually selected myosites.

b) Site selection using wrapper method:

Myosite selection was performed using the wrapper algorithm mentioned in section 4.2.3.1 on both the subject data. A raster plot of all optimal channel combinations selected by the wrapper method is shown in Fig. 4.6(a). From the raster plot the optimal combination which has maximum number of most occurring sites are selected and used as the optimal myosites for subject A. Fig. 4.6(b) shows both manually selected sites and optimally selected sites. Fig. 4.6(c) shows the check socket that was fabricated using selected myosites. From this image, it can be seen that there is similarity in the regions of sites selected manually from the image maps and sites selected using the wrapper algorithm.

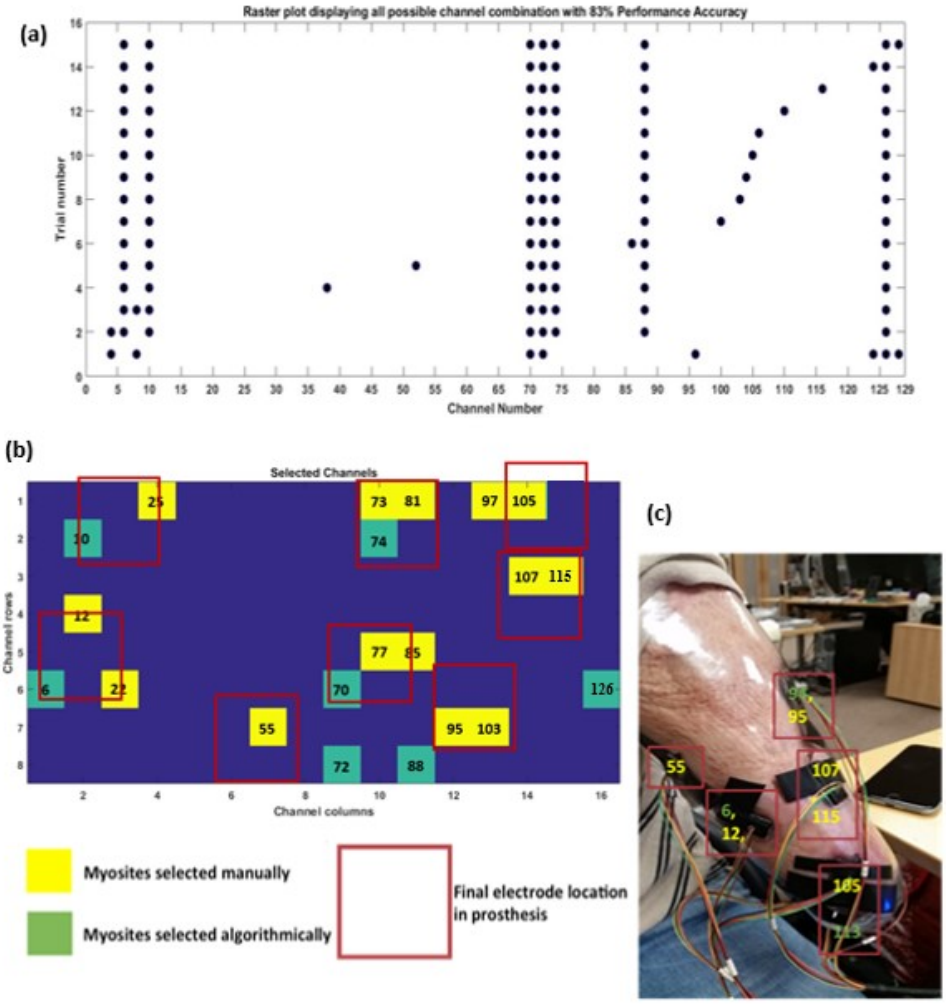

Fig. 4.6. Results for Amputee subject A: (a) Raster plot showing all possible myosite combinations with maximum classification accuracy of 83% (b) HD sEMG image map for selected electrode sites, both manually selected and algorithmically selected. (c) Subject A with custom fabricated socket showing manually selected myosites with the algorithmically selected sites marked as well.

Similar process was followed with subject B and the image maps, raster plot and selected myosites for Subject B are shown in Fig. 4.7.(a)-(f), 4.7.(g) .

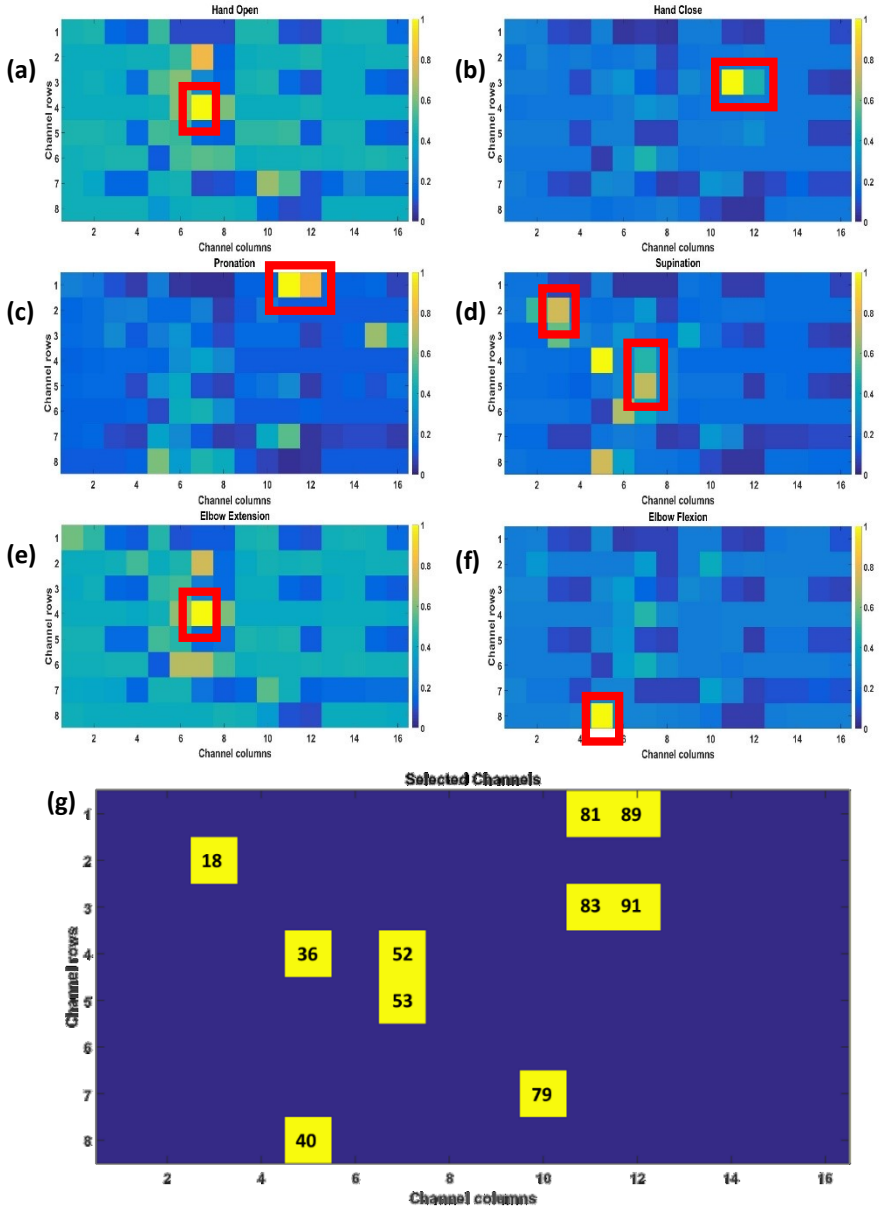

Fig. 4.7. Muscle activity map with marking of manually selected myosites for (a) HO, (b) HC, (c) PR, (d) SU, (e) EE, (f) EF (g) map of HD sEMG array showing the manually selected myosites for subject B.

Fig. 4.8 (a) shows the raster plot, Fig. 4.8 (b) shows both manually selected sites and sites selected using wrapper method for subject B. The red boxes on Fig. 4.8

(b) shows the finally selected sites for socket fabrication. Fig. 4.8 (b) shows the check socket that was fabricated for subject B using these selected myosites.

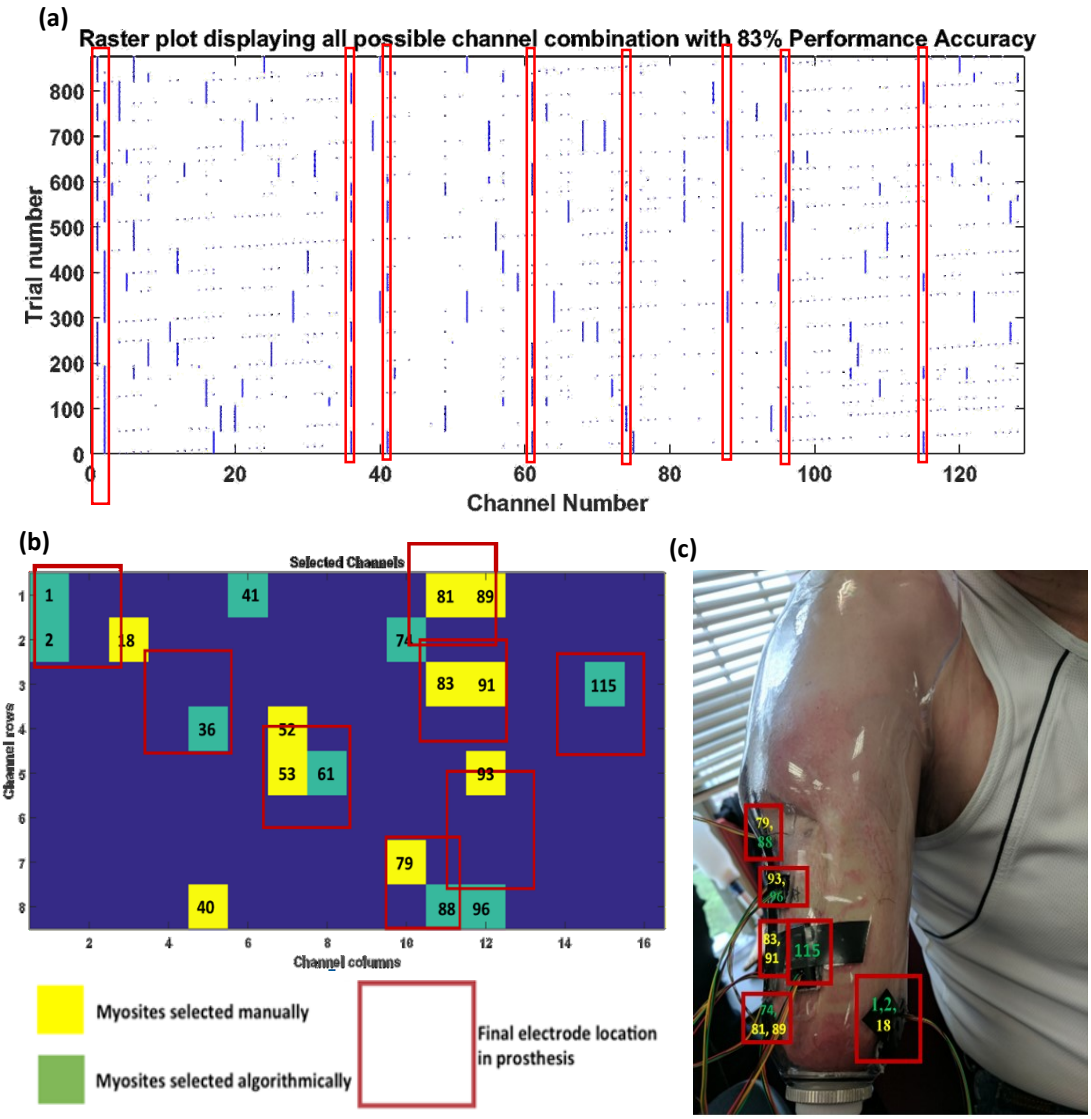

Fig. 4.8. Results for Amputee subject B: (a) Raster plot showing all possible myosite combinations with maximum classification accuracy of 83% for subject B, (b) HD sEMG image map for selected electrode sites, both manually selected and algorithmically selected, (c) subject B with custom fabricated socket showing manually selected myosites with the algorithmically selected sites marked as well.

c) Bipolar EMG Electrode Placement Orientation:

Major factors characterizing the quality of signals obtained using bipolar electrodes are shape, size, contact material, location and orientation. Hermens at al. [37] reviewed the processes and results of recommendations for sEMG sensor placement procedures. They reviewed 144 papers from 7 different journals. It was observed that the sensor configurations were not clearly specified in 40% of the papers and they reached out to the various groups in order to obtain complete information and after drafting a set of recommendations, it was reviewed by the SENIAM team and published as standards. Hermens et al. [37] found that the orientation of the electrodes was rarely mentioned. Also, it has been assumed that the location description described the location of the geometrical center of the sensor, unless specified otherwise.

Orientation is defined as the direction of the bipolar sensor with respect to the direction of the muscle fibers. The best identified orientation is placement of electrodes parallel to the muscle fibers. In the experiments performed by Young et. al. [62] the electrodes placed parallel to the muscle fibers outperformed the ones placed perpendicular in cases involving shift as well as no shift. The experimental results showed that irrespective of the size of bipolar electrodes used, parallel shift of electrodes had a lower effect on classification accuracy sensitivity. However, in case of perpendicular shifts, with increase in size the sensitivity to perpendicular shifts reduced.

Hence, while placing the electrodes on the selected myosite location, the best practice is to position it with its geometrical center of the bipolar electrode on the identified location with the contacts oriented longitudinally to the muscle that the electrode is in contact with. A prosthesis was fabricated with 8 electrodes positioned in locations selected using both

manually and algorithmically selected sites and the bipolar electrodes were oriented along the muscle's longitude.

4.2.4. Drawbacks of the wrapper algorithm:

The wrapper method is time consuming and cannot be used for online systems. The next step is to make this a HD sEMG system that can select myosites on-the-go from the 128 channels for controlling the prosthesis. This is done by a filter based method called Functionally Adaptive Myosite Selection (FAMS).

Wrapper based myosite selection method is an explorative search method and as mentioned earlier is time consuming and computationally costly. Though the sites selected using this method for the above mentioned 2 subjects worked well and they were able to use the prosthesis using the selected sites, these sites selected are specific to the movement classes performed during the experiments. The set of optimal sites may vary for a different set of movement classes and hence there will be a need to retest and refit the patient in case the patient needs to add or change the movement classes that they need their prosthetic to perform. The optimally selected sites are also different for different subjects, and hence the site selection process needs to be performed for each individual who is being fitted with the pattern recognition based myoelectric prosthesis. Also, the issues mentioned in chapter 3 with motion artifacts and electrode lift offs also apply to the conventionally used bipolar metal contact electrodes [23]. Hence, there is a need for a system that can help us get rid of the above mentioned issues and be used as an off-the-shelf system for all individuals who need a pattern recognition system. The system should also be able to adapt to changes in functionality that can be controlled by a prosthesis giving room for addition or change of movement classes.

4.3. Filter based method: Functionally Adaptive Myosite Selection (FAMS) method

4.3.1. Objective:

The ultimate goal of EMG movement-pattern classification research is to increase the number of movements that a person with amputation can reliably perform in turn increasing the functional capabilities of the myoelectric prosthesis. Our proposed functionally adaptive myosite selection (FAMS) system is a step towards achieving this by using a novel algorithm and the conformable HD sEMG electrode array to identify the myosites providing the most differentiable information a set of movement classes including both gross and fine movements.

The aim of this study is 1) to demonstrate that FAMS can identify unique myosites that provide data with minimal redundancy for optimized movement-pattern classification for a given sets of gross and fine movement classes, and 2) to compare the classification accuracies of myosites selected by FAMS against conventionally used myosite configuration in order to demonstrate the significance of myosite selection with increase in number of movement classes.

4.3.2. Introduction to filter based method

In this method, different criterion functions such as Fishers Ratio [63], Mahalanobis distance [64] and Bhattacharya distance [65] are used to select features, which provide information to a classification algorithm such that the movement classes under consideration are maximally distinguishable or separable. The Separability Index/Degree Matrix (SIM/SDM) was introduced by Han et. al [59] as a concise separability -based data organization method which effectively facilitates the feature subset selection process. In addition, some of the features in a given HD sEMG data set might be redundant or possess

similar information, thus, unnecessarily increasing the size of data. Our proposed algorithm selects features, in our case myosites, which provide information with maximum class-wise separability and minimum redundancy.

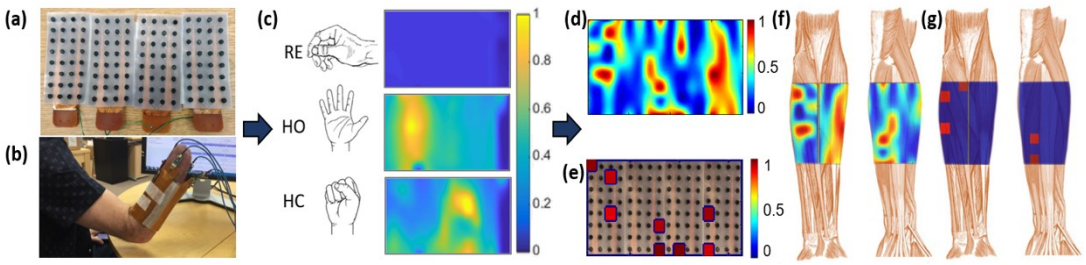

Fig. 4.9. Schematic representing FAMS method: (a) high density (HD) electrode array showing all 128 electrode contacts, (b) 128 channel HD electrode array wrapped around the subjects residual limb, (c) muscle activity image maps generated from the collected HD sEMG data for RE, HO and HC movement classes, (d) SIM for the RE, HO and HC movement classes (e) 8 OPT selected myosites using FAMS ranked in order of saliency or relevance, (f) Anatomical correspondence of separability index map and (g) anatomical correspondence of the final 8 optimal myosites selected by FAMS.

This system consists of both hardware and software components. The idea is to use the hybrid HD sEMG design inside the prosthesis along with the separability index based algorithm to improve functionality in a pattern recognition based myoelectric prosthesis. The software component of FAMS is a SIM based feature selection algorithm that selects the optimal myosites, while reducing information redundancy, from the data obtained from the HD sEMG electrode arrays. FAMS provides functional adaptability to a pattern recognition based myoelectric prosthesis, i.e., FAMS lets the pattern recognition based prosthesis functionally adapt to the increase in number of movement classes, by selecting corresponding set of optimal myosites based on the changes in separability of their muscle activity patterns, while ensuring optimum classification accuracies, without the need for refitting. A schematic representation of FAMS depicting the process of myosite selection is shown in Fig. 4.9.

4.3.3. Methods:

4.3.3.1.Subject demographics:

A total of 6 able-bodied (2 females, 4 males) and 2 amputee subjects (both male, with trans-radial, non-congenital amputations) participated in the study. Informed consent was obtained from the subjects. The study was approved by Johns Hopkins Medicine Institutional Review Board.

4.3.3.2. Protocol:

The subjects were separated into two groups based on their experience with using pattern recognition systems for prosthetic control. One group consisted of in-experienced subjects (5 able-bodied subjects), who needed training before participating in the study, while the other (1 able-bodied, 2 amputee subjects) had prior experience using a pattern recognition system for prosthetic control. All subjects were put through an initial testing phase where they were asked to train and test with a virtual training tool to analyze their level of proficiency with the system. HD sEMG data for eleven movement classes were gathered in this study: rest (RE), hand open (HO), hand close (HC), wrist pronate (PR), wrist supinate (SU), wrist flex (WF), wrist extend (WE), index point (IP), key grasp (KE), tripod (TR), and pinch (PI). The images of these 11 movement classes used for this data gathering are shown in Fig. 4.10.

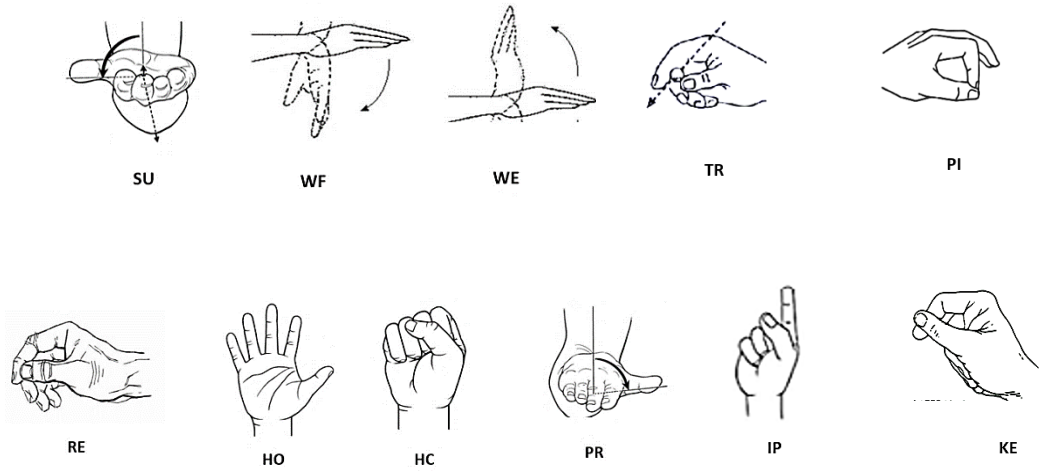

Fig. 4.10. Movement classes used for the study: RE, HO, HC, PR, SU, WF, WE, TR, PI.

4.3.3.3. Training protocol:

To evaluate the proficiency of all subjects as well as to train the inexperienced subjects, a commercially available pattern recognition system called sense was used along with a virtual training system called myotrain (Infinite Biomedical Technologies, LLC, Maryland). The training protocol loosely followed the previously published work of Powell et al. [26].

A 7-day training was given to the inexperienced subjects. The session consisted of a 20-minute training, after which myotrain tasks were performed and recorded. A HD SEMG data set for all the 11 movement classes was also recorded on all 7 days, post the training session. A 10-minute break session was included after myotrain practice and prior to HD sEMG data recording. The pattern recognition setup along with the myotrain is shown in Fig. 4.11(a). The myotrain movement class list is shown in Fig. 4.11(b).

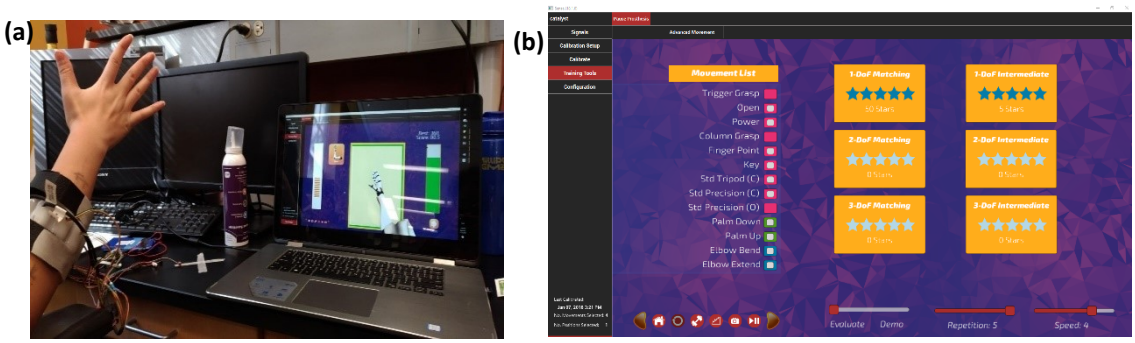

Fig. 4.11. Training setup (a) Experimental setup used for training inexperienced subjects on pattern recognition system (b)graphical user interface of myotrain showing the list of 10 classes used for this study.

On day 1, the concept of pattern recognition was explained and a demonstration of myotrain was given. Then the subjects were asked to try the virtual training system. However, myotrain data from day 1 was not considered for evaluation. On day 2 and day 3 they were trained on 4 movement classes+ rest class and their myotrain data were recorded. On day 4 and day 5, they were trained on 8 movement classes+ rest and on day 6 and 7, they were trained on all 10 movement classes+ rest. Their myotrain data were recorded on all days. Their progress was tracked based on task completion time and task completion percentage provided by the virtual training system. The progress of the 4 subjects in terms of classification accuracy based on the HD sEMG pattern classification and the task completion time and task completion percentage values are shown in Fig. 4.12(a) and 4.12(b) respectively. For representation purposes, the data from 6 days was split into 3 sessions of 2-days each. This was done in order to track progress based on number of classes included in the practice session.

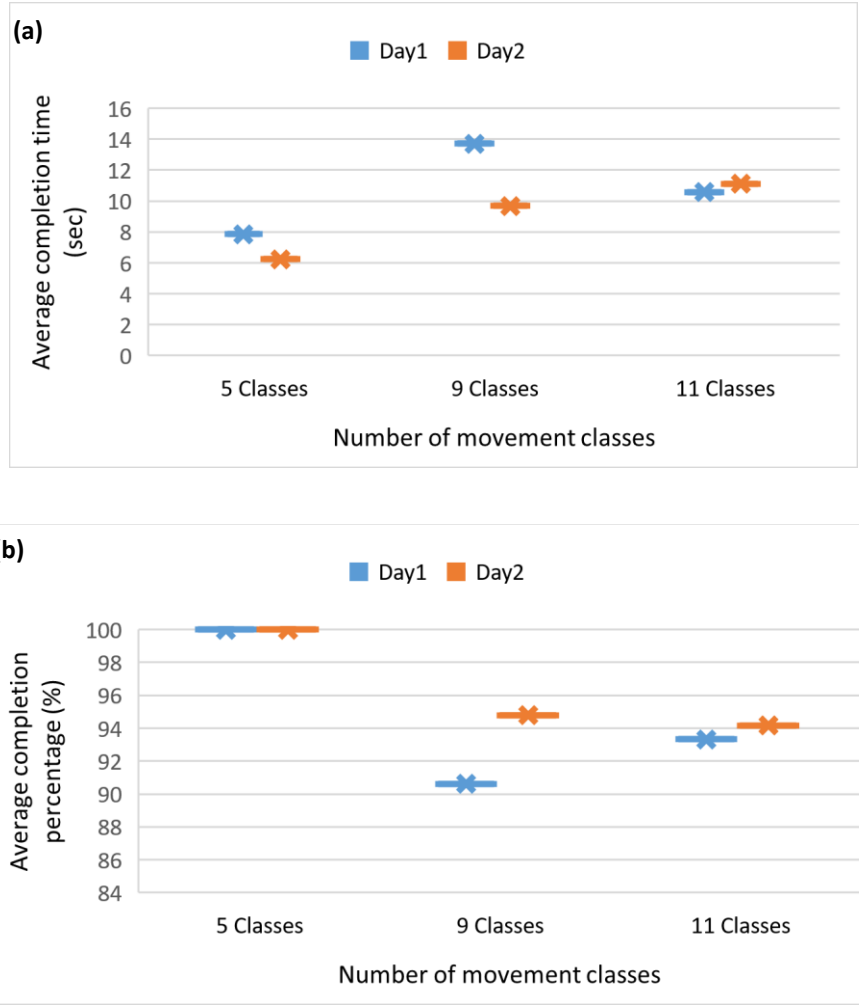

Fig. 4.12. Subject progress over time: (a) Graphical representation of average task completion times of inexperienced subjects with practice, (b) graphical representation of average task completion percentages of inexperienced subjects with practice.

From the graphs shown in Fig. 4.12, it can be seen that with inclusion of movement classes, task completion percentage reduces and task completion time increases. From Fig. 4.12(a), it can it is evident that, with practice, the subjects perform task quicker and this trend is no more seen in higher number of movement classes i.e 11 movement classes. From Fig. 4.12(b), it is seen that task completion percentage also improves with practice i.e. subjects perform better on 2nd day of every set except 5 classes, where their performance accuracy

is 100% on both days. Post this 7-day training session, the subjects were considered experienced and data collection was performed as explained below.

4.3.3.4. HDEMG data acquisition setup:

The Intan RHD2000 system (Intan Technologies, LLC, California) was used with the HD sEMG electrode arrays as described in chapter 3 for signal acquisition and recording. The experimental setup used is the standard setup described in chapter 3. The subjects were verbally and visually cued to initiate the contraction and then instructed to hold the contraction for a period of 7 s during which data was recorded. The data was gathered for 3 such trials, at a single position for the 11 movement classes mentioned the protocol. The collected data were processed as mentioned in chapter 3 to create muscle activity maps as shown in Fig. 4.13.

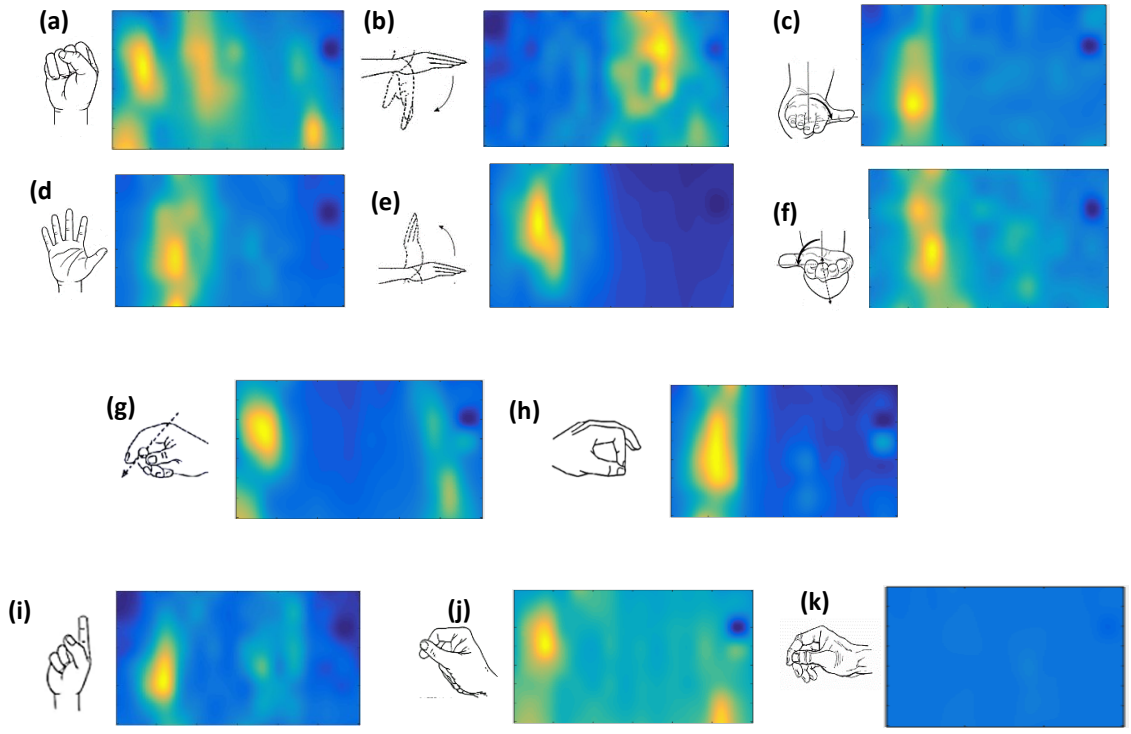

Fig. 4.13. Muscle activity map created from MAV values shown for one able-bodied subject for (a)HC, (b) WF, (c) PR, (d) HO, (e) WE, (f) SU, (g) TR, (h) PI, (i) IP, (j) KE, (k) RE.

4.3.3.5. Algorithmic Method

A major factor which impacts classification performance is the inter-class separability of the training data [59]. Our algorithm ranks the channels of recorded EMG data according to their ability to create separation among the class data clusters. However, there is a caveat to consider: multiple such channels may indeed create high separation but convey much of the same information content. Therefore, it is also necessary to factor redundancy into our ranking method so that unique information is supplied by each channel. Our algorithm, described visually and conceptually in Fig. 4.14, relies on the following metrics to quantify separability and redundancy.

Class Separation Metric: Bhattacharyya distance is a metric designed to quantify the separation between two Gaussian distributions [65]. Given a vector p containing samples drawn from an assumed normal distribution N (μ_p; σ_p) and, similarly, q drawn from N (μ_q; σ_q), the Bhattacharyya distance between these distributions is calculated as follows:

$$D_B(\mathbf{p},\mathbf{q}) = \frac{1}{4}\ln\left(\frac{1}{4}\left(\frac{\sigma_\mathbf{p}^2}{\sigma_\mathbf{q}^2}+\frac{\sigma_\mathbf{q}^2}{\sigma_\mathbf{p}^2}+2\right)\right)+\frac{1}{4}\left(\frac{(\mu_\mathbf{p}-\mu_\mathbf{q})^2}{\sigma_\mathbf{p}^2+\sigma_\mathbf{q}^2}\right) \quad (2)$$

There are similar metrics for measuring Gaussian distribution separation such as the Fisher ratio, but we found that Bhattacharyya distance achieved better experimental performance.

A Channel Redundancy Metric: Kullback-Leibler (KL) divergence is an entropy-based similarity measure used to compute the separation, or divergence, of one probability distribution from another [66]. Unlike Bhattacharyya distance, which depends on an assumption that distributions of interest are Gaussian, KL divergence requires no such

constraint on the shape of the distributions, allowing the flexibility to quantify separation among two probability mass functions (PMF) of arbitrary complexity. Given two PMFs p and q, the KL divergence DKL of p from q is computed as follows:

$$D_{\mathrm{KL}}(\mathbf{p}\|\mathbf{q}) = \sum_i p_i \log \frac{p_i}{q_i} \qquad (3)$$

where p is the distribution of interest, and q is the target distribution for comparison.

Though KL divergence is convex, it is not necessarily symmetric, so Kullback and Leibler also defined an alternative formulation is often used to obtain a bi-directional divergence of p-to-q and q-to-p:

$$D_{\mathrm{KL}}(\mathbf{p},\mathbf{q}) = D_{\mathrm{KL}}(\mathbf{q},\mathbf{p}) = D_{\mathrm{KL}}(\mathbf{p}\|\mathbf{q}) + D_{\mathrm{KL}}(\mathbf{q}\|\mathbf{p}). \qquad (4)$$

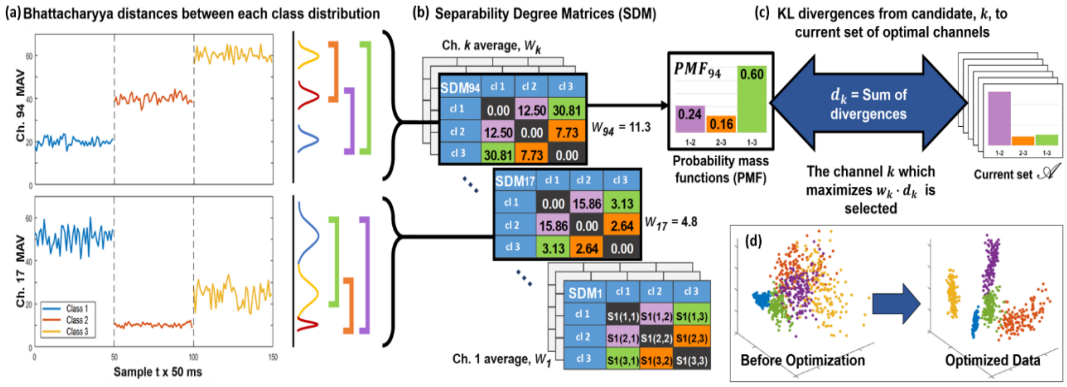

Fig. 4.14. FAMS algorithm for optimal sEMG channel ranking simultaneously maximizes inter-class separation of data while minimizing inter-channel information redundancy. (a) First, the Bhattacharyya distances are computed between each two-class combination of training data recorded from a given channel. (b) These distances are used to create a separability degree matrix (SDM) for that channel and a corresponding probability mass function (PMF). This process is repeated for all channels of the HD sEMG array. The channel of maximum average separation, W_k , is chosen first among the ranked group, A . (c) Next, for every channel k not already in A , the KL divergence is computed from its PMF to every PMF in A and summed together, d_k , providing a sense of the uniqueness of channel k's information content compared to those channels already selected. The channel k which maximizes W_k. d_k is then added to A , and this process is repeated until all 128 channels are in set A . (d) Principal component projection shows that optimized data from the first 8 channels in A creates much better class separation than untargeted channel selection.

4.3.4. Results:

4.3.4.1. Electrode configuration:

After ranking the channels based on FAMS algorithm, the performance of the LDA classifier for pattern recognition with addition of data from these optimal (N-OPT, where N is the number of optimal channels) channels were compared with the performance of 8 equispaced (8-EQUI) electrode channel configuration. Fig. 4.15(a) shows that with increase in number of OPT channels, there is an increase in accuracy until a certain N value after which it saturates. Based on empirical tests, the optimal number of channels at which this saturation occurs was identified as 17. The hypothesis tested was aimed at obtaining performance accuracies significantly greater than 8-EQUI configuration and equivalent to

using all 128 channels. Fig. 4.15(a) also shows that the sEMG from only 4-OPT myosites selected by FAMS are needed to outperform the conventional 8-EQUI configuration for all subjects (denoted by blue dashed line) for 7 movement pattern classification and 6-OPT myosites are needed for 11 movement pattern classification.

The accuracies of 8-EQUI, 6-OPT, 17-OPT and all channels (ALL) were compared and the results are presented graphically in Fig. 4.14(b) for 5, 7, 9 and 11 movement classes for all subjects and amputee subjects, respectively. In Fig. 4.15(b), it can be seen that that the rate of decrease in performance with an increase in number of classes is reduced as the N value increases. For all subjects, we see that myosite selection for 5 classes has a performance accuracy >=75% for 8-EQUI, 6-OPT, 17-OPT and ALL configurations. As more classes are added, accuracies drop to less than 70% for the 8-EQUI and 6-OPT configurations. However, performance accuracy remains >75% for classification of 9 and 11 movement classes using 17-OPT and ALL configurations. Similarly, in amputee subjects, by using 17 OPT and ALL configurations, the average classification accuracy is >80% even across the 9 and 11 movement classes, whereas, it is <60% in 8-EQUI and 6-OPT configuration as seen in Fig. 4.15(b). The p-values in table.I further reflects the aforementioned trend that the significance of using N-OPT configuration becomes more apparent with increase in the number of movement classes considered for the movement pattern classification.

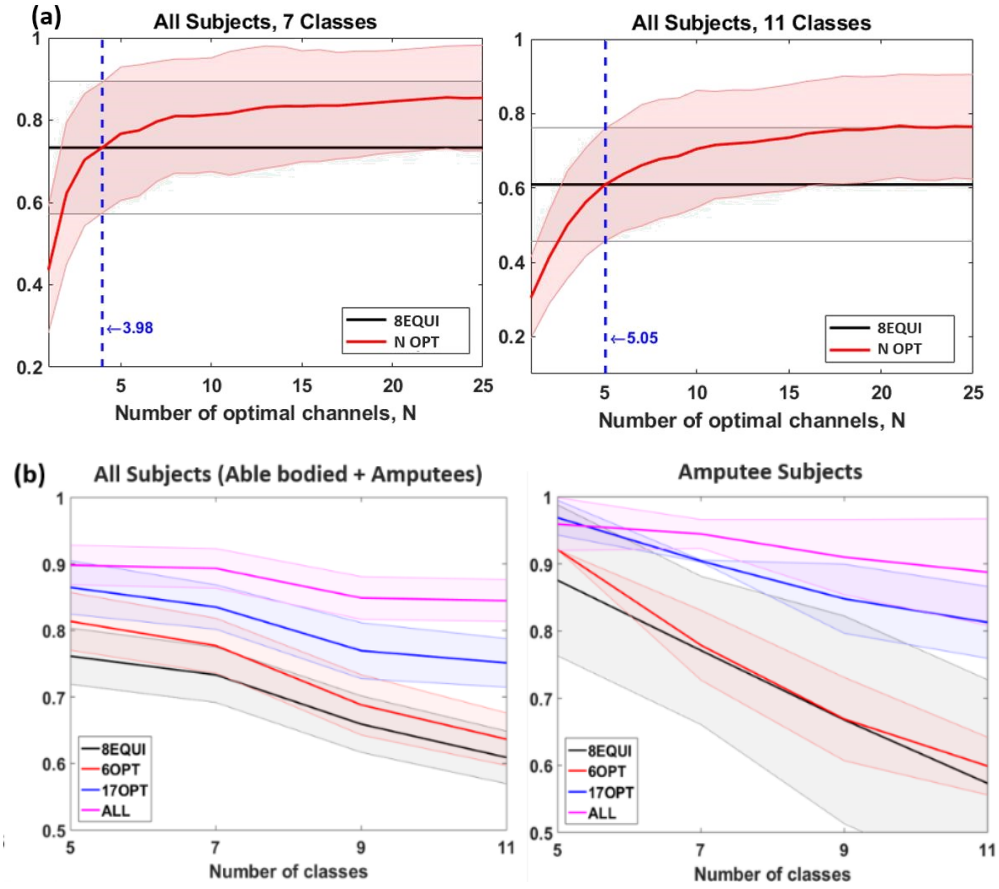

Fig. 4.15. Performance results (a) Aggregate Classification accuracy (Able-bodied + Amputees) comparison for 8EQUI myosites vs N OPT myosite configuration for 7 classes (RE, HO, HC, PR, SU, WF, WE) and for 11 classes (RE, HO, HC, PR, SU, WF, WE, IP, KE, TR, PI), (b) Classification accuracy for 8EQUI myosites, N OPT myosites and Full HDEMG configurations (for 5, 7, 9, and 11 movement classes for all subjects (Able-bodied + Amputees) and Only amputee subjects.

TABLE I

CLASSIFICATION PERFORMANCE COMPARISON OF N OPT MYOSITES WITH 8EQUI MYOSITE CONFIGURATION FOR ALL MC†

Myosite configuration	$MC = 5$	$MC = 7$	$MC = 11$
6OPT	$p = 0.20$	$p = 0.23$	$p = 0.31$
17OPT	**p=0.04**	**p=0.03**	**p=0.007**
FULL HDEMG	**p=0.009**	**p=0.003**	**p=0.0002**

†all MC stands for all movement class combinations namely 5, 7, 11

4.3.4.2. Functional Adaptation:

Myosite selection was performed on data from all subjects using the FAMS and the OPT myosites selected are shown in Figs. 4.16(a) and 4.16(b) for one able-bodied and one amputee subject, respectively. Myosite selection was performed on a set of 5 movement classes (RE, HC, HO, PR, SU), 7 movement classes (RE, HC, HO, PR, SU, WE, WF) and all movement classes (11 classes) respectively.

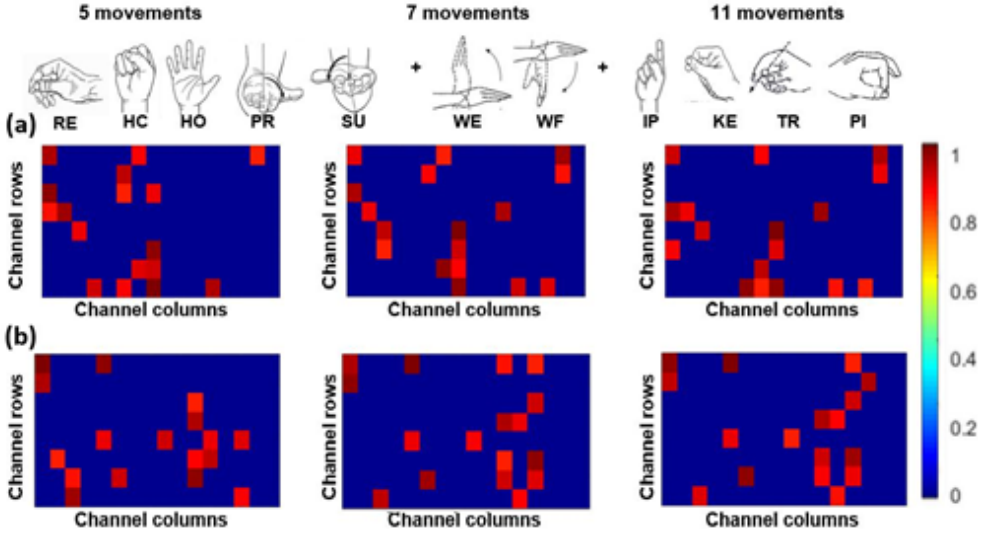

Fig. 4.16. Spatial spread of OPT selected myosites for 5, 7 and 11 movement classes (a) OPT myosites for an able-bodied subject for 5, 7 and 11 classes (b) OPT myosites for an amputee subject for 5, 7 and 11 classes.

The selected OPT sites are based on the ranks in order of saliency based on the algorithms ranking scheme presented in the Algorithm section, i.e. the sites that contribute the most differentiable or unique information are ranked higher than the others. This ranking is represented by the color gradient in the selected sites in Fig. 4.16.

It is evident from the Figs. 4.16(a) and 4.16(b) that the myosites selected for optimal performance of the pattern movement classifier for 5, 7 and 11 movement classes were

different. With inclusion of more number of classes, the myosites appear to be more dispersed covering the width of HD sEMG image map region as shown in these figures. Figs. 4.17(a) and 4.17(c) show the confusion matrices for classification performance of 8 equispaced (8EQUI) myosite configuration and 17 optimal (17OPT) myosites selected through FAMS respectively for an able-bodied subject for 5,7 and 11 movement classes. Similar results for an amputee subject are shown in Figs. 4.17(b) and 4.17(d).

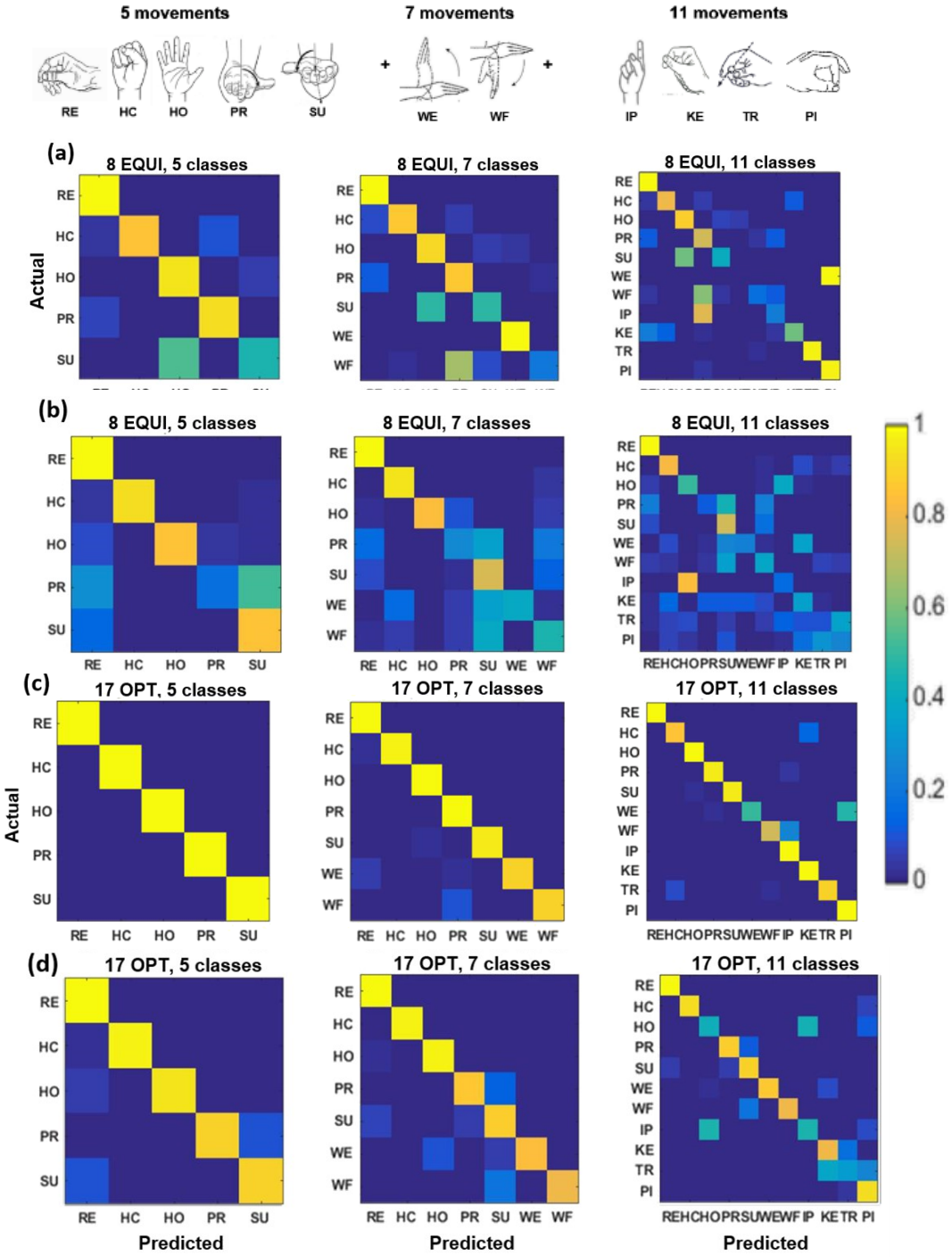

Fig. 4.17. Confusion matrix for performance for 5, 7 and 11 movement classes of (a) 8EQUI myosite configuration for an able-bodied subject (b) 8EQUI myosite configuration for an amputee subject, (c) 17OPT myosite configuration for an able-bodied subject, (d) 17OPT myosite configuration for an amputee subject.

4.3.5. Discussion:

As discussed earlier, previous studies have shown that the error rates in classification increases with addition of movement classes [43], [21]. Farrell and Weir's work [29], that showed there is not much difference in targeted and untargeted surface electrode placements, used only gross movement classes, in other words, highly differentiable classes. To exploit the maximum capabilities of the muscles of the residual limb, FAMS provides adaptation in both the number and location of selected control sites. FAMS allows selection of N-OPT channels and from the results shown in Fig. 4.15 it is evident that there is significant difference in performance of subjects when using 8-EQUI vs N-OPT myosites. FAMS selects N-OPT myosites for any given set of movement classes, based on which the amount of rise in this error rates is reduced. This can be seen in Fig. 4.15(b) from the reduction in fall of accuracy when choosing N-OPT myosites. It is also interesting to note that, since the myosite selection criteria considers the anatomical correspondence to arrive at optimal sites based on maximum separability, even as low as 4 and 6 optimally selected myosites outperform the conventional 8-EQUI configuration for 7 and 11 movement classes as seen in Fig. 4.15(a).

Daley et al's work [43] concluded that there is no significant difference in classification accuracies when the electrodes were reduced to 8 in amputee subjects, irrespective of whether they were placed optimally or distributed equally. They, thus, optimized the number of classes that a subject can perform best and showed that the amputee subjects were able to perform only 4-6 classes with a classification accuracy better than 80%. However, their optimization criterion was solely based on best possible performance accuracy using sequential forward selection, whereas, FAMS uses a more anatomically

relevant optimization criterion based on movement class separability and is able to accommodate up to 11 movement classes with >80% accuracy in amputee subjects as shown in Fig. 4.15(b).

In Fig. 4.15(a), shows that the change in performance accuracy becomes less apparent with increasing number of optimal channels. For example, after 17 optimally chosen myosites, the slope on the performance accuracy curve begins to approach 0. From Fig. 4.15(a), it is evident that while ideally, the best performance accuracy is achieved by using data from all 128 myosites, practically it may not be feasible to do so due to high computational demand. There is a trade-off between accuracy and efficiency, which limits the number of myosites that can actually be used for real time prosthesis control. However, even with this trade-off, the limited number of optimal myosites that are selected using FAMS (in this case, 17-OPT myosites), help achieve performance accuracies that are empirically equivalent to using all 128 myosites, for a large number of movement classes which includes both gross and fine motor movements. Thus, FAMS finds a balance between computational cost and improved performance and the results obtained show >80% accuracy for 11 movement classes, for amputee subjects, using 17-OPT myosites selected by FAMS.

Observing the myosites selected by FAMS in Fig. 4.16 also reveals an interesting trend in the location of sites selected with inclusion of fine movement classes. From Fig. 4.16(a), it can be seen that for an able-bodied subject more number of channels are selected in the fine motor control region, represented by the bottom half of the image map, with inclusion of fine movement classes. However, for an amputee subject, as shown in Fig. 4.16(b), the selection of myosites is based on the regions of the residual limb with intact muscle activity.

This observation also supports the significance of the anatomically relevant site selection criteria used by FAMS.

In the confusion matrices shown in Fig. 4.17, we can see that the diagonalization improves when 17-OPT myosites selected through FAMS are used for classification. In some movement classes, the related muscles activated are very similar to each other compared to the remaining movement classes. Thus, the data is closer in the feature space i.e. data points are interspersed and hard to discriminate. These are referred to as overlapping movement classes in this discussion. FAMS improves discrimination of such movement classes substantially. This is clear from the improved diagonalization of the confusion matrices in Fig. 4.17. We also see that performance gains are improved for these overlapping movement classes as the accuracy values in the diagonals are higher for 17-OPT configuration seen in Fig. 4.17.

Fig. 4.17 also shows that the precision grip classes (RE, HO, HC, TR, PI, KE, IP) separate much better while using 17-OPT myosites when compared to classification using 8-EQUI myosites. FAMS adapts the control site choice to match most separable myosites in order to provide maxi-mum distinguishability in signal patterns, which according to Powell et al. [27] is one of the major requirements for a pattern movement classifier to perform well. This reduces the need to induce pattern modifications during training sessions, as demonstrated in Powell et al.'s work [27], in order to incorporate distinguishability in such overlapping movement classes. This, in turn, is likely to reduce the pre-prosthetic training time and allow users to obtain a prosthesis earlier than currently possible.

From FAMS, we can see that the most differentiable sites may not be same as those with high muscle activity sites for a given set of movement classes. In Fig. 4.18, a comparison

between regions of high muscle activity and the sites selected by the FAMS system for optimum classification performance shows that they are not necessarily the same.

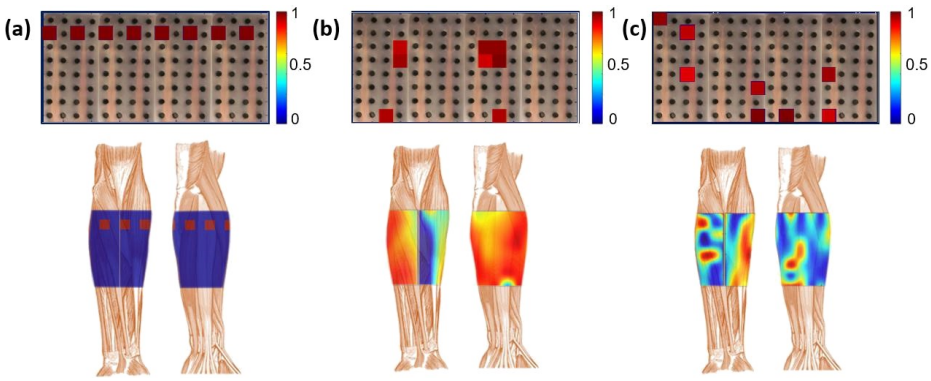

Fig. 4.18. 128 channel HD sEMG arrays showing myosites from different selection methods and anatomical correspondence of selected myosites: a) 8EQUI configuration: all 8 myosites have equal significance, b) Muscle activity map showing sites likely to be selected by palpation: high intensity sites (in red) are most likely to be selected, c) HD sEMG arrays showing 8OPT myosites selected by FAMS system and forearm with corresponding SIM showing myosites most likely to be selected.

The concept of functionally adaptive myosite selection is unique and has not been implemented before. FAMS is able to successfully quantify separability through the use of SDM and remove redundancy to output the most unique myosites for a given set of movement class patterns. In addition, the spatial distribution (spread) of myosites from our method is likely the result of minimizing the information redundancy described in the algorithm section. Clinically, this means that neighboring sites are more likely to convey similar information and since our method tries to avoid this redundancy, we achieve a good spatial spread. The ability of FAMS to provide adaptation can be utilized by the user to customize the classes that the prosthesis controls based on the individuals needs and can be dynamically change over the course of the use. Users could also customize movement classes that the prosthesis needs to control based on the place of use or need for repetitive tasks in a given scenario where reliability of a fewer movement classes are of importance.

FAMS uses LDA with only one EMG feature and still produces accuracy values comparable to previous study [8] which uses a combination of time domain (TD) and autoregressive (AR) features. Hence, there is further scope for FAMS to be tested with more number of features and better pattern movement classifiers to improve its efficiency.

Chapter 5: Conclusion and future directions

5.1. Conclusion:

In this work, we developed a custom designed HD sEMG array and an adaptive algorithm to go with the arrays in order to make myosite selection for pattern recognition more adaptable to the needs of the user as well as to improve the functionality of the pattern recognition based myoelectric systems. This work provides a reliable, more quantitative approach for selecting N OPT control sites for an upper limb myoelectric prosthesis system. Results show that myosite selection becomes more significant with increase in number of movement classes. This is seen from the statistical significance of difference in performance accuracies of the sites selected by the FAMS system over current untargeted electrode placements. Performance of 6 and 17 optimal sites selected by the FAMS system was compared with performance of untargeted electrode configuration for 5, 7 and 11 movement classes. Table I in chapter 4 shows that the p-value of a 2 sample t-test - left tailed with unequal variances, improves from 0.2 to 0.007 for 6 optimal myosites selected by the FAMS method (5 movement classes) and 17 optimal myosites selected by FAMS (11 movement classes), respectively. Results of FAMS study also show that >80% accuracy can be achieved for 11 movement classes for amputee subjects, using 17 optimal myosites selected by FAMS even while using a single sEMG feature (MAV) along with the basic LDA classifier. FAMS system provides the ability to expand the functionality of the fitted prosthesis and pattern recognition system without the need to go through the process of prosthesis refitting. While this method of functionally adaptive site selection can be expanded for use by people with higher level of amputations, like trans-humeral amputations or shoulder disarticulations, more experiments and further validations need to

be performed to prove similar performance gains as the trans-radial case. While offline results are promising, we cannot make definitive claims about the superiority of this method over existing methods. In order to do so, real-time decoding performance and functional evaluations are warranted to ensure the improvement in decoding accuracy that can translate into real-world usability.

In this chapter, we will discuss the future directions of this work in an attempt to suggest other capabilities of FAMS and to work out steps to make this a feasible system to be used in a commercial myoelectric prosthesis.

5.2. Future directions:

5.2.1. FAMS for temporal adaptation of control sites in myoelectric prosthesis:

The muscles activated during a contraction become capable of producing more localized signals with practice over time, i.e. noise or co-contraction is reduced and hence, the optimal myosites selected for a given set of classes migrate over time with practice. FAMS has the capability to provide adaptation to such temporal variations and can be a highly useful alternative to the current system of using fixed myosites. Preliminary studies were conducted to confirm the hypothesis that there is migration of optimal myosites with practice over time, and FAMS system can be used to adapt to this migration. FAMS system can thus provide temporal adaptation to changing capability of the residual limb muscles. This can enable the users to get access to a pattern recognition based prosthesis sooner as well as use the same system during and after training, to gain maximum performance with the capability of the muscles at any given time. The results of these studies are presented below.

5.2.1.2. Preliminary work:

a) Methods:

As explained in chapter 4, inexperienced subjects were trained over a period of 7 days and HD sEMG data for all 11 movement classes were collected on all 7 days. The HD sEMG data collected from these 4 inexperienced subjects were used as preliminary data to test if the above mentioned hypothesis is true. For this analysis only 4 movement classes, namely hand open (HO), hand close (HC), wrist pronation (PR) and wrist supination (SU) were used since those were the only 4 classes that the subjects practiced with using the virtual training system on all 7 days of the training.

The HD sEMG muscle activity maps were created as described in chapter 3 section 3.2.1 and the normalization was performed across data of 7 days for each movement class. The muscle activity maps thus produced for one able bodied subject for HO class from all 7 days is shown in Fig. 5.1 to represent the validity of this hypothesis.

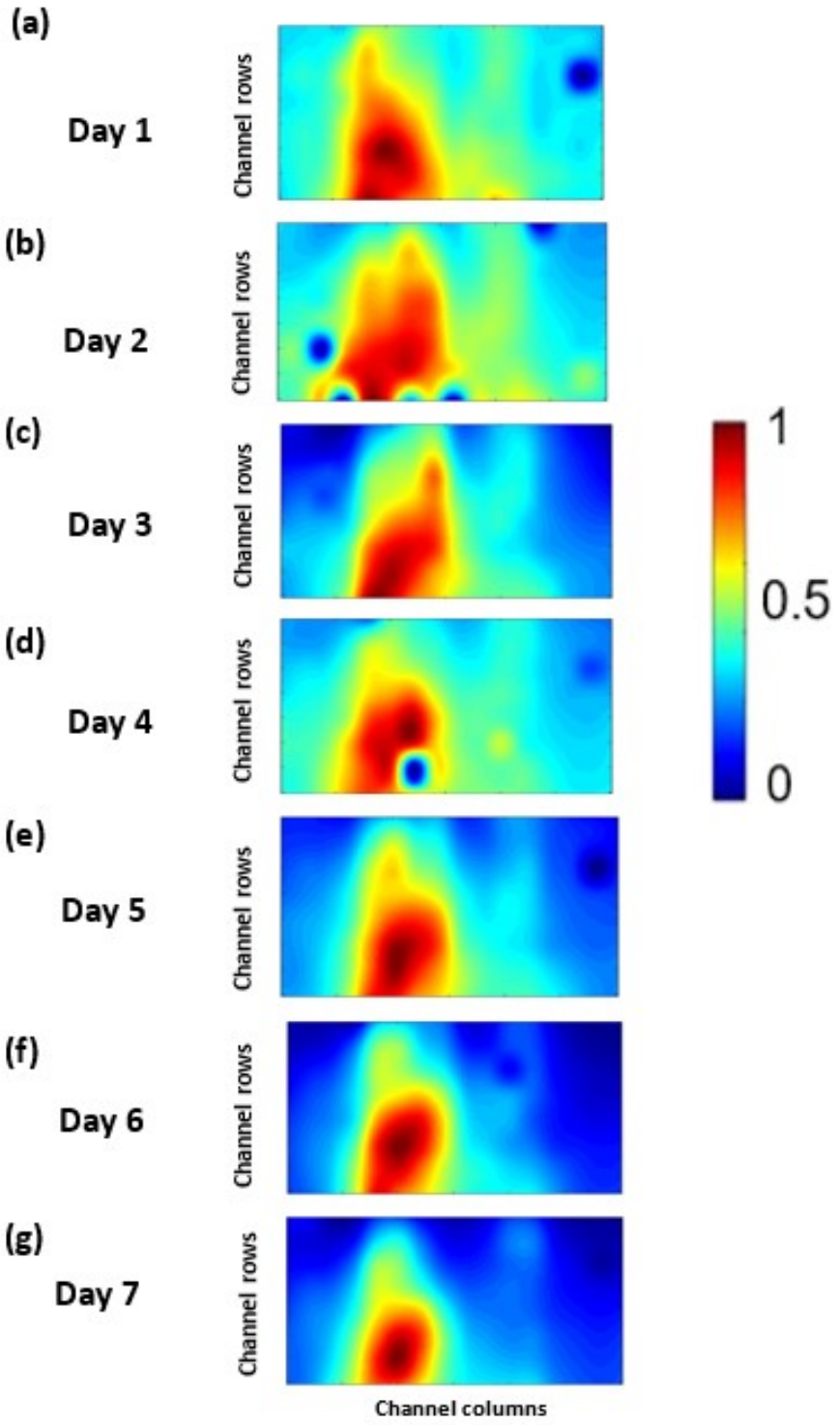

Fig. 5.1. HD sEMG muscle activity map for one able-bodied subject for HO class from (a) Day 1, (b) Day 2, (c) Day 3, (d) Day 4, (e) Day 5, (f) Day 6, (g) Day 7. The image maps shown here are normalized [values from 0 to 1] across 7 days for comparing region of muscle activity for a given subject for HO class from the 7-day training.

Similar image patterns were created for HC, PR and SU data. It is important to note that these are normalized image maps and hence the amount of contraction does not affect these image patterns. On visual inspection of image maps in Fig. 5.1, it can be seen that the muscle activation gets localized over the 7 days. For quantitative evaluation of this trend, color segmentation was performed on the 4 movement classes mentioned above for all 7 days using thresholding method. To select image thresholds, the RGB color thresholder app from MATLAB was used. To remove regions of inactivation, histogram threshold mask was created with lower and upper bound of 0 and 141 on the blue color space and 0 to 255 on the red and green color space, in order to preserve only the regions of muscle activation and remove the inactive muscle regions. These thresholds were arrived at using visually inspecting the image maps while changing the image thresholds to identify the best threshold values. The segmented regions of muscle activity are shown as black and white images with white spaces indicating the region of interest from the color map images in Fig. 5.1 is shown below in Fig. 5.2.

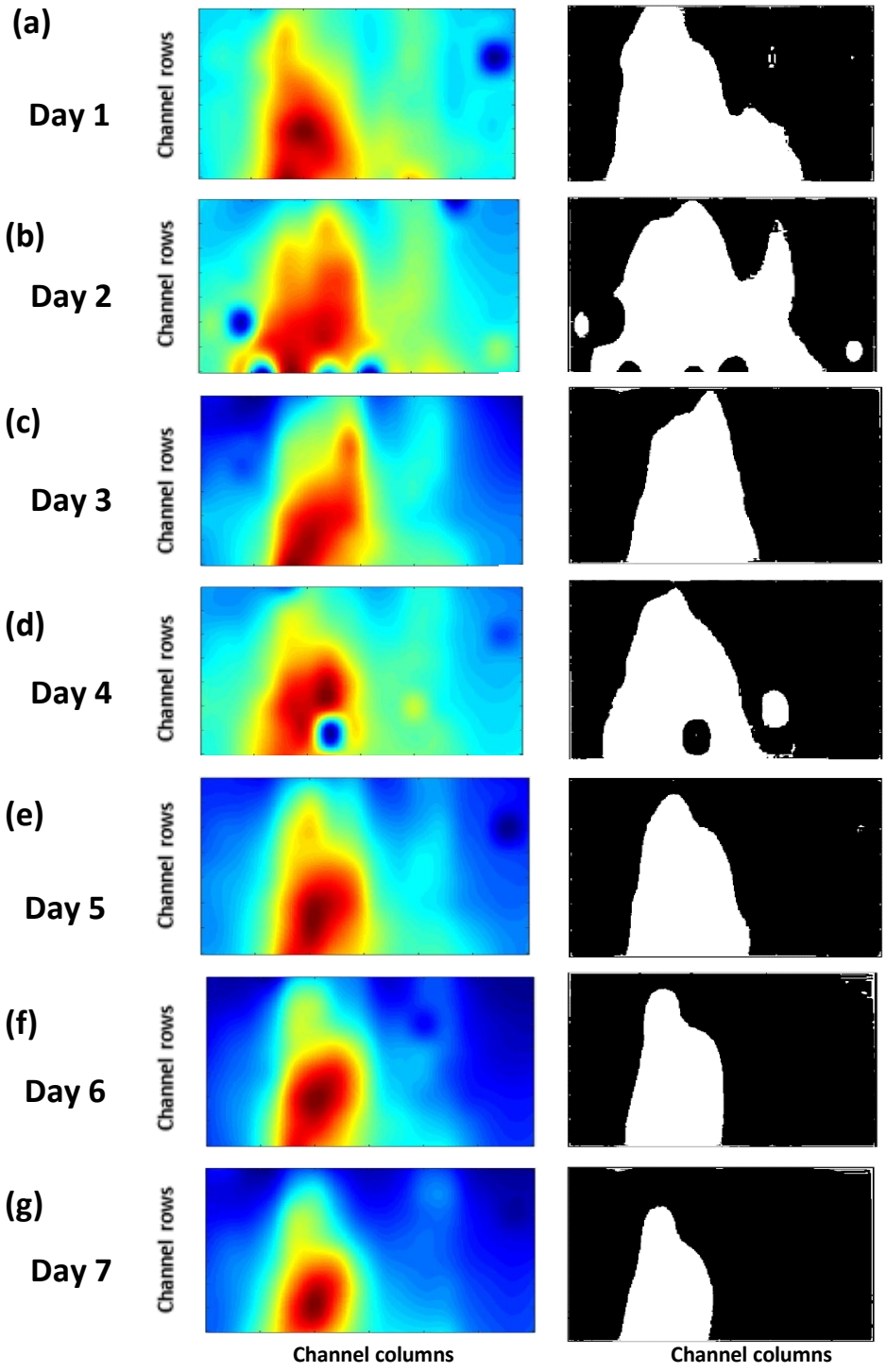

Fig. 5.2. Muscle activity maps and corresponding segment masks created from HD sEMG data for one able-bodied subject for HO class from all 7 days of training to quantify localization of region of muscle activation. Muscle activity maps are normalized and same scale as Fig.5.1. The masks are shown as binary images with white regions corresponding to area of interest or muscle activation regions.

This segmentation was performed for all 4 classes and all 4 subjects, and the segmented area as a percentage of the whole HD sEMG image map region was averaged across all 4 classes, 4 subjects for 7 days. This is represented graphically in Fig. 5.3.

Here the "regions of muscle activations" are regions which have muscle activity and show up in the color segment masks shown in Fig.5.2.

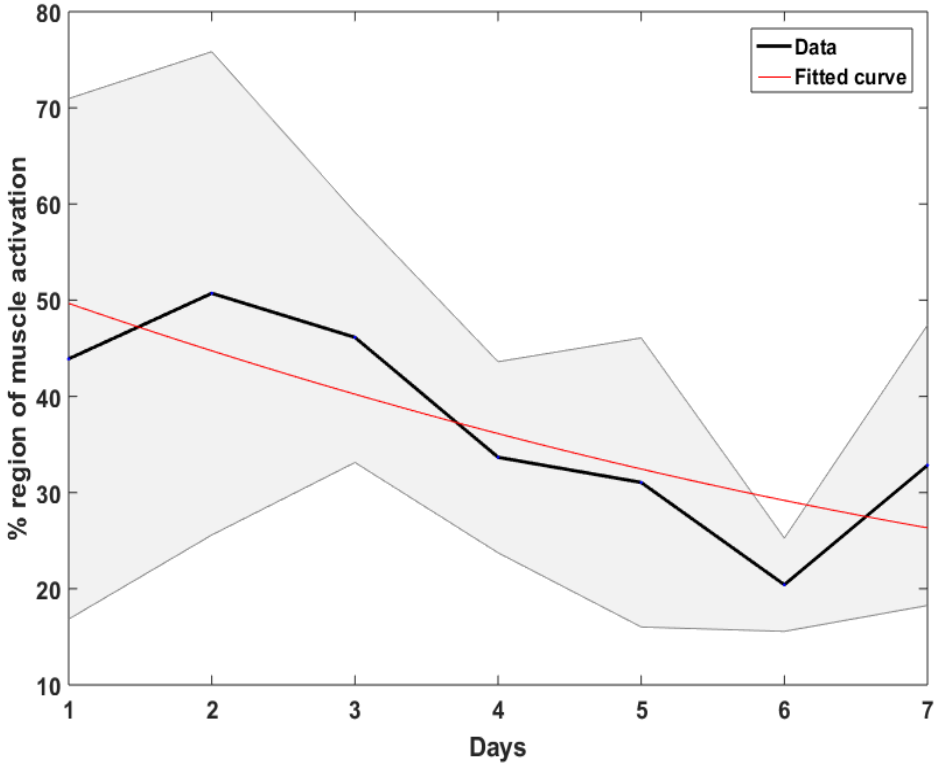

Fig. 5.3. Effects of training on muscle activity: Average percentage muscle activation region with practice over a period of 7 days of 4 subjects for 4 movement classes is shown here. The graph clearly shows that the region of muscle activation gets more localized or decreases with practice represented by the fitted curve (red line) in the graph.

Fig. 5.3 shows average muscle activation region of all 4 classes and 4 subjects over a period of 7 days. From Fig. 5.3, it can be seen that the total region of muscle activation reduces with practice resulting in more localized muscle activation with the least amount of noise.

This is shown by the fitted curve in the graph in Fig. 5.3. This result support the hypothesis that, with practice, subjects are able to produce more localized, cleaner signals for each of the motion classes. With this kind of localization of muscle activation, optimal myosites selected based on the separability index maps (explained in chapter 4) also change. To demonstrate this, the separability index maps along with the performance metric for the above mentioned 4 movement classes for one of the subjects are shown in Fig.5.4 and 5.5 respectively; the maps show the results from Day 1 to Day 7.

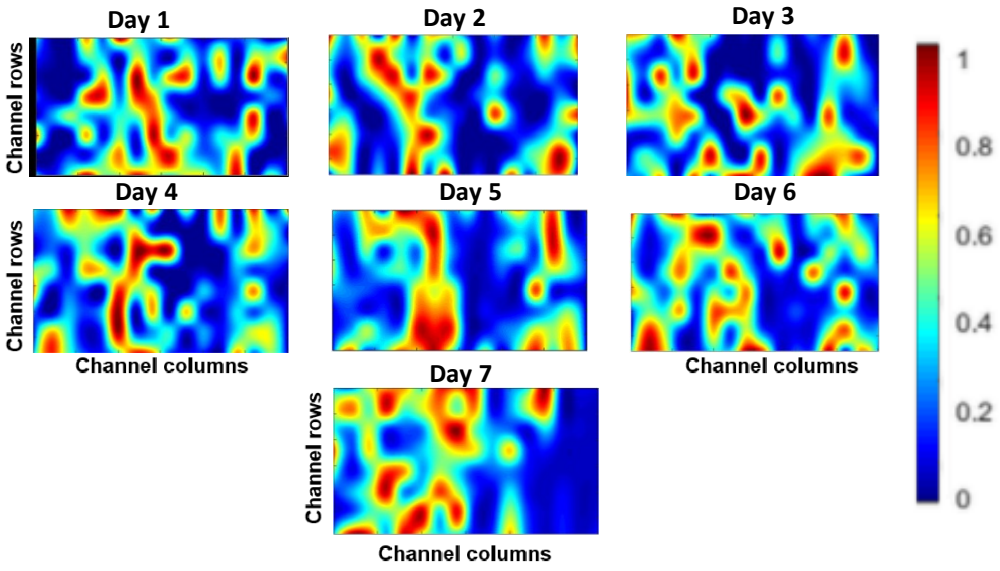

Fig. 5.4. Migration of optimal channels over time and performance results: Separability index map(SIM) for one able-bodied subject for 4 classes (HO, HC, PR, SU) through 7 days to show migration of optimal regions represented by high intensity or red colored areas in the SIM.

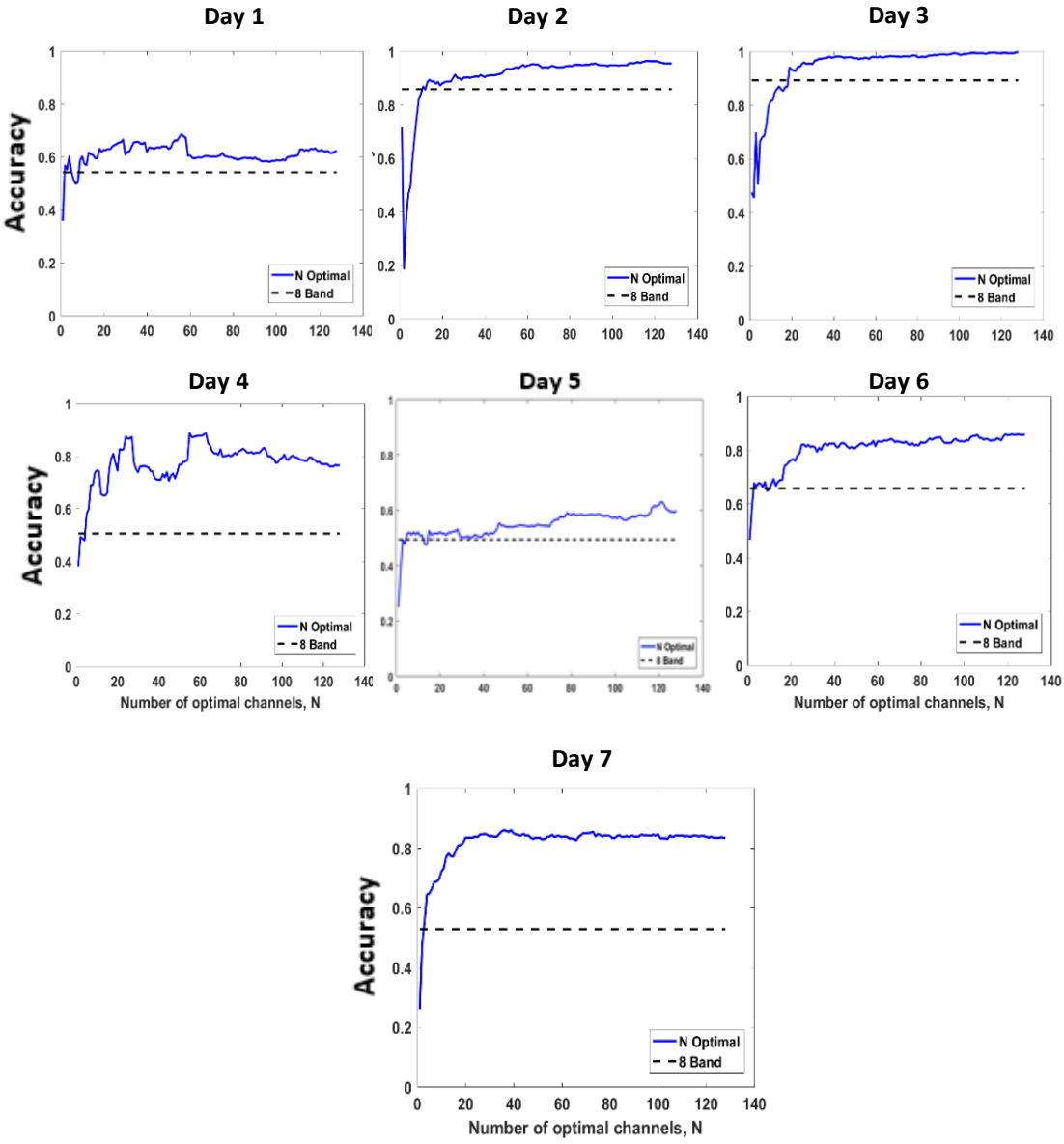

Fig.5.5. Performance accuracy vs number of optimal channels graph showing the performance of N-optimal channels (represented by blue lines) and 8 equispaced configuration (represented by horizontal dotted lines) for comparison of current untargeted electrode placement configuration and electrode configuration selected by FAMS system.

As shown in Fig. 5.4 there is a clear migration of regions with high separations indicated by the red regions. However, the aim of the proposed system is to provide the best possible performance on any given day/ phase of training, irrespective of the optimal myosite

locations. This can be seen in the N optimal vs 8 equispaced electrode configuration (explained in Chapter 4) performance graphs shown in Fig. 5.5.

Thus, we claim that the FAMS system is also capable of adapting to the temporal changes in the muscle physiology that is brought about by practice. This system can, thus, serve as a desirable solution to the issues with myoelectric prosthetic control arising from the configuration and orientation of electrode placements. However, this conclusion is reached only from the preliminary data presented here, and further long term study needs to be done to support this claim.

5.2.2. FAMS as a universal electrode interface:

The ultimate goal of this project is to have an off-the-shelf universal electrode system along with an add-on algorithm that can be used in a myoelectric prosthesis for people with any level and type of amputation. For this, the system should also accommodate site selection for direct control so that the user can switch to direct control in case of emergencies when pattern recognition fails to work or repetitive tasks that require antagonistic muscle movements where direct control can be easier to use.

The criteria for achieving good performance in direct control system is that there should be minimal cross talk between the antagonistic muscle activities [67]. Currently, a prosthetist selects myosites using the palpation method and/or by moving bipolar electrodes on to the region of interest to locate the sites with maximum amplitudes. However, the HD sEMG system provides the capability to simultaneously obtain muscle activity of the whole residual muscle and hence, the best 2 sites for direct control can be quantitatively selected.

5.2.2.1. Preliminary work:

a) Method:

Signal to noise ratio(SNR) is used as the criterion function [67] for direct control site selection. Here, signal amplitude from the electrode contact on the flexor muscle during wrist flexion is considered the "signal" and the signal amplitude from the electrode contact on the extensor muscle during wrist flexion is regarded as noise since that is not the signal of interest. Based on these criterion, the SNR value is calculated for all the 128 channels and the myosites with the maximum SNR is selected as the best sites for direct control.

The validity of this proposed method is demonstrated by selecting sites on an able-bodied subject using the manual myosite selection procedure and the SNR based myosite selection technique, and the signals from both sets of selections are then evaluated by visualizing the signals from these myosites using bipolar electrodes.

b) Method for manual site selection:

Muscle locations were manually selected to place bipolar electrodes for a direct control system by palpating/ moving bipolar electrodes on the site of interest to get the location with highest intensity signal. These sites were marked as shown in Fig. 5.6 (a). The process of manual selection was done both by a prosthetist as well as a novice in order to demonstrate how the level of experience of a person can affect the process of myosite selection. Bipolar electrodes, namely the IBT Element^{TM} electrodes (Infinite biomedical technologies, Baltimore), were placed on the selected antagonistic muscle pair as shown in Fig. 5.6 (b). Signals from both electrodes are visualized on the Element^{TM} GUI for visual inspection of SNR. The signals from these electrodes are shown in Fig. 5.6 (c).

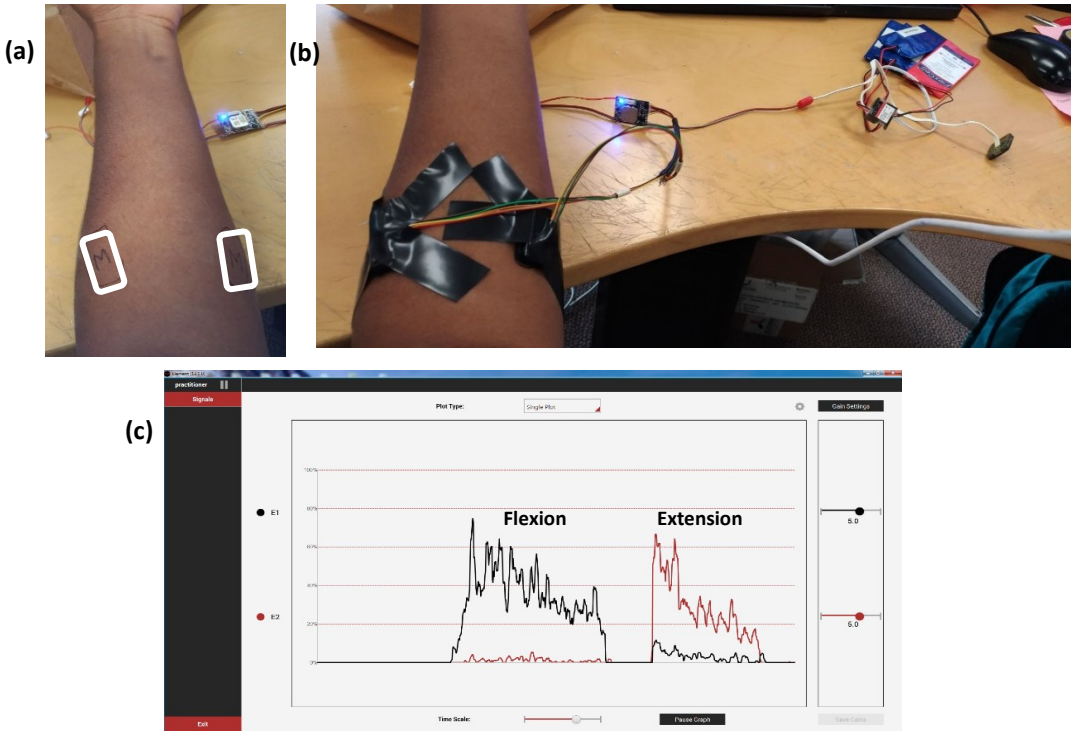

Fig. 5.6. Manual site selection by novice personnel: (a) Sites manually selected by a novice on an able-bodied subject for direct control, (b) electrode setup for signal visualization, (c) element electrode GUI showing signals from wrist flexion and extension. The black signal corresponds to the electrode placed on the wrist flexor region and red signal corresponds to the electrode placed on the wrist extensor region.

Similarly, the sites selected by an experienced person on the same subject along with the signals from these sites are shown in Fig. 5.7 (a) and 5.7 (b) respectively.

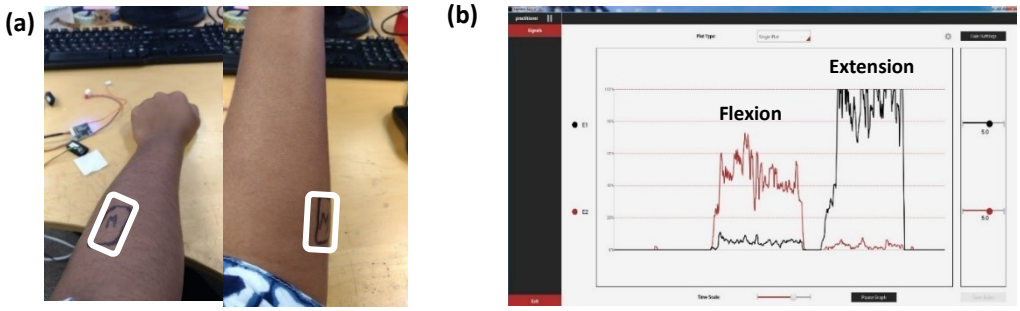

Fig. 5.7. Manual site selection by experienced personnel (a) Sites manually selected by an experienced person on an able-bodied subject for direct control, (b) element electrode GUI showing signals from wrist flexion and extension. The red signal corresponds to the electrode placed on the wrist flexor region and black signal corresponds to the electrode placed on the wrist extensor region.

c) Experimental setup:

HDEMG electrodes were wrapped over the limb and signals are acquired as mentioned in chapter 3. Signals were acquired for flexion and extension for 3 trials and were processed using the MATLAB codes as explained in chapter 3.

d) Results and discussion:

The muscle activity image maps and normalized SNR image maps, as shown in Fig. 5.8 (a), (b) and 5.8 (c), (d) respectively, suggest the best locations for placing the electrodes. The SNR image maps along with the sites selected by a trained personnel, a novice personnel and the algorithm are shown in Fig. 5.8.

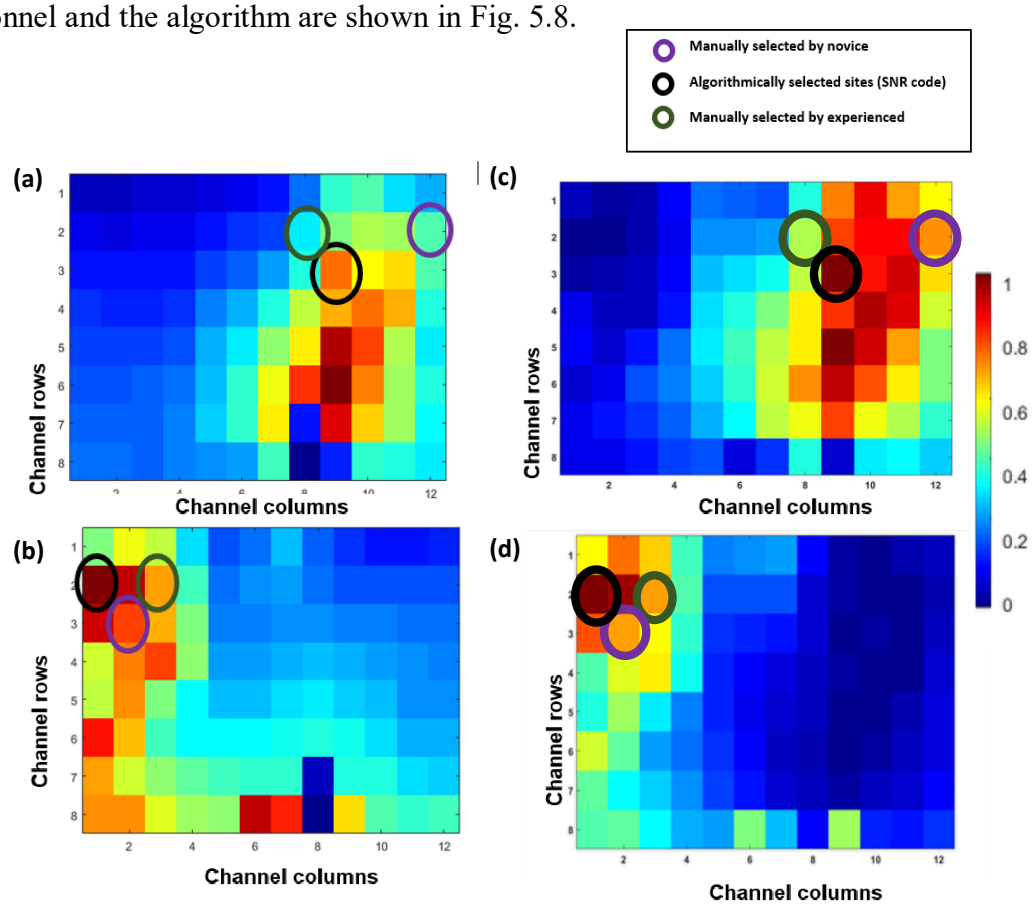

Fig. 5.8. Image maps for Algorithmic site selection (a) Muscle activity map for wrist extension (WE) showing selected sites, (b) muscle activity map for wrist flexion (WF) showing selected sites, (c) normalized SNR maps with WE as signal and WF as noise, (d) normalized SNR maps with WF as signal and WE as noise.

These locations were mapped back on to the subject's arm and marked as shown in Fig. 5.9(a). Bipolar electrodes were placed with the center on the selected location and the electrode parallel on the muscle along the longitudinal axis, as explained in chapter 4 section 4.2.3.5, on the selected antagonistic muscle pair and signals from both electrodes are visualized on the element GUI for visual inspection of SNR and are shown in Fig. 5.9 (b).

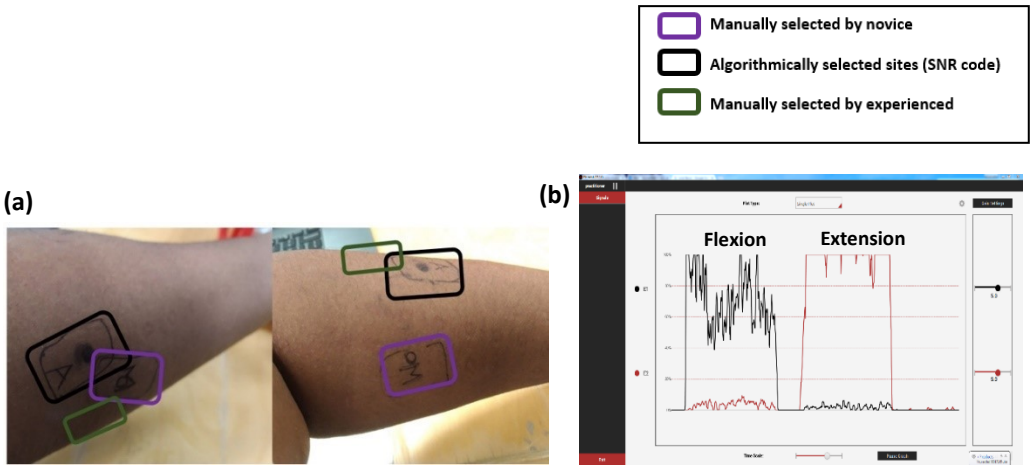

Fig. 5.9. Algorithmically selected myosites: (a) Selected sites marked on the subject's forearm, (b) Element™ electrode GUI showing the integrated EMG envelope signals from wrist flexion and extension tasks for algorithmically selected sites. The black signal corresponds to the electrode placed on the wrist flexor region and red regnal corresponds to the electrode placed on the wrist extensor region.

Results suggest that the sites selected with the HDEMG electrodes have a much better SNR even when tested with bipolar electrodes. Higher SNR values should help provide better usability since the threshold would be much cleaner and chances for false positives are highly reduced.

5.2.3. HD sEMG array design to fit into a prosthetic socket:

The next step to incorporate the FAMS system into a myoelectric prosthesis is to incorporate the design to fit inside a prosthetic socket. For this, the HD sEMG electrode

arrays were made smaller and denser to pick up as much information as possible from the residual limb. The flex array design was made using Altium designer software (Altium LLC, CA). To make the arrays more flexible, unwanted areas of polyimide material was removed and made minimal. The proposed design to be used with a prosthetic socket is shown below in Fig. 5.10.

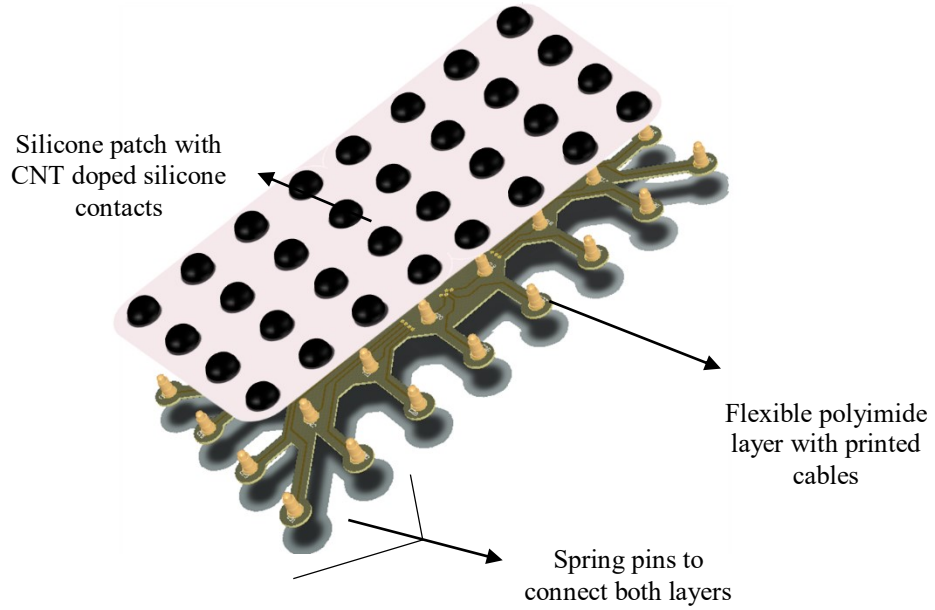

Fig. 5.10. Compact hybrid array design to fit inside of a prosthetic socket.

The prototype based on this design was fabricated and assembled. Flexible connectors were also designed and prototyped to connect these arrays to the existing Intan data acquisition setup used in the previous studies (Refer section 3.2.1 for more information). Images of the prototypes along with the connectors and setup is shown in Fig. 5.11.

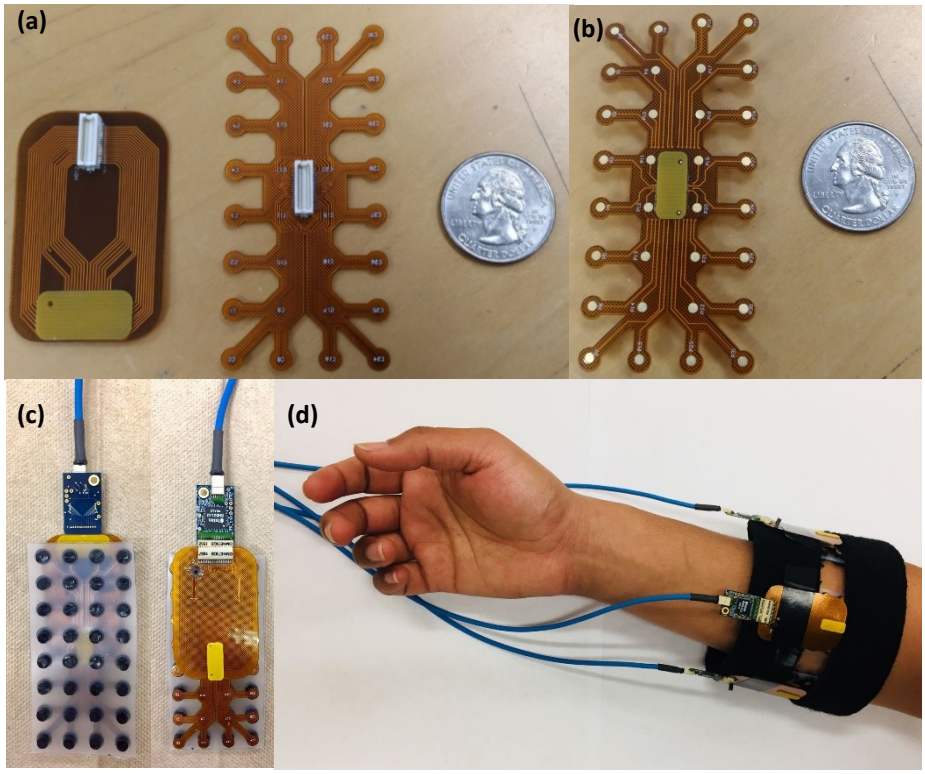

Fig. 5.11. Compact hybrid array prototype: (a) Compact hybrid array design with custom fabricated flexible connectors, (b) compact hybrid array showing the contact side, (c) Assembled and connected arrays, (d) array setup for data collection.

The compact hybrid arrays were used to gather sEMG data from an able-bodied subject. sEMG data were also gathered from the same subject using the hybid arrays (DI3) used in chapter 3 and 4. The compact hybrid arrays were positioned such that it covered the mid region of the hybrid array placement. The HD sEMG image maps of data collected from one of the able-bodied subjects is shown in Fig. 5.12.

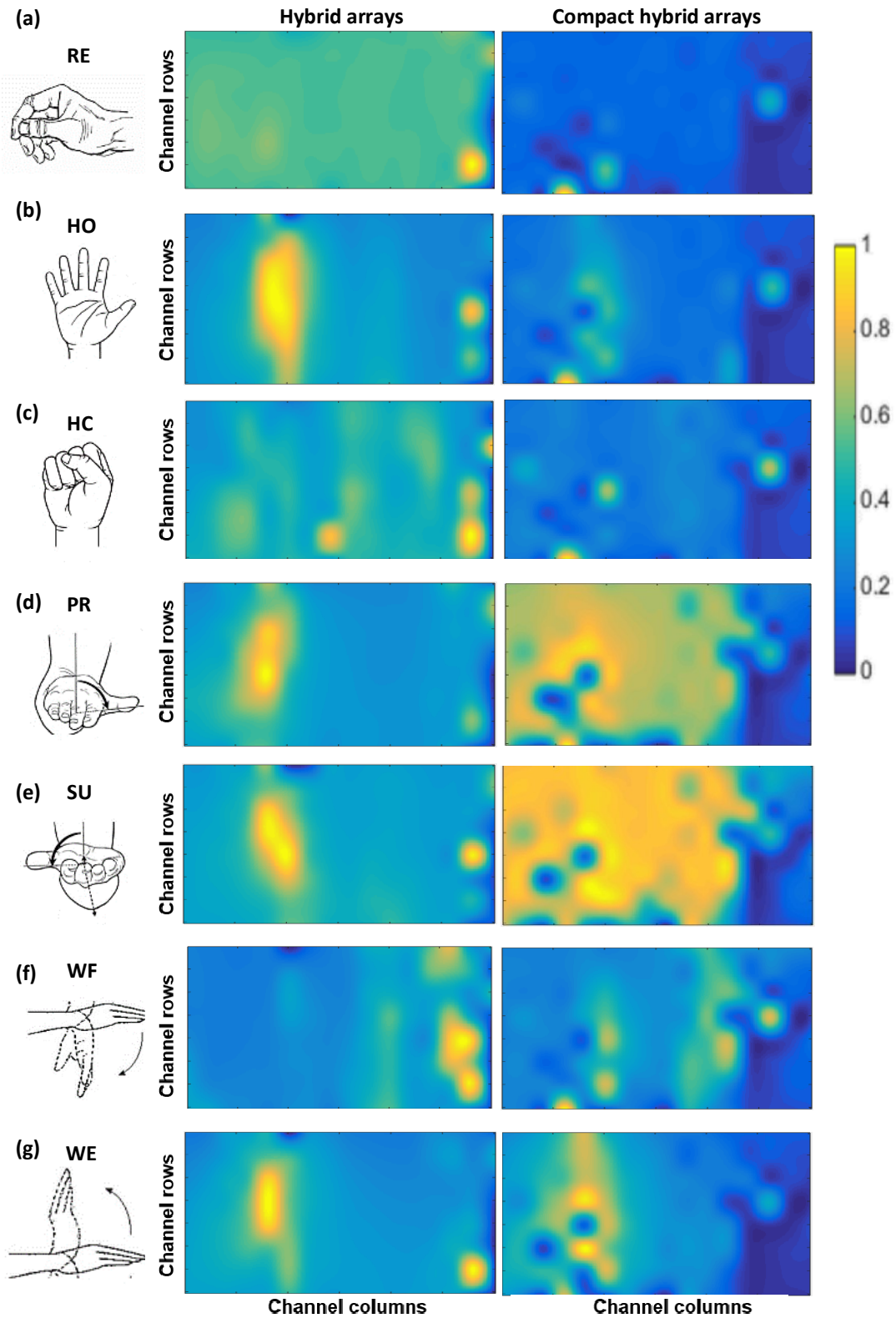

Fig. 5.12. Muscle activity map comparison: Muscle activity map created from MAV values shown for one able-bodied subject for the hybrid arrays and compact hybrid arrays (a)RE, (b) HO, (c) HC, (d) PR, (e) SU, (f) WF, (g) WE.

The one final step to making FAMS a reality is to build an online HD sEMG system and an HD sEMG based training system. Ideally a user should be able to put on the HD sEMG arrays embedded in a socket and train using the online training system. A universal off-the-shelf system like this could reduce a lot of fitting and training effort and time and bring standardize the system of fitting of a pattern recognition based myoelectric prosthesis.

REFERENCES:

[1] P. A. Parker and R. N. Scott, "Myoelectric control of prostheses," Crit. Rev. Biomed. Eng., vol. 13, no. 4, pp. 283–310, 1986.

[2] K. Norton, "A brief History of Prosthetics," InMotion, vol. 17, no. 7, pp. 1–3, 2007.

[3] May, Bella J., and Margery A. Lockard. Prosthetics & orthotics in clinical practice: a case study approach. FA Davis, 2011.

[4] K. Ziegler-Graham, E. MacKenzie, P. Ephraim, T. Travison, and R. Brookmeyer, "Estimating the prevalence of limb loss in the United States: 2005 to 2050.," Arch. Phys. Med. Rehabil., vol. 89, no. 3, pp. 422–9, 2008.

[5] F. Cordella et al., "Literature review on needs of upper limb prosthesis users," Frontiers in Neuroscience, vol. 10, no. MAY. 2016.

[6] K. Østlie, I. M. Lesjø, R. J. Franklin, B. Garfelt, O. H. Skjeldal, and P. Magnus, "Prosthesis rejection in acquired major upper-limb amputees: A population-based survey," Disabil. Rehabil. Assist. Technol., vol. 7, no. 4, pp. 294–303, 2012.

[7] E. Biddiss and T. Chau, "Upper limb prosthesis use and abandonment: A survey of the last 25 years," Prosthetics and Orthotics International, vol. 31, no. 3. pp. 236–257, 2007.

[8] M. D. Northmore-Ball, H. Heger, and G. a Hunter, "The below-elbow myo-electric prosthesis. A comparison of the Otto Bock myo-electric prosthesis with the hook and functional hand.," J. Bone Joint Surg. Br., vol. 62, no. 3, pp. 363–367, 1980.

[9] K. Bhaskaranand, A. K. Bhat, and K. N. Acharya, "Prosthetic rehabilitation in traumatic upper limb amputees (an Indian perspective).," Arch. Orthop. Trauma Surg., vol. 123, no. 7, pp. 363–6, 2003.

[10] Reid, D., and A. Fay. "Survey of juvenile hand amputees." J Assoc Child Prosthet Orthot Clin 22.3 (1987): 51-55.

[11] M. Asghari Oskoei and H. Hu, “Myoelectric control systems-A survey,” Biomed. Signal Process. and Control, vol. 2, no. 4. pp. 275–294, 2007.

[12] C. Pylatiuk, S. Schulz, and L. Döderlein, “Results of an internet survey of myoelectric prosthetic hand users,” Prosthet. Orthot. Int., vol. 31, no. 4, pp. 362–370, 2007.

[13] E. Biddiss and T. Chau, “Upper limb prosthesis use and abandonment: A survey of the last 25 years,” Prosthetics and Orthotics International, vol. 31, no. 3. pp. 236–257, 2007.

[14] C. H. Jang et al., “A Survey on Activities of Daily Living and Occupations of Upper Extremity Amputees,” Ann. Rehabil. Med., vol. 35, no. 6, pp. 907, 2011.

[15] E. Scheme and K. Englehart, “Electromyogram pattern recognition for control of powered upper-limb prostheses: State of the art and challenges for clinical use”, J. Rehabil. Res. Dev., vol. 48, no. 6, p.643,2011.

[16] Coapt. Homepage Available at: http://coaptengineering.com/. Accessed December 10, 2017.

[17] M. M. White et al., Usability Comparison of Conventional Direct Control Versus Pattern Recognition Control of Transradial Prostheses, IEEE Trans. Human-Machine Syst., vol. 47, no. 6, pp. 11461157, 2017.

[18] L. J. Hargrove, L. A. Miller, K. Turner, T. A. Kuiken,“Myoelectric Pattern Recognition Outperforms Direct Control for Transhumeral Amputees with Targeted Muscle Reinnervation: A Randomized Clinical Trial,” Sci. Rep., vol. 7(1), pp. 1-9, 2017.

[19] Roche, H. Rehbaum, D. Farina, O. Aszmann, “Prosthetic Myoelectric Control Strategies: A Clinical Perspective,” Curr. Surg. Reports, vol. 2(3), pp. 1-11, 2014.

[20] H. Daley, K. Englehart, L. Hargrove, U. Kuruganti, High density electromyography data of normally limbed and transradial amputee subjects for multifunction prosthetic control, J. Electromyogr. Kinesiol., vol. 22(3), pp. 478-484, 2012.

[21] Michael, John W., and John H. Bowker, eds. Atlas of amputations and limb deficiencies: surgical, prosthetic, and rehabilitation principles. American Academy of Orthopaedic Surgeons, 2004.

[22] L. M. Smurr, K. Yancosek, K. Gulick, O. Ganz, S. Kulla, M. Jones, C. Ebner, A. Esquenazi, P. F. Pasquina, R. A. Cooper, "Occupational Therapy for the Poly trauma Casualty with Limb Loss" in Care of the Combat Amputee, Falls Church, Va. and Washington, DC: United States. Dept. of the Army. Office of the Surgeon General., Borden Institute (U.S.), pp. 493-533, 2009.

[23] Training Protocol for Therapists, Touch Bionics, Part Number: MA01243, Issue No. 1, July 2014.

[24] Chadwell, L. Kenney, S. Thies, A. Galpin, and J. Head, “The reality of myoelectric prostheses: Understanding what makes these devices difficult for some users to control,” Front. Neurorobot., vol. 10, no. AUG, 2016.

[25] N. Celadon, S. Doen, I. Binder, P. Ariano, and D. Farina, “Proportional estimation of finger movements from high-density surface electromyography, J. Neuroeng. Rehabil., vol. 13, no. 1, 2016.

[26] W. Geng, Y. Du, W. Jin, W. Wei, Y. Hu, and J. Li, “Gesture recognition by instantaneous surface EMG images,” Sci. Rep., vol. 6, 2016.

[27] H. Huang, P. Zhou, G. Li, and T. A. Kuiken, "An analysis of EMG electrode configuration for targeted muscle reinnervation based neural machine interface," IEEE Trans. Neural Syst. Rehab. Eng., vol. 16, no. 1, pp. 37–45, Feb. 2008.

[28] G. Li, Y. Li, L. Yu, and Y. Geng, "Conditioning and sampling issues of EMG signals in motion recognition of multifunctional myoelectric prostheses." Ann. Biomed. Eng., vol. 39, no. 6, pp. 17791787, 2011.

[29] D. C. Tkach, A. J. Young, L. H. Smith, E. J. Rouse, and L. J. Hargrove, "Real-time and offline performance of pattern recognition myoelectric control using a generic electrode grid with targeted muscle reinnervation patients," IEEE Trans. Neural Syst. Rehabil. Eng., vol. 22, no. 4, pp. 727–734, 2014.

[30] H. Daley, K. Englehart, L. Hargrove, U. Kuruganti, "High density electromyography data of normally limbed and transradial amputee subjects for multifunction prosthetic control, J. Electromyogr. Kine-siol., vol. 22(3), pp. 478-484, 2012.

[31] Mesa, A. Rubio, I. Tubia, J. De No, and J. Diaz, "Channel and feature selection for a surface electromyographic pattern recognition task", Expert Syst. Appl., vol. 41, no. 11, pp. 51905200, 2014.

[32] Y. Geng, X. Zhang, Y.-T. Zhang, and G. Li, "A novel channel selection method for multiple motion classification using high-density electromyography", Biomed. Eng. Online, vol. 13, no. 1, p. 102, 2014.

[33] M. Paleari, M. Di Girolamo, N. Celadon, A. Favetto, and P. Ariano, "On optimal electrode configuration to estimate hand movements from forearm surface electromyography," in Proceedings of the Annual International Conference of the

IEEE Engineering in Medicine and Biology Society, EMBS, 2015, vol. 2015–November, pp. 6086–6089.

[34] M. A. Powell and N. V Thakor, "A Training Strategy for Learning Pattern Recognition Control for Myoelectric Prostheses.," J. Prosthet. Orthot., vol. 25(1), pp. 30-41, 2013.

[35] T. R. Farrell and R. F. Weir, "A comparison of the effects of electrode implantation and targeting on pattern classification accuracy for prosthesis control.," IEEE Trans. Biomed. Eng., vol. 55(9), pp. 2198-211, 2008.

[36] F. V. G. Tenore, A. Ramos, A. Fahmy, S. Acharya, R. Etienne-Cummings, and N. V Thakor, "Decoding of individuated finger movements using surface electromyography.," IEEE Trans. Biomed. Eng., vol. 56, no. 5, pp. 1427–34, 2009.

[37] H. J. Hermens, B. Freriks, C. Disselhorst-Klug, and G. Rau, "Development of recommendations for SEMG sensors and sensor placement procedures," J. Electromyogr. Kinesiol., vol. 10, no. 5, pp. 361–374, 2000.

[38] H. Al-Timemy, G. Bugmann, J. Escudero, and N. Outram, "Classification of finger movements for the dexterous hand prosthesis control with surface electromyography, IEEE J. Biomed. Heal. Informatics, vol. 17, no. 3, pp. 608618, 2013.

[39] Chan and G. Green, "Myoelectric control development toolbox," presented at the 30th Conf. Can.Med. Biol. Eng. Soc., Toronto, ON, Canada, 2007.

[40] R. Khushaba, A. Al-Ani, and A. Al-Jumaily, "Orthogonal fuzzy neighborhood discriminant analysis for multifunction myoelectric hand control," IEEE Trans. Biomed. Eng., vol. 57, no. 6, pp. 1410–1419, Jun. 2010.

[41] Y. Fang and H. Liu, “Robust sEMG electrodes configuration for pattern recognition based prosthesis control,” in Conference Proceedings - IEEE International Conference on Systems, Man and Cybernetics, 2014, vol. 2014–January, no. January, pp. 2210–2215.

[42] M. C. Castro, S. P. Arjunan, and D. K. Kumar, “Selection of suitable hand gestures for reliable myoelectric human computer interface,” Biomed. Eng. Online, vol. 14, no. 1, 2015.

[43] P. Zipp, “Recommendations for the standardization of lead positions in surface electromyography,” Eur. J. Appl. Physiol. Occup. Physiol., vol. 50, no. 1, pp. 41–54, 1982.

[44] J. V. Mayor, R. M. Costa, A. Frizera Neto, and T. F. Bastos, “Dexterous hand gestures recognition based on low-density sEMG signals for upper-limb forearm amputees”, Res. Biomed. Eng., vol. 33, no. 3, pp. 202217, 2017.

[45] O. Fukuda, T. Tsuji, M. Kaneko, and A. Otsuka, “A human-assisting manipulator teleoperated by EMG signals and arm motions,” IEEE Trans. Robot. Autom., vol. 19, no. 2, pp. 210–222, 2003.

[46] G. Li, A. E. Schultz, and T. A. Kuiken, “Quantifying pattern recognition- based myoelectric control of multifunctional transradial prostheses,” IEEE Trans. Neural Syst. Rehabil. Eng., vol. 18, no. 2, pp. 185–192, 2010.

[47] D. Agarwal, “Flexible Electronics for High-Density EMG Based Signal Acquisition for Upper Limb Myoelectric Prosthesis Control”, 2016.

[48] W. Sensinger, B. A. Lock, and T. A. Kuiken, “Adaptive pattern recognition of myoelectric signals: Exploration of conceptual framework and practical

algorithms," IEEE Trans. Neural Syst. Rehabil. Eng., vol. 17, no. 3, pp. 270–278, 2009.

[49] J. Hargrove, K. Englehart, and B. Hudgins, "A comparison of surface and intramuscular myoelectric signal classification," IEEE Trans. Biomed. Eng., vol. 54, no. 5, pp. 847–853, 2007.

[50] http://www.otbioelettronica.it/index.php?option=com_content&view=article&id=29&Itemid=265&lang=en

[51] J. S. Head, D. Howard, S. W. Hutchins, L. Kenney, G. H. Heath, and A. Y. Aksenov, "The use of an adjustable electrode housing unit to compare electrode alignment and contact variation with myoelectric prosthesis functionality: A pilot study," Prosthet. Orthot. Int., vol. 40, no. 1, pp. 123–128, 2016.

[52] C. M. Light, P. H. Chappell, and P. J. Kyberd, "Establishing a standardized clinical assessment tool of pathologic and prosthetic hand function: Normative data, reliability, and validity," Arch. Phys. Med. Rehabil., vol. 83, no. 6, pp. 776–783, 2002.

[53] H. Huang, F. Zhang, Y. L. Sun, and H. He, "Design of a robust EMG sensing interface for pattern classification," J. Neural Eng., vol. 7, no. 5, 2010.

[54] Yokus and J. S. Jur, "Fabric-based wearable dry electrodes for body surface biopotential recording," IEEE Trans. Biomed. Eng., vol. 63, no. 2, pp. 423–430, 2016.

[55] T. Degen and H. Jäckel, "Continuous monitoring of electrode - Skin impedance mismatch during bioelectric recordings," IEEE Trans. Biomed. Eng., vol. 55, no. 6, pp. 1711–1715, 2008.

[56] Cömert and J. Hyttinen, “Impedance spectroscopy of changes in skin-electrode impedance induced by motion,” Biomed. Eng. Online, vol. 13, no. 1, 2014.

[57] H. Liu, X. Tao, P. Xu, H. Zhang, and Z. Bai, “A dynamic measurement system for evaluating dry bio-potential surface electrodes,” Meas. J. Int. Meas. Confed., vol. 46, no. 6, pp. 1904–1913, 2013.

[58] COAPT complete control handbook, COAPT LLC, Chicago, IL, Unites States, 2017. Accessed on: Mar. 19, 2017 [Online]. Available: https://www.coaptengineering.com/uploads/1/0/5/1/105156115/coapt complete control handbook apr2017.pdf

[59] J. S. Han, S. W. Lee, Z. Bien, “Feature subset selection using separability index matrix”, Inf. Sci. (Ny)., vol. 223, pp. 102-118, 2013.

[60] Liu, Huan, and Hiroshi Motoda. Feature selection for knowledge discovery and data mining. Vol. 454. Springer Science & Business Media, 2012.

[61] Prime, Y. Losier, and U. Kuruganti, “Clinical investigation of high-density electromyography data and pattern classification accuracy for prosthetic control,” J. Prosthetics Orthot., vol. 27, no. 1, pp. 8–14, 2015.

[62] J. Young, L. J. Hargrove, and T. A. Kuiken, “The effects of electrode size and orientation on the sensitivity of myoelectric pattern recognition systems to electrode shift,” IEEE Trans. Biomed. Eng., vol. 58, no. 9, pp. 2537–2544, 2011.

[63] K. Fukunaga, “Introduction to statistical pattern recognition”, second ed., Academic Press,vol. 22., 1990.

[64] P. C. Mahalanobis, “On the generalized distance in statistics”, Proc. Indian Nat. Inst. Sci. (Calcutta), vol. 2, pp. 49-55, 1936.

[65] Bhattacharyya, “On a measure of divergence between two statistical populations defined by their probability distributions,” Bull. Calcutta Math. Soc., vol. 35, pp. 99-109, 1943.

[66] S. Kullback and R. Leibler, “On Information and Sufficiency,” Ann. Math. Statist. vol. 22(1), pp. 79-86, 1951.

[67] P. Parker, K. Englehart, and B. Hudgins, “Myoelectric signal processing for control of powered limb prostheses,” J. Electromyogr. Kinesiol., vol. 16, no. 6, pp. 541–548, 2006.

BIOGRAPHY:

Sapna Kumar was born in Tirupati, Andra Pradesh, India on 29 November 1992. She received B. Tech in Biomedical engineering from Sathyabama University, Chennai, TN, India in the year 2014. She is currently pursuing Master's degree in biomedical engineering at the Johns Hopkins University, Baltimore, Maryland. She worked as a research assistant at the Neuroengineering and biomedical instrumentation laboratory headed by Dr. Nitish. V. Thakor. She is interested in the study of electrode interface to measure surface Electromyography (sEMG) and its signal source in people with upper limb amputations. Her work involves developing an electrode interface for EMG signal source optimization to improve performance of upper limb Myoelectric control systems. She also worked as a teaching assistant for courses including Robot sensors and actuators, Principles of design of biomedical instrumentation and Biomedical Engineering Pract and Innovation Lab courses.